

DIGITAL SIMULATION OF SHIP PROPULSION TRAINS  
UTILIZING GAS TURBINE AND DIESEL PRIME MOVERS

Ernest Raymond Freeman



DIGITAL SIMULATION OF SHIP PROPULSION TRAINS  
UTILIZING GAS TURBINE AND DIESEL PRIME MOVERS

by

ERNEST RAYMOND FREEMAN

LIEUTENANT COMMANDER, UNITED STATES NAVY

B.S., United States Naval Academy

(1963)

Submitted in Partial Fulfillment of the  
Requirements for the Degree of  
Ocean Engineer and the Degree of  
Master of Science in Mechanical Engineering

at the

MASSACHUSETTS INSTITUTE OF TECHNOLOGY

May, 1972

7/20/12  
5-1686-2

ABSTRACT

Digital Simulation of Ship Propulsion Trains Utilizing  
Gas Turbine and Diesel Prime Movers

Ernest R. Freeman

A computer simulation of some power plants, transmission systems, and propellers has been developed.

Theoretical models have been established mainly from published models for the following components.

1. prime movers
  - a. aircraft derivative gas turbines
  - b. low speed diesel engines
  - c. medium speed diesel engines
2. transmissions
  - a. direct drive (low-speed diesel)
  - b. reduction gear with and without reversing clutch arrangement
3. propulsors
  - a. conventional fixed pitch propellers
  - b. controllable reversible pitch propellers

The computer simulation utilized the Dynamic System Simulation Program (DYSYS) on an IBM 1130 computer. DYSYS was developed by the Department of Mechanical Engineering at N.I.T. Representative accelerations and crashback maneuvers were computed using the various propulsion systems. Several critical situations were established involving the sequencing of power plant, transmission, and propulsion transients.

Thesis supervisor: A. Douglas Carmichael  
Title: Professor of Power Engineering

Thesis Reader: Henry H. Paynter  
Title: Professor of Mechanical Engineering



## TABLE OF CONTENTS

### ABSTRACT

### INTRODUCTION

1.	GAS TURBINE MODELS	1
1.1	Introduction	1
1.2	Aircraft Gas Turbine Models	1
1.3	Marine Gas Turbine Models	5
1.4	Torque-Speed Characteristics Model	5
1.5	An Improved Model	6
2.	DIESEL ENGINE	12
2.1	Introduction	12
2.2	Presentation of Models	12
2.3	Low Speed Diesel Model	18
2.4	Medium Speed Diesel Model	18
2.5	Delays	19
2.6	Discussion	19
3.	CLUTCHES AND HYDRODYNAMIC TORQUE CONVERTERS	20
3.1	Introduction	20
3.2	Falk Marine Airflex Clutch	20
3.3	SQ500 Synchoclutch (Dental Clutch Type)	22
3.4	Hydraulic Transmissions	23
3.5	Discussion	27
4.	PROPELLER MODELS	29
4.1	Introduction	29



TABLE OF CONTENTS (Cont'd)

4.	PROPELLER MODELS (Cont'd)	
4.2	Propeller Characteristics	29
4.3	Modelling the Wageningen B-Screw Series	31
4.4	Controllable Reversible Pitch Propellers (CRPP)	35
4.5	Pitch Control System Model	39
4.6	Discussion	40
5.	SHIP CHARACTERISTICS	44
5.1	Wake Fraction and Thrust Deduction Factor	44
5.2	Added Mass of Ship and Propeller	46
5.3	Ship Resistance	46
5.4	Shaft Friction	47
6.	RESULTS	48
6.1	Introduction	48
6.2	Coastdown from 30 Knots (FT4A-2)	48
6.3	Accelerating from 5 Knots (FT4A-2)	48
6.4	Crashback from 30 Knots (FT4A-2)	49
6.5	Accelerating from 15 Knots (LM2500-A)	49
6.6	Crashback from 30 Knots (LM2500-A)	49
6.7	Crashback from 9 Knots (KV Major 12)	50
6.8	Crashback from 12 Knots (B & W 7K98FF)	51
7.	CONCLUSIONS	83
8.	RECOMMENDATIONS	84
	REFERENCES	85
	APPENDIX A Gas Turbine Models	89
	APPENDIX B Diesel Particulars	107



TABLE OF CONTENTS (Cont'd)

APPENDIX C	Clutches	116
APPENDIX D	Propeller Subroutines	121
APPENDIX E	Ship Dynamics	129
APPENDIX F	FT4A-2 Drive Train	131
APPENDIX G	LM2500-A Drive Train	135
APPENDIX H	KV Major 12 Drive Train	145
APPENDIX I	B & W 7K98FF Drive Train	150



## INTRODUCTION

The rapid advances made in the field of automatic controls since World War II have found more and more applications in the area of ship propulsion. One of the principal driving forces behind this is the desire to operate plants safely and at or near their "optimal" operating point. The safe coordinated operation of some ship power plants consisting of high performance prime movers, sophisticated couplings, and propellers is no trivial matter. This is especially true during periods when fast ship response is desired, e.g., emergency stopping or accelerating.

To be able to control a propulsion plant, one must be able to model it and know how it behaves under various disturbances or changes in inputs. The alternative is a costly experimental program for each system. The problem for the control engineer now becomes one of developing or choosing a model that suitably describes the characteristics of the particular power train components. These component models may be either physical or functional. A physical model may accurately describe a component's characteristics using, for example, Newton's Laws of Motion, thermodynamic relationships, conservation of mass relations, etc. These provide a valuable insight of the physical processes occurring in the operation of a component, and enable one to perceive what simplifications can be made to a model. Some components, on the other hand, may prove to be very non-linear and to describe their operational characteristics using physical laws may result in mathematical expressions which are not suitable for use in a simulation study. In this situation a simpler mathematical expression is developed which closely approximates the component's characteristics over a reasonable range of inputs.



## INTRODUCTION (Cont'd)

The philosophy behind the study described in this thesis has been to keep the models simple, but yet reasonable. To quote P. J. Kiviat, who prepared a RAND memorandum on digital simulation modeling concepts,

"the model should only be as detailed as is necessary to answer the question at hand; it should be so designed, however, so it can be expanded to include more detail without inordinate cost in those model areas which have a high probability of becoming subsequent subjects of concern."(1)

Once the component models are selected, drive train models can be synthesized and prepared for simulation. No discussion will be made concerning the relative merits of digital simulation compared to analog or analog-digital (hybrid) simulation. The simulation literature is replete with these discussions. Digital simulation was decided at the outset.

A major part of this study has been concentrated on writing computer programs for prime movers, propellers, and transient operations. These programs were developed to investigate various control schemes for marine power plants.

The gas turbines selected for simulation are the Pratt and Whitney FT4A-2 and the General Electric LM2500-A. A medium speed and a low speed diesel were also selected. The medium speed diesel selected is the Mirrless KV Major 12; the low speed diesel selected is the Burmeister and Wain 7K98FF. The main reasons for selecting these particular engines were the availability of suitable data at reasonable power levels.



## 1. GAS TURBINE MODELS

### 1.1 Introduction

Gas turbines, as applied to ship propulsion, usually connote the inclusion of a power turbine or "free" turbine, which provides the driving torque. The power turbine is driven by the hot exhaust gases of the "gas generator." Thus when marine engineers refer to gas turbines, they usually include the combination of gas generator and power turbine in their meaning.

There are, of course, exceptions to the statement concerning separate power turbines. The Koelin Class escort frigates built for the German Federal Navy are driven by gas turbines which do not have a separate power turbine. The gas generator is coupled through a clutch to the drive train.(2)

### 1.2 Aircraft Gas Turbine Models

During the literature survey part of this study, several gas turbine models useful for aircraft propulsion simulation were found. In Reference (3), for example, Cottington presents a simulation study of a two-spool turbojet engine, and also covers the design of a digital three-term controller using digital simulation methods. In trying to determine an "optimum" set of gains, he treated the high pressure rotor system as a critically damped second order system. Values of these optimized gain settings for varying values of high pressure rotor speeds are presented.

Mueller has developed a single spool gas turbine model from one-dimensional flow relationships.(4) He assumes that the only important dynamics are those of the rotating compressor-



## 1. GAS TURBINE MODELS (Cont'd)

### 1.2 Aircraft Gas Turbine Models (Cont'd)

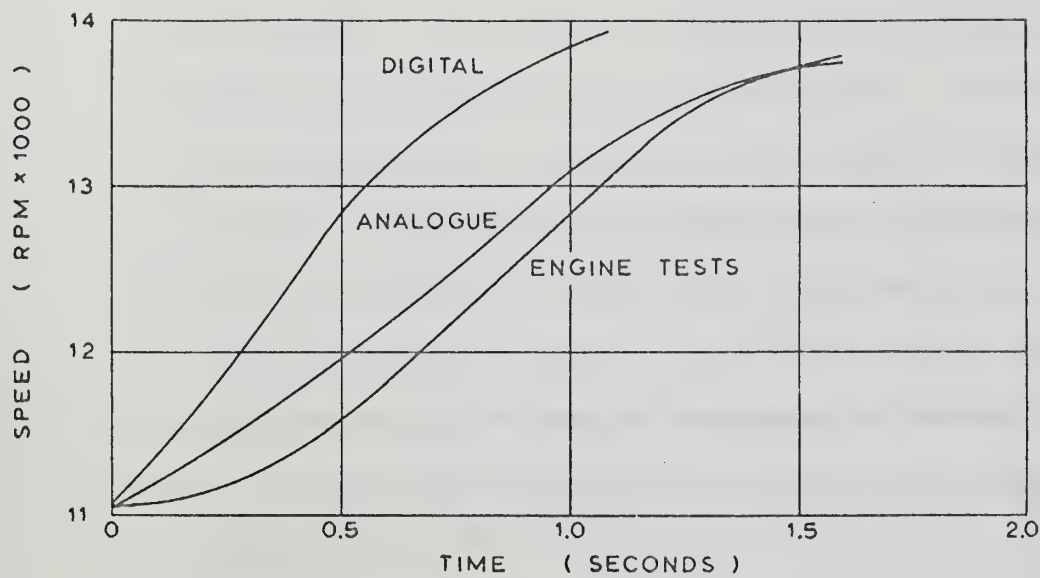
turbine spool. Mueller justifies this by noting that gas disturbances travel through the engine at the speed of sound, whereas a spool acceleration or deceleration takes some seconds. No results of his simulations are presented.

In References (5) and (6), models are derived from a linear analysis of gas turbine dynamics. The model presented in the latter reference is highly detailed and is developed using non-dimensionalized parameters. To use this model, one must have access to the machinery performance maps. The prominent feature of this model is that it assumes stepwise linearity. The compressor performance map is utilized to obtain the coefficients in the linearized equation at each operating point.

In References (7) and (8), Saravanamuttoo and Fawke discuss the application of both analog and digital computer methods of simulating gas turbine dynamic performance. They approached the problem from the viewpoint of engineering thermodynamics, using the normal compressor and turbine characteristics.

Figure (1-1) shows the results obtained by Saravanamuttoo and Fawke for a single-spool turbojet simulation, both digital and analog, along with the results of actual engine tests. It can be seen that the acceleration predicted by both simulations was much faster than the actual engine. An examination of the test results on the engine showed that there was a lag in the rise of turbine entry temperature following a fuel change.





RESULTS OF SARVANALUTTO-FAMKE SIMULATIONS COMPARED WITH  
ENGINE TESTS

Fig. (1-1)



## 1. GAS TURBINE MODELS (Cont'd)

### 1.2 Aircraft Gas Turbine Models (Cont'd)

Saravanamuttoo and Fawke's model, however, had assumed immediate response, although they realized there would be some lag due to the dynamics of the fuel injection system. They decided to simulate this lag by postulating that after a sudden change in fuel flow, the combustion efficiency drops instantaneously and then recovers exponentially. This drop in efficiency was made proportional to the percentage increase in fuel flow. The constant of proportionality was determined such that the turbine entry temperature before and after the transient was unchanged from the steady state values. The time constant for the recovery of combustion efficiency was taken to be inversely proportional to the air flow through the combustor, i.e.,

$$\tau = \tau_0 \cdot \frac{W_0}{W}$$

$\tau$  - time constant for recovery of combustion efficiency

$\tau_0$  - time constant at design speed

$W_0$  - air flow at design speed

$W$  - air flow

To achieve flow compatibility in their digital model, Saravanamuttoo and Fawke added lags in the propagation of pressure signals through the engine. The lags were introduced by considering the engine components to be separated by specified volumes; these volumes produced the desired capacitive effect.



## 1. GAS TURBINE MODELS (Cont'd)

### 1.3 Marine Gas Turbine Models

During the early parts of the literature survey, a Russian title on analog and digital models of marine gas turbines was found in a gas turbine newsletter. This book, listed as Reference (9), was written by Bichayev and published by the Shipbuilding Press of Leningrad in 1969. Although it is still untranslated, the book appears to be a major work in the field of marine gas turbine simulation, judging from the many analog computer diagrams, compressor maps, and equations. The cost of having it translated (over \$900) was prohibitive.

An unedited rough translation of a Russian work by Lurye discusses mathematical modeling of a marine gas turbine engine with a real fuel apparatus.(10) Lurye's model is presented in the form of linearized differential equations. The equations describing Lurye's model are reproduced in Appendix A.

Using Saravanamuttoo's technique, one can extend his model to a gas turbine having a free turbine. This is also presented in Appendix A.

### 1.4 Torque-Speed Characteristics Model

C. J. Rubis has developed a method based on the free turbine torque-speed characteristics to model a gas turbine's action.(11,12) The free turbine torque-speed characteristics can be derived from the steady-state power-speed characteristics which show lines of constant SFC. The corresponding curves for the Pratt and Whitney FT4A-2 and General Electric LM2500-A



## 1. GAS TURBINE MODELS (Cont'd)

### 1.4 Torque-Speed Characteristics Model (Cont'd)

are given in Appendix A. The torque-speed characteristics have been used here as the model selected for simulating the performance of the marine gas turbine.

The unrefined model, used to describe the transient performance of the turbine operates in the following manner. Referring to Figure (12), assume that the initial steady-state operating point is at A operating at torque  $T_0$  and speed  $N_0$ , and assume that the engine is to accelerate to point B. In a time interval  $\Delta t$ , fuel is increased by  $\Delta F$ . This increase in fuel produces an instantaneous change in torque  $\Delta T$  such that the new torque is  $T_0 + \Delta T$ . This increase in torque will result in a change in power turbine rotation  $\Delta N$  along the constant fuel rate line  $F_0 + \Delta F$ . The new starting point for the next time interval is at the intersection of the  $F_0 + \Delta F$  constant fuel rate line and the new rotational speed  $N_0 + \Delta N$ . The dotted lines illustrate the paths taken during the time steps, while the heavy line is the torque path.

### 1.5 An Improved Model

The methodology of this model is not new. The torque-speed characteristics have been used in the past to model diesel engines. The idea of obtaining instantaneous torque for a change in fuel rate is much closer to the real thing in a diesel than it is in a gas turbine. Comparisons with engine tests have shown that the predicted values of torques obtained from the gas turbine characteristics are higher than the



POWER TURBINE STEADY-STATE  
TORQUE-SPEED CHARACTERISTICS  
FOR CONSTANT VALUES OF  
FUEL FLOW

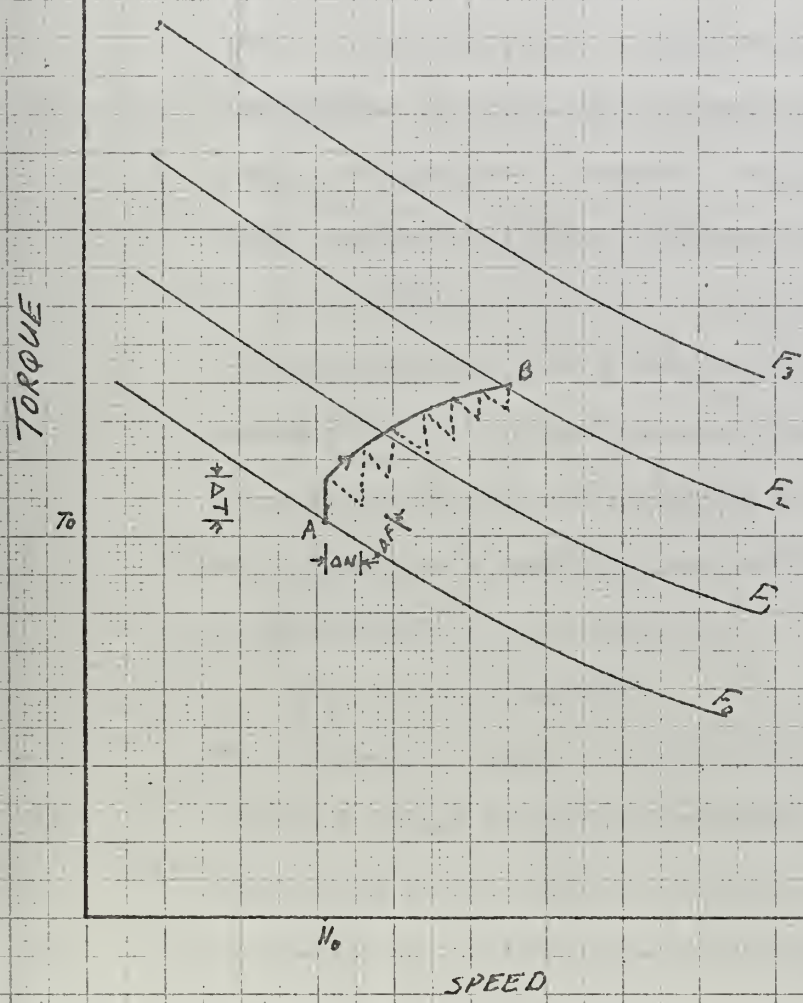


FIG. (1-2)



## 1. GAS TURBINE MODELS (Cont'd)

### 1.5 An Improved Model (Cont'd)

measured values. The differences in torque and the resulting differences in speed were measured by Rubis who conducted engine tests with the FT4A-2. He also used the torque-speed curves in a simulation between the same two power levels.

Figure (1-3) shows how the simulation results in a higher acceleration because of the higher torques. This graph should be compared with figure (1-1).

It is evident from the comparison of figures (1-1) and (1-3) that what is needed to improve this model is a correction factor, which could have a physical explanation similar to that offered by Saravanamuttoo and Fawke for their model; namely a reduction in combustion efficiency. The results of other transient tests conducted with the FT4A-2 were presented by Rubis in Reference (13). In this paper, Rubis presents correction factors to the torque-speed curve model for engine accelerations. This curve is reproduced herein as figure (1-4). One can observe that the curve for accelerations from idle can be expressed as a decaying exponential similar to the proposal by Saravanamuttoo and Fawke, viz.,

$$K_e = .3 + .7 (1 - e^{-\frac{t}{2.5}})$$

This expression, which creates a form of delay or lag in the transient torque produced by the model, was included in the simulations in this study. It should be clear that this lag is applied to the transient torque obtained from the model and not to the whole torque.



RESULTS OF RUBIS' SIMULATION  
COMPARED WITH ENGINE TEST

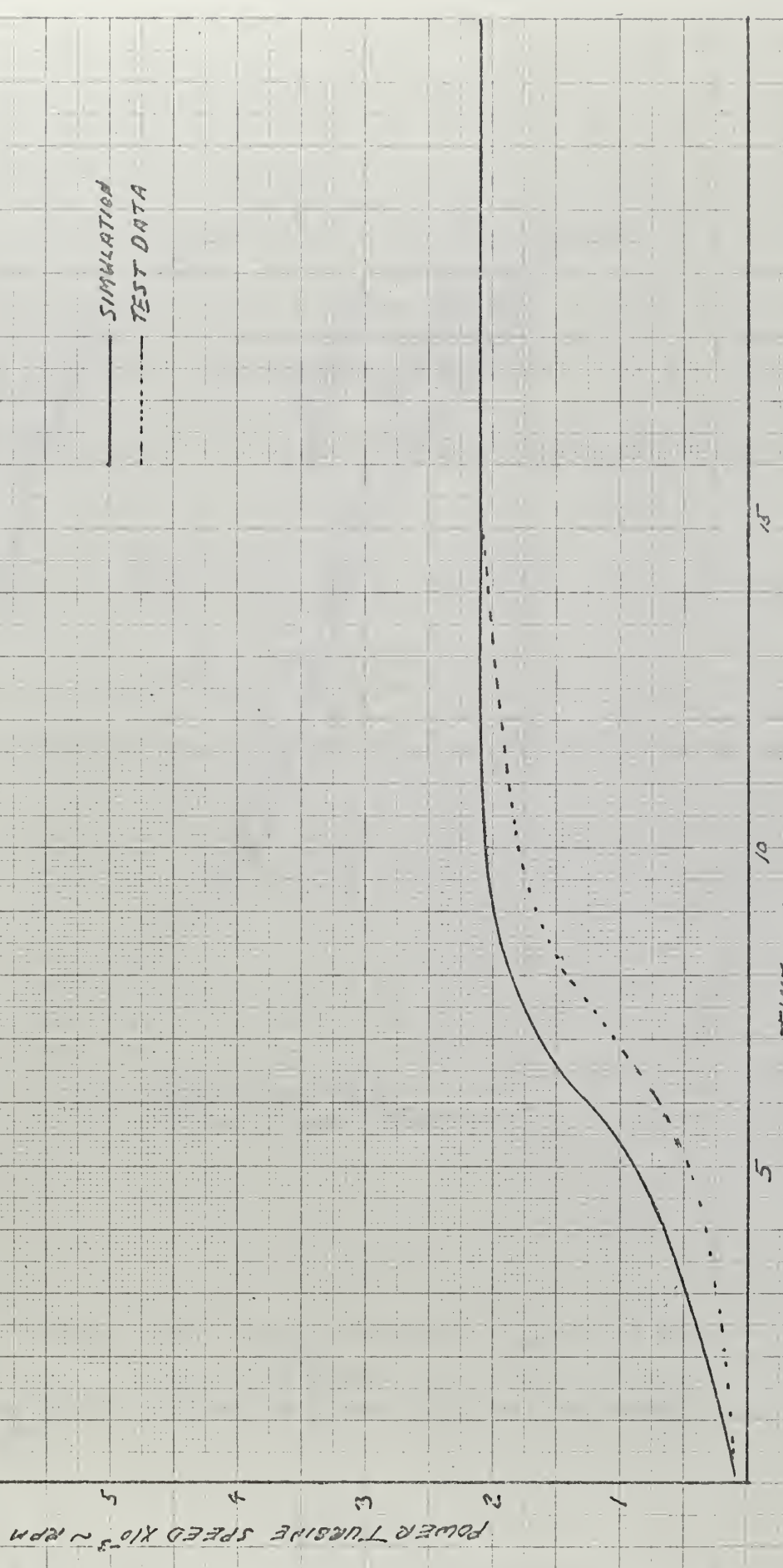
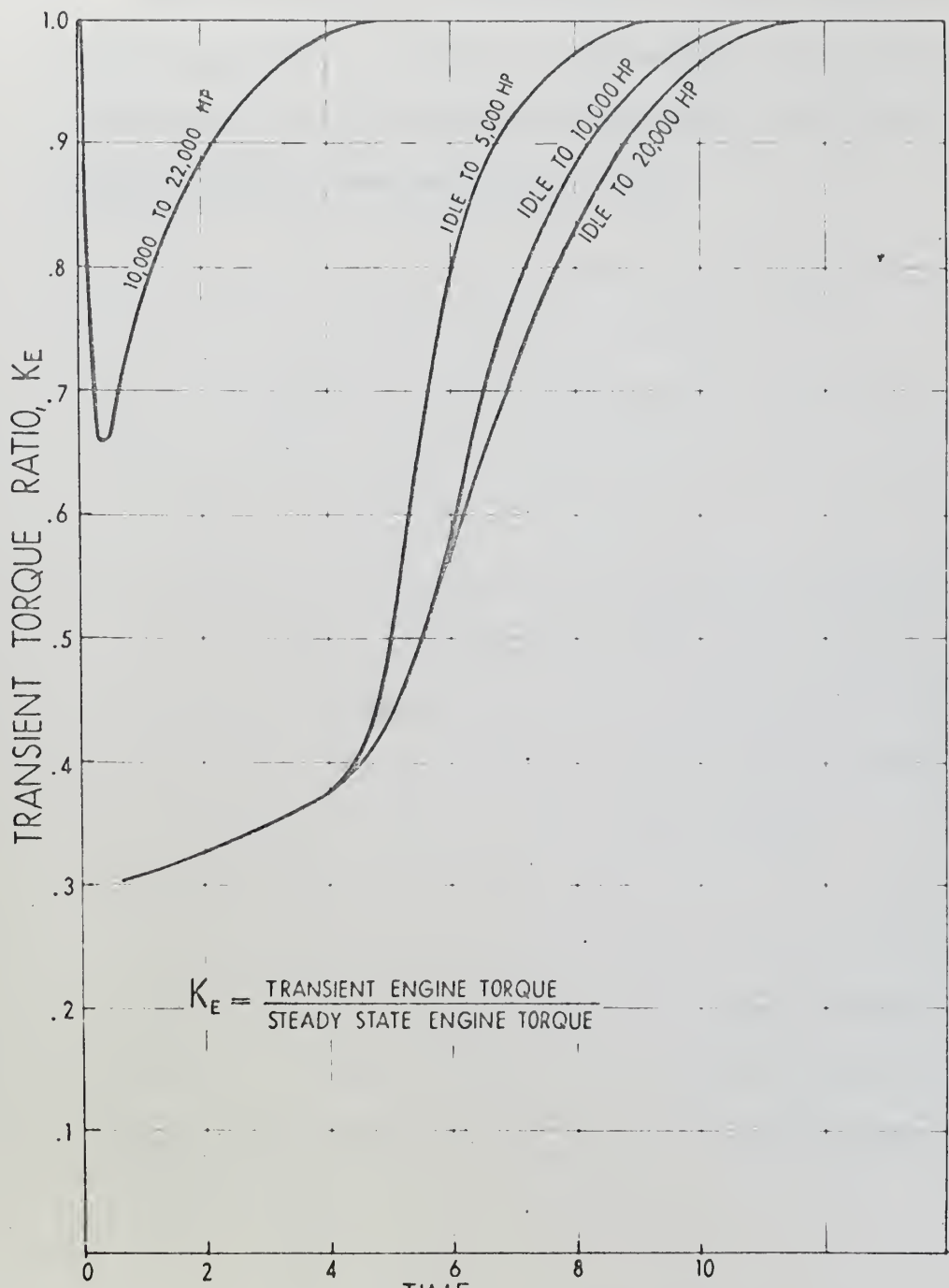


FIG (1-3)





CORRECTION FACTORS TO STEADY STATE ENGINE TORQUE  
MODEL

Fig. (1-4)



## 1. GAS TURBINE MODELS (Cont'd)

### 1.5 An Improved Model (Cont'd)

The model appears to be acceptable for ship propulsion studies because it is simple; it also permits loading other characteristics of the ship drive train into a medium sized computer without exceeding its core size.



## 2. DIESEL ENGINE

### 2.1 Introduction

The traditional use of steam power plants to propel large American built ships has created somewhat of a void in this country's technical literature on diesel ship propulsion. The successful use of diesel engines for ship propulsion by foreign shipbuilders, on the other hand, has been an established fact long before the first digital computer was ever built, and long before analog and digital simulations became established as accurate techniques for modeling and testing ship propulsion plants prior to their construction. Consequently there has been very little demand from industry, either foreign or domestic, for diesel plant simulations. However, some published data were obtained and used in this study. Since the use of high speed diesels has been fairly restricted to small craft, the simulations have been limited to medium and low speed diesels.

### 2.2 Presentation of Models

Woodward presents in Reference (14) a simple, straightforward treatment of the diesel engine as applied to ship propulsion. A widely used expression given in Reference (14) and other engine textbooks, is the formula for indicated horsepower (IHP):

$$IHP = \frac{PLAN}{33000} \quad (HP)$$

P = indicated mean effective pressure ( $\text{lbs/in}^2$ )

L = stroke (ft)

A = total piston area ( $\text{in}^2$ ) for a multi-cylinder engine

N = RPM (two-stroke engine),  $\frac{RPM}{2}$  (four-stroke engine)



## 2. DIESEL ENGINE (Cont'd)

### 2.2 Presentation of Models (Cont'd)

This power is that produced in the engine cylinders, and is greater than that available at the output shaft because of friction and other internal loads (e.g., water pumps, fuel pumps, turbochargers, etc.). What is available at the output shaft is termed brakehorsepower (BHP). The ratio of brakehorsepower (BHP) to indicated horsepower (IHP) is the mechanical efficiency ( $\eta_m$ ) of the engine, i.e.,

$$\eta_m = \frac{\text{BHP}}{\text{IHP}}$$

$$\text{or BHP} = \frac{\eta_m \text{ IHP}}{33000}$$

The product  $N_m P$  is called the brake mean effective pressure (BMEP). The indicated mean effective pressure,  $P$ , can be directly measured and is proportional to the energy released by combustion in the cylinder. This energy is proportional to the amount of fuel injected in each power stroke. Most diesels utilize positive displacement pumps for fuel injection. The amount injected per power stroke for this type of pumping system should be the same. The stroke,  $L$ , and the total piston area,  $A$ , are, of course, fixed for a particular diesel. If one assumes constant mechanical efficiency, then it can be seen that for a particular fuel setting, BHP is a linear function of  $N$ , i.e.,

$$\text{BHP} = KN$$

$$K = \frac{N_m \text{ PLA}}{33000} \quad \text{for a particular fuel injection setting}$$



IDEAL DIESEL ENGINE  
TORQUE-SPEED CURVES  
FOR CONSTANT FUEL  
SETTING "F".

TORQUE

$F_3$

$F_2$

$F_1$

RPM

FIG (2-U)



IDEAL DIESEL ENGINE  
POWER-SPEED CURVES  
FOR CONSTANT FUEL  
SETTING "F"

$$F_3 > F_2 > F_1$$

BHP

RPM

FIG (2-2)



## 2. DIESEL ENGINE (Cont'd)

### 2.2 Presentation of Models (Cont'd)

Since rotational power is the product of torque,  $\tau$ , and speed,  $\omega$ , it then follows that for a two stroke engine,

$$\omega = 2\pi N \quad (\text{rad/min})$$

$$\tau\omega = \tau 2\pi N \quad (\text{ft-lb/min})$$

$$\tau = \frac{K}{2\pi} \quad K \text{ as previously defined}$$

i.e., torque is constant for particular fuel injection setting.

The above is known as the ideal torque-rpm and power-rpm diesel relationships, and are graphically illustrated in Figure 2-1 and 2-2.

The important assumption of this model is the one concerning constant mechanical efficiency. How close does this approach the actual case? In Reference (15), Pounder devotes an entire chapter to the Burmeister and Wain Engines and states a mechanical efficiency of 91% in his discussion on B & W low speed diesels. (Note: this figure was confirmed by a representative of the Burmeister & Wain Corporation on a recent visit to MIT).

It was indicated before that the indicated mean effective pressure is proportional to the fuel injected rate. An extension of the ideal model then is to say that torque is not only constant for a given fuel setting, but also proportional to that fuel setting. In other words, torque is a linear function of fuel setting. Obviously, other extensions can be made such as relating torque to fuel rack position or to



## 2. DIESEL ENGINE (Cont'd)

### 2.2 Presentation of Models (Cont'd)

the movement of some fuel control actuator.

Lewis, Lecourt, and Scoville used a variation of the ideal diesel engine in Reference (16). The torque developed within the engine was designated  $Q_{DE}$  and the friction torque  $Q_{fe}$ . The output torque is the difference between the two torques.  $Q_{DE}$  was postulated as linearly related to fuel rack position,  $z$ , i.e.,

$$Q_{DE} = Kz$$

and the friction torque was taken as linearly related to engine speed,

$$Q_{fe} = A_0 + A_1 \cdot N.$$

It can be seen that this model does not assume constant mechanical efficiency.

In Reference (17), Garvey presents a linearized differential equation describing the motion of a diesel engine. He assumed the output torque developed by the engine to be proportional to governor position, i.e.,

$$T = Cz$$

$T$  - change in torque

$z$  - governor position

$c$  - governor gain

Parker uses the same model with a delay (18),

$$T = ce^{-sT} z$$

$T$  = Torque

$c$  = governor gain

$z$  = governor position



## 2. DIESEL ENGINE (Cont'd)

### 2.2 Presentation of Models (Cont'd)

$s$  = differential operator

$\tau$  = time delay

### 2.3 Low Speed Diesel Model

The ideal diesel engine model in conjunction with a delay in the form of an exponential lag was chosen as the method to simulate a Burmeister & Wain 7K98FF low speed diesel.

In Reference (19), Meulengracht presents the results from test-bed trials of a 7K98FF. From these results, and assuming the ideal diesel characteristics, one can get a brakehorse-power-speed curve and from this curve, derive the flat torque speed characteristics for constant fuel settings. These curves are all included in Appendix B.

### 2.4 Medium Speed Diesel Model

Reference (20) describes the development of high performance medium speed diesel, the Mirrless KV Major 12. Since the fuel map for this diesel is included in this article, it was selected as the diesel to model. From the fuel map, and using the elementary relations presented earlier, one can derive the engine's torque speed characteristics for constant fuel settings. In the process of drawing these characteristics, it was observed that torque could be approximated quite well as being proportional to fuel setting. Thus the expression,

$T = Kx$  (torque)

$x$  = fuel setting

$K$  = proportionality constant

was used in the simulations.



## 2. DIESEL ENGINE (Cont'd)

### 2.5 Delays

As in the gas turbine, the diesel engine does not instantaneously produce a change in torque with an increase in fuel rate. For a four-stroke cycle multi-cylinder diesel engine, Parker recommends a value of  $\frac{15}{N}$  when N equals engine rpm; this is an approximation for diesel engines with two or more cylinders firing per revolution.(21) For the more general case, Reference (16) recommends

$$\frac{15}{N_{Re}} < T_{DELAY} < \frac{15}{N_{Re}} + \frac{60}{N_{Re}^p}$$

$N_{Re}$ : designed engine speed

p : number of cylinders firing per revolution

### 2.6 Discussion

The torque-fuel setting characteristics were found to be linear for the medium speed diesel but not quite linear for the low speed engine. The characteristics for the low-speed diesel were therefore stored in the computer. For each diesel, a change in fuel setting results in a change in torque. This torque was tempered by a delay in the form of a decaying exponential. This method is much simpler than that employed for the gas turbine models since diesel torque is independent of speed in the engine's operating range.

For ship propulsion studies being considered here, it was not considered necessary to seek a model which would produce the oscillatory torque that is characteristic of internal combustion engines (cf. Reference 16).



### 3. CLUTCHES AND HYDRODYNAMIC TORQUE CONVERTERS

#### 3.1 Introduction

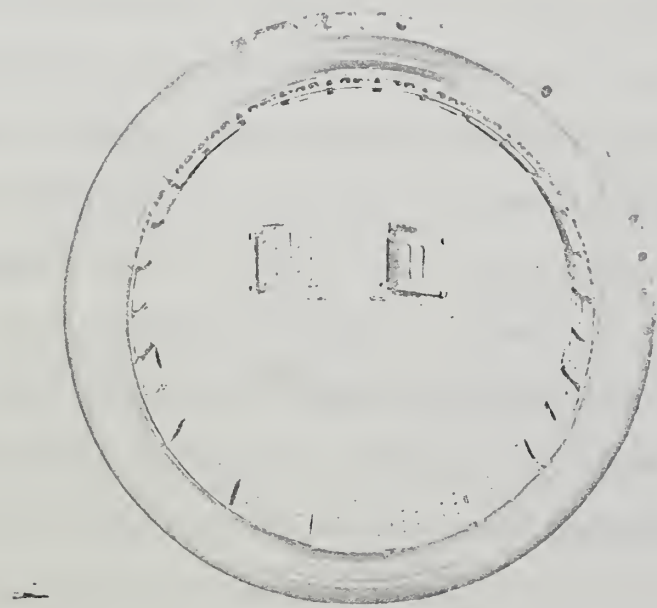
The selection of a fixed pitch propeller and a non-reversing prime mover will necessarily mean the incorporation of a clutch or torque converter in the drive train. Gas turbines, for example, are limited to undirectional movement; and some diesels, on the other hand, are designed for operation in two directions. It will be observed later that clutch engagement and disengagement times play a critical part in the emergency stopping of a ship. The selection of a proper clutch for a drive train thus is no trivial matter. In the same vein, the selection of a suitable clutch model to simulate the emergency stopping of a ship is important in order to avoid erroneous results.

#### 3.2 Falk Marine Airflex Clutch

Figure 3-1 shows the principal part of the Airflex clutch. The clutch is pneumatically operated drum-type dry friction clutch consisting of an annular rubber/fabric air gland bonded to an outer, flanged steel rim and lined with friction shoes which engage an inner iron drum when the gland is inflated. A newer air-cooled version utilizes extruded aluminum shoe blocks with axial air passages, to which the friction brake block liners are riveted to insulate the rubber gland from the heat generated at the friction surface (cf. Reference 22).

Rubis was able to obtain from the Falk Corporation the torque expressions for the clutches.(11) The torque capacity was found to be directly related to the number of brake liners





FALK MARINE AIRFLEX CLUTCH

Fig. (3-1)



### 3. CLUTCHES AND HYDRODYNAMIC TORQUE CONVERTERS (Cont'd)

#### 3.2 Falk Marine Airflex Clutch (Cont'd)

and the net air pressure used to engage the clutch. For a 35-inch-diameter clutch with eight liners, the maximum clutch torque capability,  $Q_c$ , is given by the expression

$$Q_c = 2275 P_{net} \quad (\text{lb-ft})$$

$P_{net}$  = net air pressure activating the clutch (psi)

One of the important features to consider in this clutch is that the inward expansion of the clutch glands during engagement is opposed by the centrifugal force of the rotating clutch assembly. The retarding force has been transformed to an equivalent air pressure,  $p_c$ , and is expressed by the relation

$$p_c = 5 + (5.9 \times 10^{-5}) N_g^2 \quad (\text{psi})$$

$N_g$  = speed of the frame housing the clutch glands (rpm)

Rubis states that typical inflation and deflation rates are 5 psi per second and 30 psi per second respectively; and a typical supply pressure is 150 psi.

#### 3.3 SQ500 Synchroclutch (Dental Clutch Type)

The SQ500 Synchroclutch is manufactured by the Philadelphia Gear Corporation. Literature on the description and operation was furnished by the manufacturer and is included in Appendix C. This particular clutch is recommended for gas turbines in the 25000 HP at 3600 rpm range (e.g. FT4A-2 & LM2500). For a typical application, the torque history for the synchronizing (friction) clutch may be approximated by:



### 3. CLUTCHES AND HYDRODYNAMIC TORQUE CONVERTERS (Cont'd)

#### 3.3 SQ500 Synchroclutch (Dental Clutch Type) (Cont'd)

$$T = T^1(1-e^{-t/26})$$

T = torque at time t (ft-lb)

t = time (sec)

$$T^1 = 11,600 \text{ (ft-lb)}$$

Both  $T^1$  and the time constant may be changed to suit specific operating conditions.(23) Other information and details on this clutch are included in Appendix C.

Another clutch which operates in a similar manner to the SQ500 is the BLH-Dynetic synchronizing clutch manufactured by Koppers Co, Inc. Although no torque-time history expression was provided by the manufacturer, information was provided on the operation and design of the clutch. This is included in Appendix C for information purposes only.

#### 3.4 Hydraulic Transmissions

One of the problems inherent in a plant driven by a diesel or gas turbine prime mover with a fixed pitch propeller that is not found in a comparable steam plant is that the former prime movers have minimum speeds at which they can be operated. The Coast Guard Ship Hamilton (WPG-715), for example, is powered by two FT4-A-6 gas turbines and two Fairbanks Morse Model 38TD-1/8 turbo-supercharged opposed-piston marine diesel engines driving two controllable pitch propellers. With the propeller at full pitch, and the diesel at idle, the vessel will attain a speed of approximately 12 knots, and 18 knots with full pitch



### 3. CLUTCHES AND HYDRODYNAMIC TORQUE CONVERTERS (Cont'd)

#### 3.4 Hydraulic Transmissions (Cont'd)

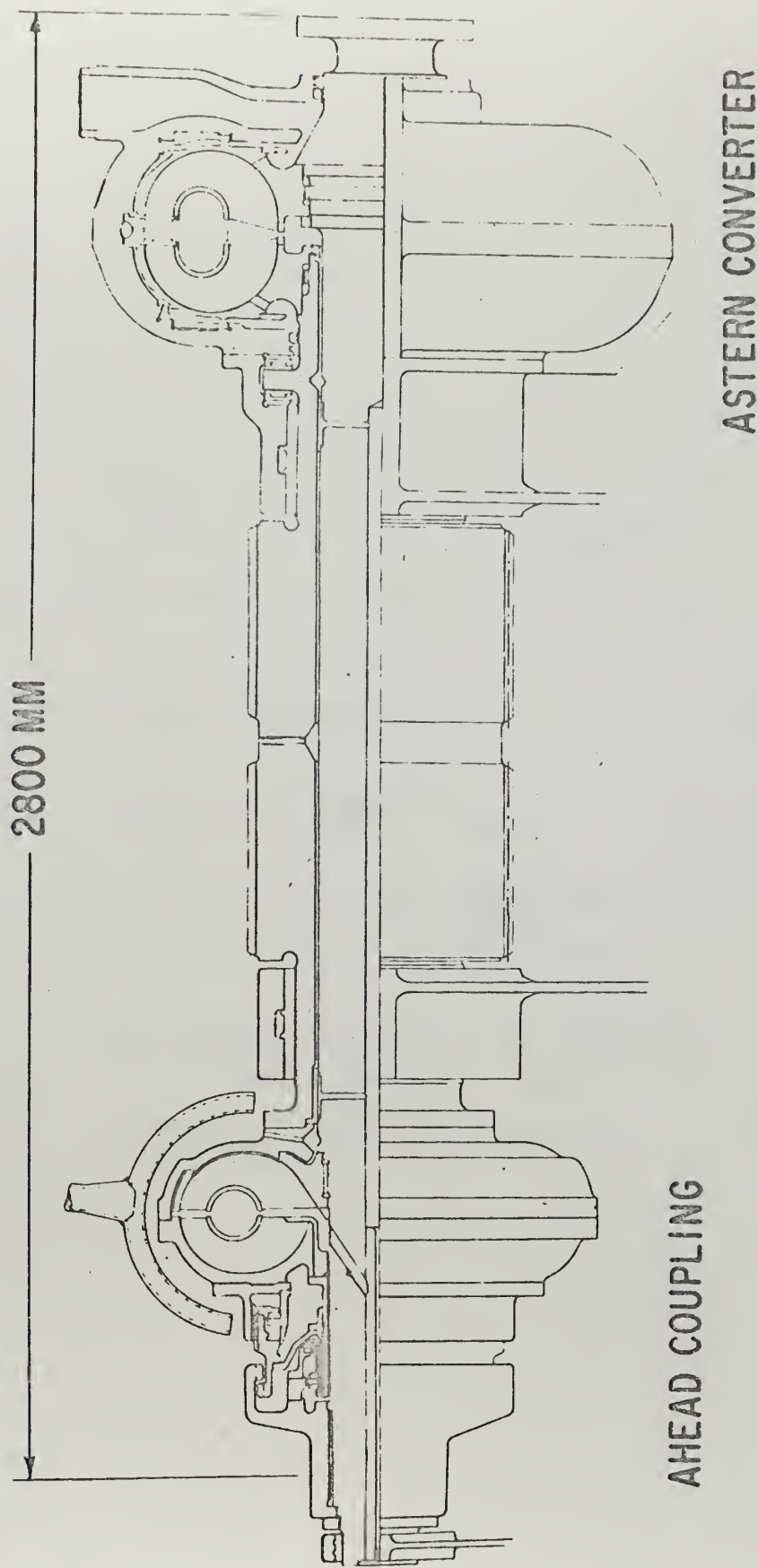
and turbine at idle.(24) Richardson describes a method whereby the Falk clutch can be partially inflated thereby permitting continuous operation or maneuvering at shaft speed below that corresponding to minimum turbine (or diesel) idle.(25) For some applications, however, the heat rate may be prohibitive for continually doing this, and its effect on the life of the clutch is not clear.

In Reference (26), Rowen describes a hydraulic transmission system that permits propeller speeds in the low rpm's with a diesel or gas turbine. The system has a hydraulic reversing gear which incorporates a fluid coupling for ahead rotation of the propeller and a reversing torque converter for astern operation. In addition, a positive drive clutch is included for normal operation in the ahead direction at sea. Figure 3-2 is a cross section of the hydraulic transmission system. The torque characteristics on a "per unit" basis of the two hydraulic elements are presented in figure 3-3.\* Speed ratio, as defined by Rowen, is the ratio of the output speed to the input speed (positive for ahead rotation, negative for astern rotation). He assumed that the hydraulic element efficiencies were constant over the speed ratio range, and defined the output torque by the relation,

$$T_c = Q_{of} \times N_{pm}^2 \times F$$

\* "Per Unit" is defined as the actual value divided by the design point value.

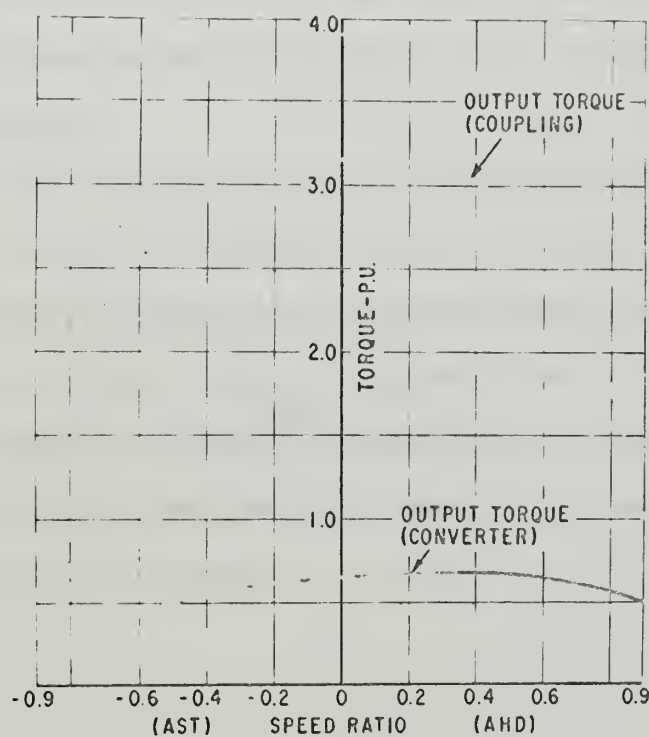




CROSS SECTION OF HYDRAULIC TRANSMISSION SYSTEM

Fig. (3-2)





HYDRAULIC TRANSMISSION TORQUE  
CHARACTERISTICS

Fig. (3-3)



### 3. CLUTCHES AND HYDRODYNAMIC TORQUE CONVERTERS (Cont'd)

#### 3.4 Hydraulic Transmissions (Cont'd)

$T_c$  = converter or coupling output torque

$Q_{of}$  = oil flow to converter or coupling

$N_{pm}$  = input speed of prime mover

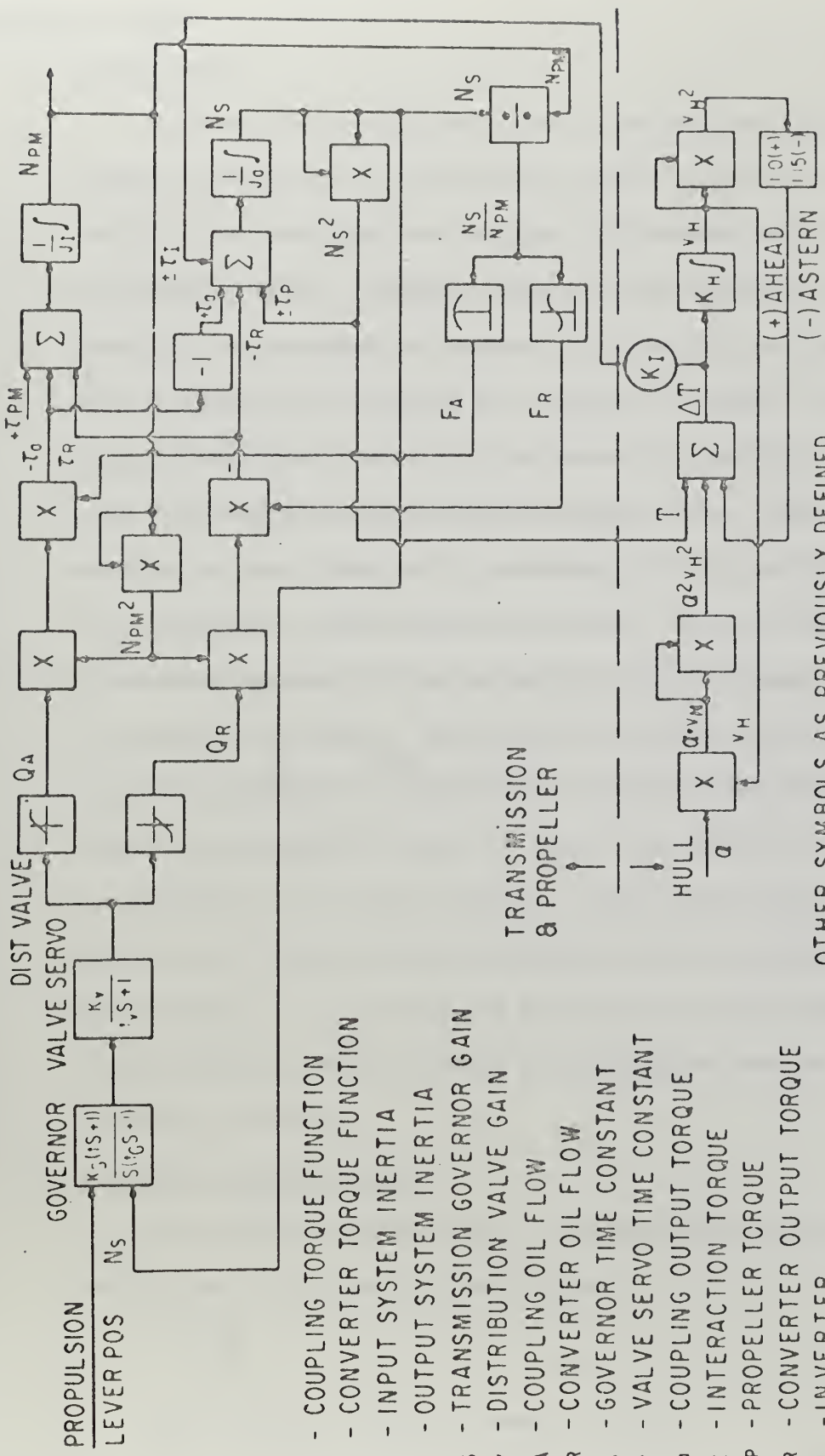
$F$  = a function of the speed ratio (Fig. 3-3)

Figure 3-4 is a block diagram of the hydraulic transmission simulation used by Rowen.<sup>(27)</sup> No numbers were given by him for the various parameters involved in the simulation.

#### 3.5 Discussion

The Falk clutch and the Philadelphia Gear synchroclutch were selected for inclusion in the simulation because of their simplicity and because of their wide spread use in ship propulsion trains. Since no expression for clutch disengagement was provided by Philadelphia Gear, it was assumed that the clutch torque decreased as an exponential decay with a time constant of 5 seconds.





וינכט 31 מילון אס פאל אונדרו גראנדה

## BLOCK DIAGRAM OF HYDRAULIC

TRANSMISSION SIMULATION USED BY ROWEN

Fig. 3.



#### 4. PROPELLER MODELS

##### 4.1 Introduction

The propeller simulation proved to be the most challenging aspect of this study. An excellent study of propellers under conditions of reversing was written by Miniovich and is listed as Reference (28). Miniovich questions the validity of using propeller characteristics measured under equilibrium conditions in the simulation of backing and reversing of ships. To answer this, he performed reversing experiments with models in a towing tank and measured the propeller characteristics. These characteristics were found to be in agreement with those measured in equilibrium or quasi-stationary tests. The only notable discrepancy appeared to lie in the zero thrust region. From his equations of motion, Miniovich also calculated the values of basic variables that characterize the reversing process (e.g., time required to stop the ship, time required to stop the propeller, and maximum values of thrust and torque) and found these to differ from experimental data by a maximum of 10 percent. It thus appears that one can use the steady state propeller characteristics in a simulation and get a reasonable accuracy.

##### 4.2 Propeller Characteristics

The traditional definition of the propeller advance coefficient is the familiar expression,

$$J = \frac{V_A}{ND}$$

$V_A$  = propeller speed of advance (ft/sec)



#### 4. PROPELLER MODELS (Cont'd)

##### 4.2 Propeller Characteristics (Cont'd)

$N$  = propeller rate of rotation (rev/sec)

$D$  = propeller diameter (ft)

This coefficient can be derived from a dimensional analysis for propellers (cf. Reference 29). It is obvious that relating fixed pitch propeller coefficients to  $J$  might prove to be unwieldy for ship propulsion studies since  $J$  becomes unbounded as the shaft goes from positive rotation (providing thrust to move the ship ahead) to negative rotation (providing thrust to move the ship astern). Miniovich solved this dilemma by defining the propeller characteristics in terms of both  $J$  and its inverse, viz.,  $\frac{ND}{V_A}$ . The result is two graphs of propeller characteristics instead of one; when either one of the coefficients tends to large values he changes to the alternate definition.

At the Ninth International Towing Tank Conference (1957), Stephanson demonstrated how the  $J$  and the  $1/J$  propeller characteristics could be combined with a new term, called the modified advance coefficient defined by,

$$J' = \frac{V_A}{(V_A^2 + N^2 D^2)^{1/2}}$$

where all the terms are defined as before. (30) (Miniovich ascribes a similar expression to Kalmakov in 1940). It can be seen that  $J'$  will not become unbounded as  $N$  or  $V_A$  approach zero values.



#### 4. PROPELLER MODELS (Cont'd)

##### 4.2 Propeller Characteristics (Cont'd)

In Reference (31) Baker and Patterson discuss Miniovich's work and present his propeller characteristics using the modified advance coefficient. Other forms of advance coefficients are offered by the two authors to make the task of simulating a propeller easier than as performed by Miniovich.

##### 4.3 Modeling the Wageningen B-Screw Series

In 1969, Van Lammeren, Van Manen, and Oosterveld presented a new technique of reproducing the propeller characteristics of the Wageningen B-Screw Series.(32) The nondimensionalized thrust and torque coefficients are presented in the form of a Fourier series. The series is given as a function of the hydrodynamic pitch angle,  $\beta$ , defined by,

$$\beta = \arctan \left( \frac{V_A}{0.7\pi N D} \right)$$

where  $V_A$ ,  $N$ , and  $D$  are as previously defined. The nondimensionalized thrust coefficient,  $C_T^*$ , and torque coefficient,  $C_Q^*$ , are then given by

$$C_T^* = \sum_{K=0}^M A(K) \cos \beta K + B(K) \sin \beta K$$

$$10 C_Q^* = \sum_{K=0}^M A(K) \cos \beta K + B(K) \sin \beta K$$

Once the coefficients are obtained, thrust,  $T$ , in pounds, and torque,  $Q$ , in ft-lbs can be calculated using,

$$T = C_T^* \left\{ \frac{1}{2} \rho \left[ V_A^2 + (0.7\pi N D)^2 \right] \frac{\pi}{4} D^2 \right\}$$



#### 4. PROPELLER MODELS (Cont'd)

##### 4.3 Modeling the Wageningen B-Screw Series (Cont'd)

$$Q = C_q^* \left\{ \frac{1}{2} \rho [V_A^2 + (0.7 N \pi D)^2] \frac{\pi}{4} D^3 \right\}$$

where

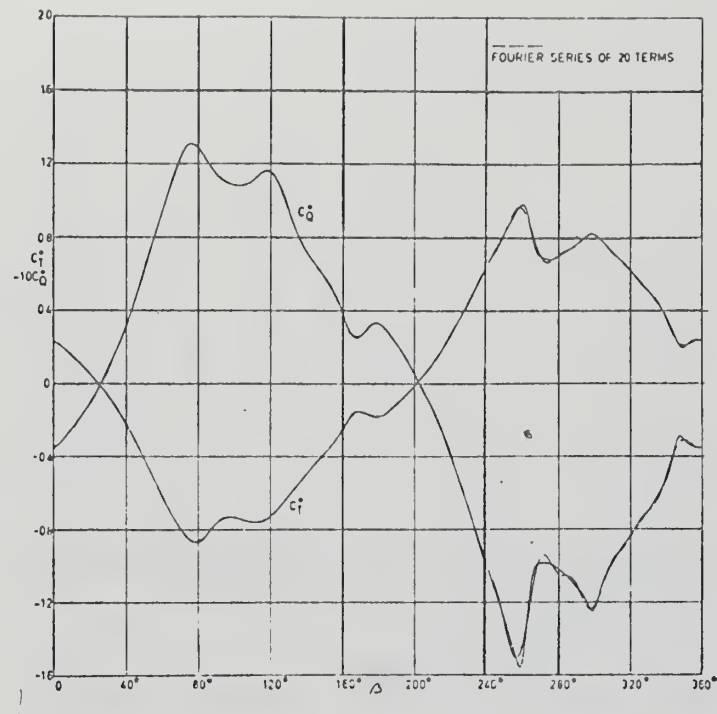
$\rho$  = fluid density

$V_A$ ,  $N$ ,  $D$  as previously defined

The factor "10" in the expression for nondimensionalized torque coefficient apparently through omission, does not appear in two different published versions of Reference (32). Simulations were performed without this factor and resulted in excess propeller torques (10 times that predicted from hand calculations). Figure (40) of Reference (32) was reproduced by the IBM 1130 computer without the factor of 10 in the expression. Examination of Figure (40) revealed that the ordinate is labeled  $C_T^*$  and  $-10 C_q^*$ , the minus sign being introduced to avoid overlapping of curves. It was thus deduced that the expression for  $C_q^*$  should include a factor of 10.

The values of the coefficients  $A(K)$  and  $B(K)$  for a series of 20 terms, i.e.  $K = 1-20$ , are presented in Reference (32). These coefficients are presented for a wide range of B-Screw series. Figure 4-1 illustrates how closely a series of 20 terms matches the measured characteristics of a B 4-70 screw with a pitch ratio of 1.0. Figure 4-2, furthermore, illustrates how well a series of 10 terms approximates the measured characteristics for the same propeller.

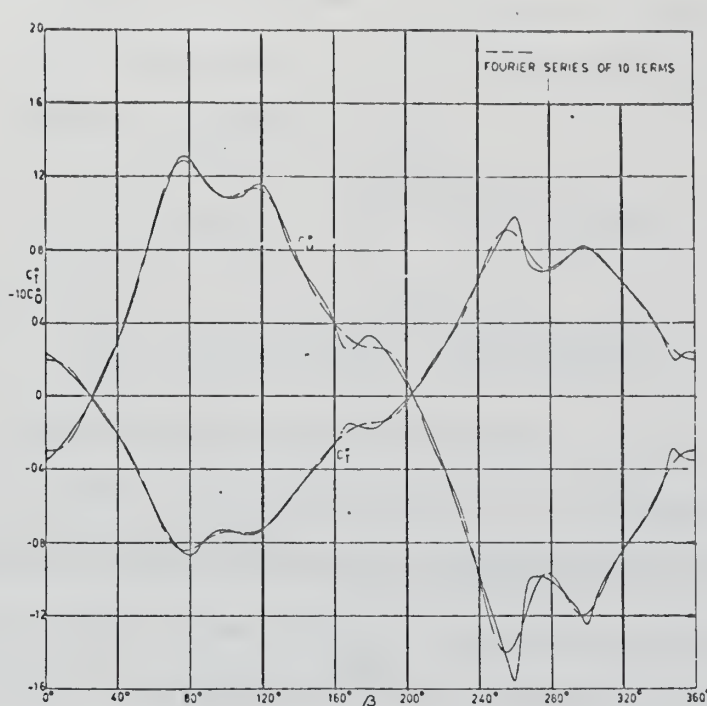




A COMPARISON OF A 20 TERM FOURIER SERIES  
WITH ACTUAL PROPELLER CHARACTERISTICS

Fig. (4-1)





A COMPARISON OF A 10 TERM FOURIER SERIES  
WITH ACTUAL PROPELLER CHARACTERISTICS

Fig. (4-2)



#### 4. PROPELLER MODELS (Cont'd)

##### 4.3 Modeling the Wageningen B-Screw Series (Cont'd)

It was probably noticed that the definition of  $\beta$  does not avert the problems previously associated with the traditional definition of  $J$ , i.e., dividing when  $n=0$ . It would seem more appropriate to use

$$\beta = \arcsine \frac{V_A}{(V_A^2 + (0.7 \pi ND)^2)^{\frac{1}{2}}}$$

or  $\beta = \arccosine \frac{0.7 \pi ND}{(V_A^2 + (0.7 \pi ND)^2)^{\frac{1}{2}}}$

instead of the arctangent definition of  $\beta$ . The IBM scientific subroutine library on the IBM 1130 digital computer that was used did not have subroutines for calculating arccosine or arcsine. The arctangent subroutine had to be used. It should be also noted that the IBM subroutine for arctangent generates values only between  $-\frac{\pi}{2}$  to  $+\frac{\pi}{2}$ . It is the writer's opinion that if a numerical overflow should occur in the argument for the arctangent subroutine, that this subroutine will yield either  $\pi/2$  or  $-\pi/2$  depending on the sign of the overflow. No numerical overflow problems were experienced using the arctangent subroutine.

##### 4.4 Controllable Reversible Pitch Propellers (CRPP)

A simple model of a CRPP was presented by Rowen in Reference (26). The "per unit" equation for thrust is given by

$$\text{Thrust} = (\text{pitch} \times \text{rpm})^2$$



#### 4. PROPELLER MODELS (Cont'd)

##### 4.4 Controllable Reversible Pitch Propellers (CRPP) (Cont'd)

and the "per unit" equation for torque is given by

$$\text{Torque} = [0.3 \times (\text{rpm})^2] + [0.7 + (\text{rpm})^2 \times (\text{pitch})^3]$$

In Reference (33), Read presents a study of gas turbines driving a CRPP, and includes the torque and thrust characteristics for the propeller. Apart from the characteristics, all that is known about the propeller is that it has 4 blades and has a polar moment of inertia of 7050 lb-ft-sec<sup>2</sup>. Wendel and Dunne apparently found a small error in the values of modified torque coefficient given by Read and applied a correction to the torque characteristic.(34) The modified advance coefficient,  $J'$ , is as previously defined, viz.,

$$J' = \frac{V_A}{(V_A^2 + N^2 D^2)^{\frac{1}{2}}}$$

The modified thrust coefficient is defined by

$$K_T' = \rho \frac{T}{D^2 (V_A^2 + N^2 D^2)}$$

and the modified torque coefficient is defined by

$$K_Q' = \rho \frac{Q}{D^3 (V_A^2 + N^2 D^2)}$$

where  $T$  = thrust in lbs

$Q$  = torque ft-lbs

$\rho$ ,  $V_A$ ,  $N$ ,  $D$  are as previously defined

(Note the absence of  $\pi$  in the denominator in the expressions for  $K_T'$  and  $K_Q'$ ;  $\pi$  is included in the similar expressions



#### 4. PROPELLER MODELS (Cont'd)

##### 4.4 Controllable Reversible Pitch Propellers (CRPP) (Cont'd)

given by Van Lammeren. Baker and Patterson discuss the "W" question in Reference (31)).

Figures (4-3) and (4-4) are the CRPP characteristics, and include the Wendel-Dunne correction.

##### 4.5 Pitch Control System Model

The only analytical description of a CRPP pitch control system found was that described by Read in Reference (33).

Pitch,  $R$ , and angular rotation,  $\theta$ , are related by the expression

$$R = \frac{\tan \theta}{0.455}$$

The pitch-changing cylinder has a total capacity of 40 gallons, and the blade angle varies very nearly linearly with ram stroke, such that

$$\frac{d\theta}{dt} = \frac{55}{57.3} \times \frac{F_0}{48} \quad (\text{Rad/sec})$$

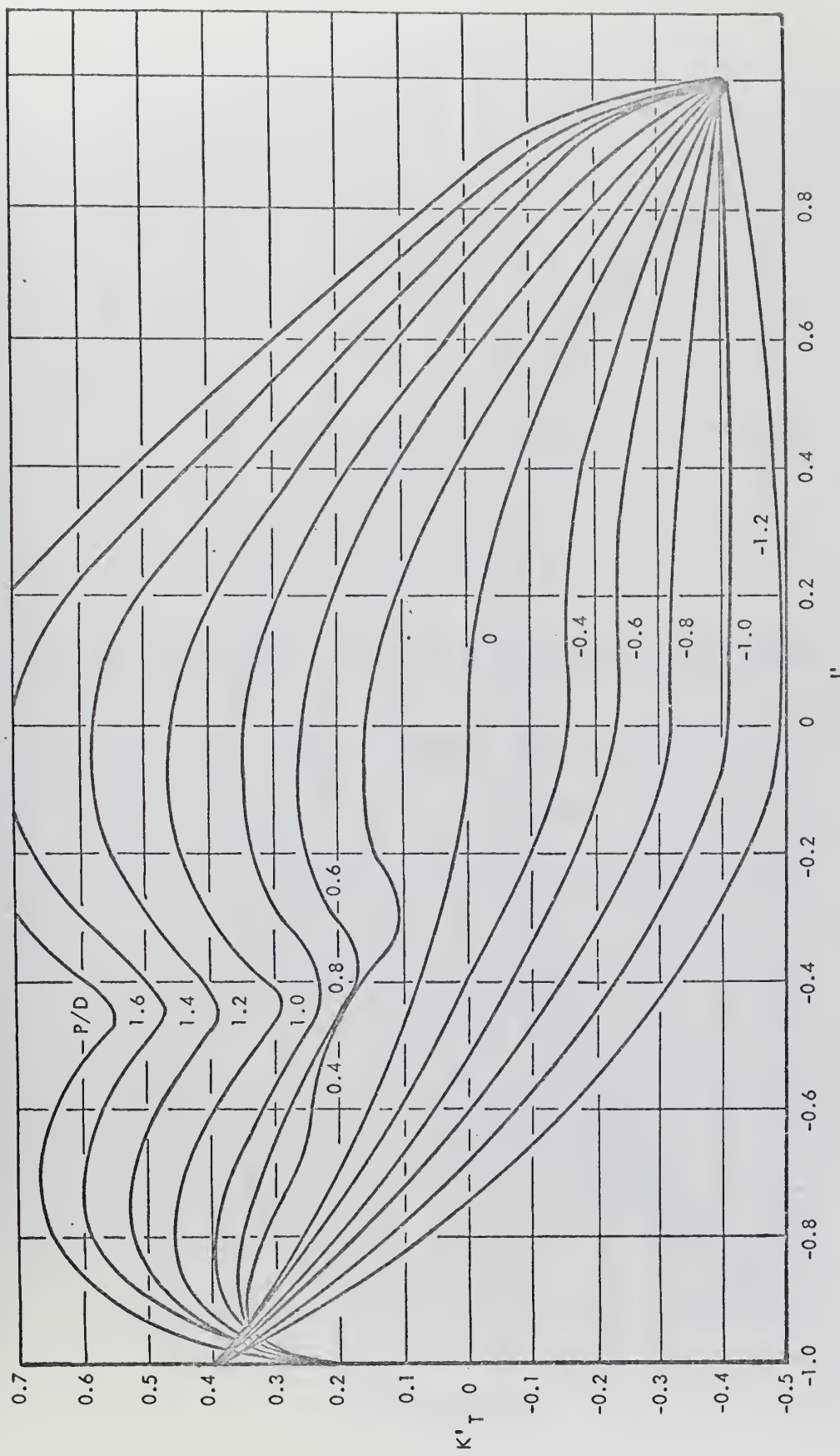
$F_0$  = oil flow in gal/sec

By manipulating the two equations, one can arrive at the expression

$$\frac{dR}{dt} = \pm 0.0528 + 0.0109 R^2 F_0$$

There are two pumps supplying the oil flow,  $F_0$ . One is motor driven and the other is shaft driven. The motor driven pump has a maximum capacity of 60 gal/min and the shaft driven pump has a maximum capacity of 100 gal/min. The pumps are pressure controlled such that any alteration in pitch demand causes the motor-driven pump to provide 60

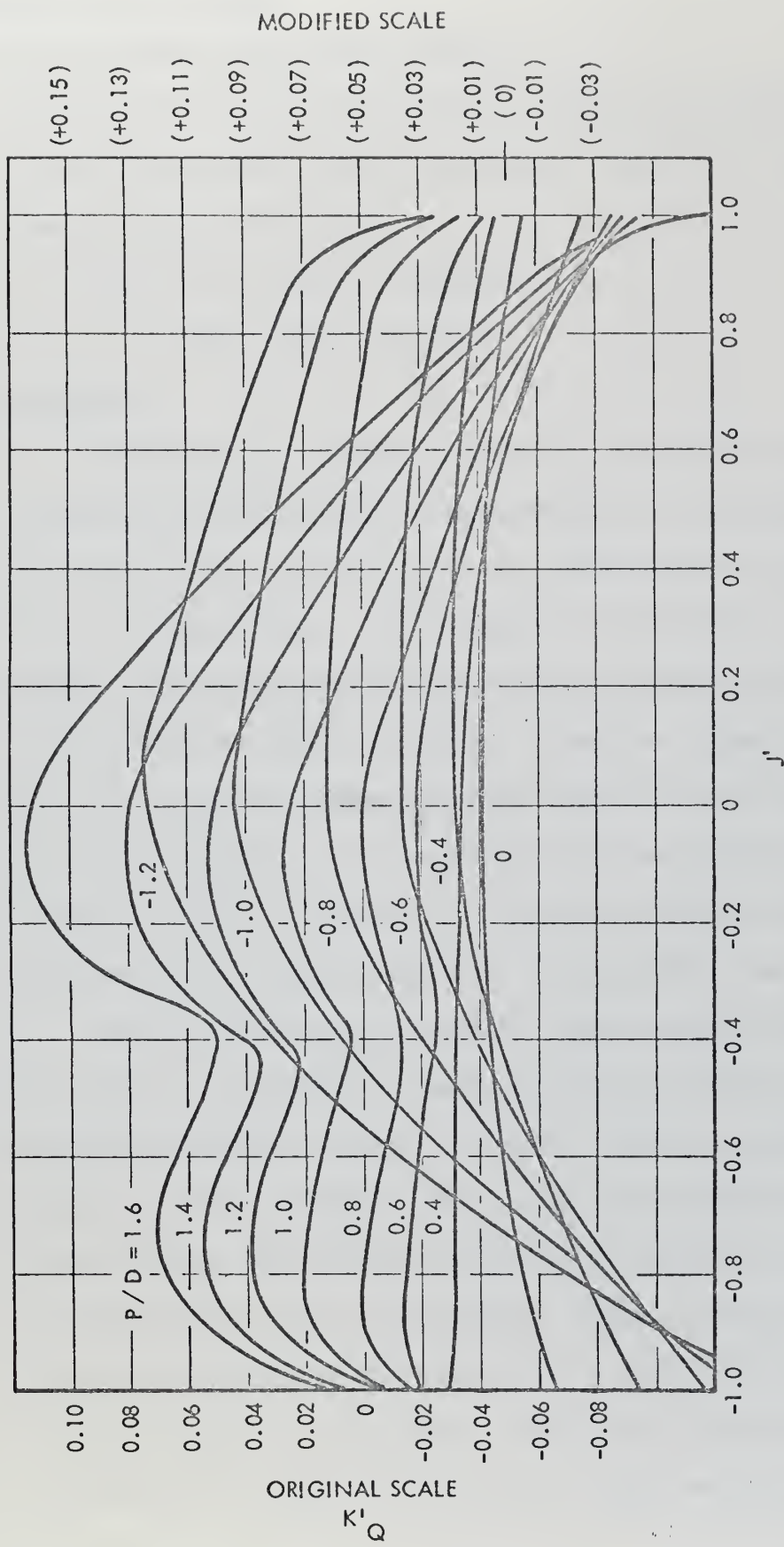




CRPP: THRUST COEFFICIENT VS. ADVANCE COEFFICIENT

Fig. (4-3)





CRAPP: TORQUE COEFFICIENT VS. ADVANCE COEFFICIENT  
FIG. (4-14)



#### 4. PROPELLER MODELS (Cont'd)

##### 4.5 Pitch Control System Model (Cont'd)

gal/min and the shaft-driven pump to provide its maximum output at the shaft speed in question. The result is that during a pitch alteration,

$$F_0 = (1 + 0.435 N) \text{ (gal/sec)}$$

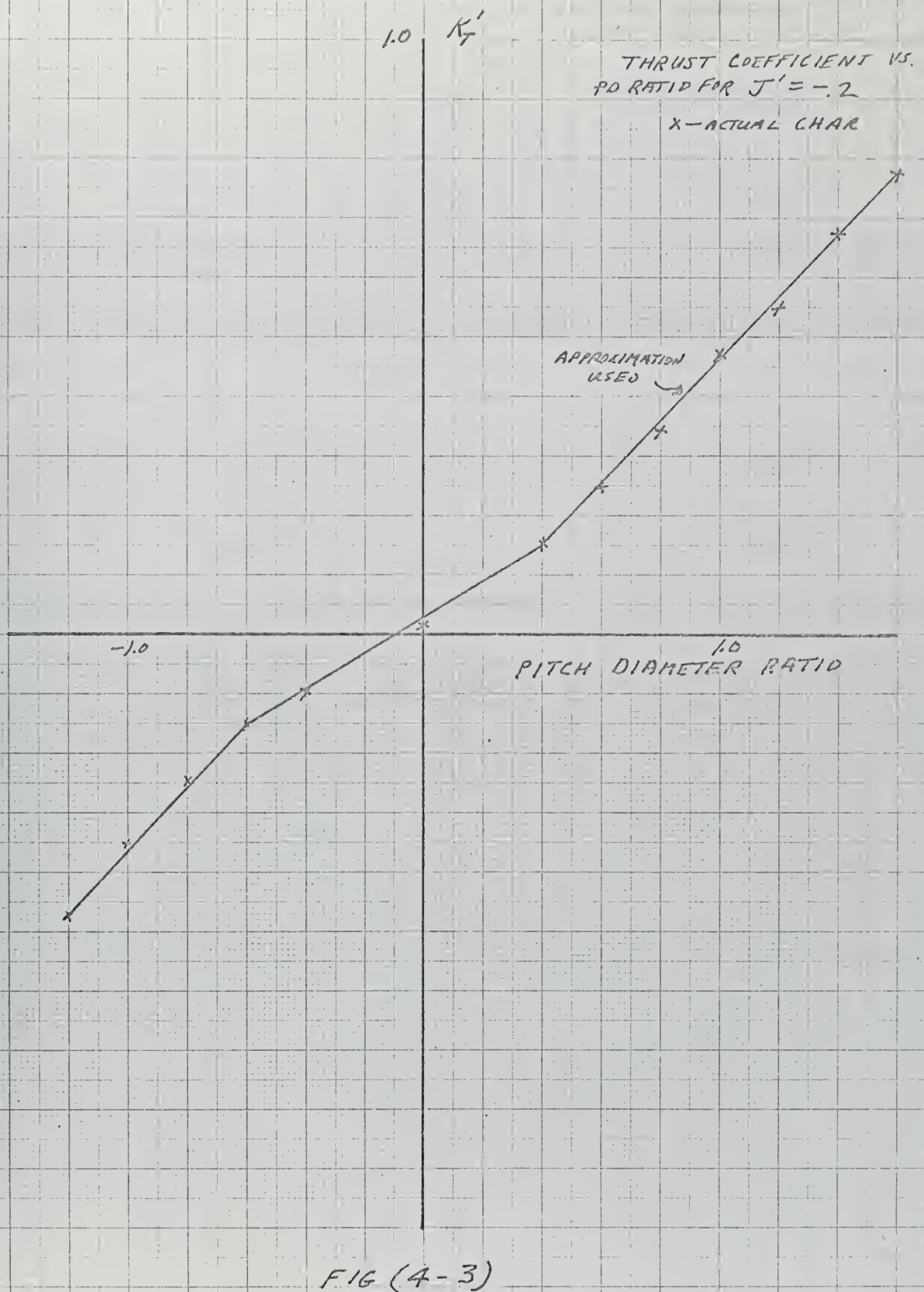
N = shaft speed (rev/sec)

##### 4.6 Discussion

The fixed pitch propeller model selected was the Fourier representation of propeller characteristics as presented in Reference (32). Only the first ten coefficients were used in the representation. The resistance characteristics of the vessel, and the propeller diameter are two important factors in selecting the proper propeller. Since the characteristics for the B-4 series with an expanded area ratio of .7 were readily available, it was decided to use this type of propeller. A plot of  $K_T/J^2$  indicated a pitch-diameter ratio of 1.0 would give the maximum efficiency; hence this propeller was chosen.

Read's controllable reversible pitch propeller (CRPP) was chosen. The propeller characteristics as modified in Reference (34) were redrawn for constant values of modified advanced coefficient ( $J'$ ). The independent variable was taken as pitch diameter (PD) ratio and the dependent variables were thrust and torque coefficients. Figure (4-3) shows the thrust coefficient vs. PD ratio for  $J' = -0.2$ . This curve is fairly typical of the others. The linear approximations are indicated. Figure (4-4) shows the torque coefficients







TORQUE COEFFICIENT VS. PD  
RATIO FOR  $J' = -.2$

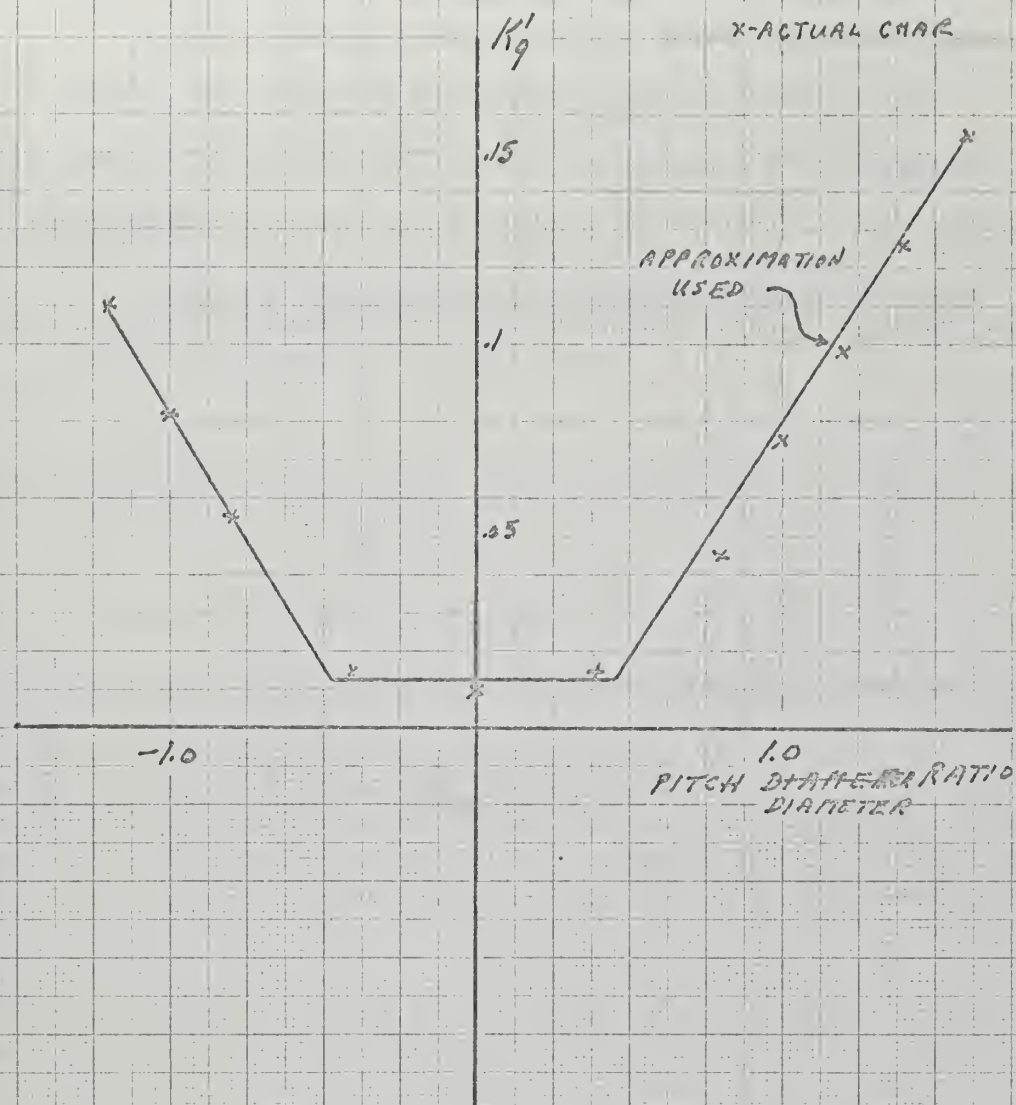


FIGURE (4-4)



#### 4. PROPELLER MODELS (Cont'd)

##### 4.6 Discussion (Cont'd)

vs PD ratio for  $J' = -0.2$  with the linear approximations used. This curve is also fairly typical of the other curves of torque coefficients for constant  $J'$  and varying PD ratio.

Read's pumping system as described earlier was also used in conjunction with the CRPP.



## 5. SHIP CHARACTERISTICS

### 5.1 Wake Fraction and Thrust Deduction Factor

Wake fraction,  $w$ , determines the velocity the propeller is advancing at in relation to the ship velocity,

$$V_A = (1-w) V$$

$V_A$  = propeller speed of advance

$V$  = ship speed

$w$  = wake fraction

Thrust deduction factor,  $t$ , indicates how much propeller thrust is reduced due to hull interaction,

$$T_l = T_{ow} (1-t)$$

$T_{ow}$  = open water propeller thrust

$T_l$  = actual thrust

$t$  = thrust deduction factor

(For a physical explanation of " $t$ " and " $w$ ", and other useful relationships involving these two terms, see Reference (29), Chapter VII, Section 13).

The implication in the two above definitions is that they are steady state quantities. Thus at equilibrium, the actual thrust equals ship resistance. Since  $t \ll 1$ ., the definition shows how much more thrust is required over resistance to keep ship speed constant.

Wake fraction and thrust deduction factor are not, as one would expect, constant over a range of speed. The variation in  $t$  and  $w$  depend on the degree of interaction between propeller and hull. Harvald performed several towing tank tests to



## 5. SHIP CHARACTERISTICS (Cont'd)

### 5.1 Wake Fraction and Thrust Deduction Factor (Cont'd)

measure "t" and "w" under transient conditions for two different hull shapes.(35) He performed his towing tank tests under conditions of constant model ship velocity and varying shaft rpm and vice versa. Although his work provided good insight into the behavior of "t" and "w" under these two conditions, it was difficult to assess how his results could be applied for conditions of varying shaft rpm and ship velocity. How did others treat this phenomena? In the solution of his backing equations, Miniovich assumed both factors to be equal to zero.(36) Rubis assumed varying values of "t" and "w" from two curves of bell shaped form.(37) Read considered wake fraction to be negligible, but formulated linear relations for thrust deduction factor for positive and negative values of propeller thrust.(38). Lewis, Lecount, and Scoville assumed thrust deduction factor and wake fraction to be a function of vessel speed only; for negative speeds thrust deductions and wake fractions were neglected.(39) Thus, it can be seen that there is no general agreement on the treatment of these two factors. The feeling appears to be that these two factors are so small that any errors in their treatment will have negligible effects on the total simulation. For simulations performed here, constant values of wake fraction ( $w=0.04$ ) and thrust deduction factor ( $t=0.02$ ) were assumed.



## 5. SHIP CHARACTERISTICS (Cont'd)

### 5.2 Added Mass of Ship and Propeller

As with thrust deduction and wake fraction, the treatment of added mass of ship and propeller is also varied. The added mass of the ship is usually taken to be between 8-10% of the displacement. This study used 10%. Lewis, Lecount, and Scoville used a different approach to account for added mass as will be discussed later. The added mass of a fixed pitch propeller is usually assumed to be about 25% of the inertia. (cf., e.g., Reference (40)) Twenty-five percent was assumed here. There is nothing fixed about this figure as Burrill and Robinson found the percentage addition should be as high as 46% for one particular propeller. (41)

For his CRPP, Read proposed in Reference (33) the expression,

$$I = 325 + 1050 / R$$

I = added mass due to entrained water ( $lb \cdot ft \cdot sec^2$ )

R = pitch diameter ratio

This expression was used in the simulation with the B & W 7K98FF low speed diesel - CRPP combination.

### 5.3 Ship Resistance

Accurate representation of ship resistance is, of course, vital to the proper selection of propeller(s). One of the basic assumptions of the popular "Propeller Law" (cf. References (14) & (15) ) is that resistance is proportional to the square of velocity for ships where the wave drag is small. For those cases where it is desired to simulate transients on a particular ship, it is, of course, more accurate to use that



## 5. SHIP CHARACTERISTICS (Cont'd)

### 5.3 Ship Resistance (Cont'd)

vessel's characteristics as determined from towing tank tests.

Lewis, LeCount, and Scoville included acceleration effects in their expression for ship resistance,

$$R_H = R_{ss} + C_{AD} M \frac{dv_s}{dt}$$

M = mass of ship

$v_s$  = ship speed

$R_{ss} = R_{ss} (v_s)$  = steady-state resistance

$C_{AD}$  = "added mass" coefficient

No values for  $C_{AD}$  were provided by the authors.

For simulations performed here, resistance was assumed to be of the form,

$$R = 104.8 v^2 \quad (\text{lbs})$$

v = ship velocity (ft/sec)

### 5.4 Shaft Friction

Read used the expression

$$Q_f = 2890 N^{1.23} \quad (\text{ft-lb})$$

N = propeller speed (assumed to be rev/sec)

to represent shaft friction.(33) Rubis, on the other hand, represented shaft friction characteristics in the form of a "table-look-up" in his computer simulations. These characteristics were approximated in simulations performed here by the expressions

$$Q_f = 2500 \text{ (ft-lb)} \quad 0 \leq N \leq 25$$

$$Q_f = 100/N \quad (\text{ft-lb}) \quad N > 25$$

N = propeller shaft rpm



## 6. RESULTS

### 6.1 Introduction

The following maneuvers were performed with the drive trains as indicated:

FT<sup>4</sup>A-2 Gas Turbine - Fixed pitch propeller

1. Coastdown from 30 knots
2. Accelerating from 5 knots
3. Crashback from 30 knots

LJ2500-A Gas Turbine - controllable reversible pitch propeller

1. Accelerating from 15 knots
2. Crashback from 30 knots

Mirrless KV Major 12 - Fixed Pitch propeller

1. Crashback from 9 knots

Burmeister & Wain 7K98FF - Controllable reversible pitch propeller

1. Crashback from 12 knots

### 6.2 Coastdown from 30 knots (FT<sup>4</sup>A-2)

At zero time, fuel rate was decreased from 9500 lb/hr to 1600 lb/hr exponentially with a 1-second time constant.

Results of this simulation are presented in figures (6-1) - (6-4).

### 6.3 Accelerating from 5 knots (FT<sup>4</sup>A-2)

At zero time, fuel rate was increased exponentially with a 1-second time constant from 2500 LB/hr to 12000 LB/hr.

Figures (6-5) - (6-11) are plots of the results. A copy of the computer program used is included in Appendix F.



## 6. RESULTS (Cont'd)

### 6.4 Crashback from 30 knots (FT4A-2)

This maneuver was accomplished in three phases:

1. Coastdown\* - opening clutch
2. engaging reverse clutch
3. stopping the ship

Results of this simulation are plotted in figures (6-12) - (6-17). Time for forward clutch disengagement was 4.8 seconds. The reverse clutch was engaged at 11.2 seconds and the ship stopping time was 43.4 seconds. Head reach was 1229 ft. A copy of the computer program used in phase 3 is included in Appendix F.

### 6.5 Accelerating from 15 knots (LM2500-A)

A description of the control strategy and the controller used is in Appendix G. Initially the ship is at 15 knots with a pitch ratio of 1.0 on the CRPP. Pitch was increased to 1.6 in 8 seconds. At that instant the controller acted to increase shaft rpm to 216. Results of this simulation are shown in figures (6-18) - (6-20).

### 6.6 Crashback from 30 knots (LM2500-A)

The problem to consider here was whether or not the power turbine would overspeed while the CRPP goes through a zero value of torque coefficient. This ship is initially at a speed of about 30 knots with full pitch ratio (1.6). The

\*Coastdown as used hereafter implies setting fuel rate to idle.



## 6. RESULTS (Cont'd)

### 6.6 Crashback from 30 knots (LM2500-A) (Cont'd)

first simulation that was tried used the following sequence of events:

- a. reduce fuel to idle
- b. decrease pitch to -1.2
- c. increase fuel to 9900 lb/hr

In performing this simulation, it was observed that the pitch changing operation took a rather lengthy time. The end result would have been a time to stop in excess of 60 seconds. The simulation was stopped and a new sequence of events was attempted,

- a. simultaneously decrease fuel to idle and decrease pitch
- b. when pitch equals -.8, increase fuel to 9900

Using this sequence of events, a stopping time of 44.3 seconds resulted. Results of this simulation are plotted in figures (6-21) - (6-24). A copy of the computer program used in sequence (a) is included in Appendix G.

### 6.7 Crashback from 9 knots (KV Major 12)

The same sequence of events described in section 6.4 were used here, viz.,

1. coastdown - opening clutch
2. engaging reverse clutch
3. stopping the ship

Forward clutch disengagement occurred at 11 seconds, and 6.2 seconds later, the reverse clutch engaged. The ship



## 6. RESULTS (Cont'd)

### 6.7 Crashback from 9 knots (KV Major 12) (Cont'd)

was stopped in 95.2 seconds with a head reach of 1208.7 feet.

Results of this computer simulation are plotted in figures (6-25) - (6-27). Copies of the programs used in all three sequences are included in Appendix H.

### 6.8 Crashback from 12 knots (B & W 7K98FF)

This simulation successfully illustrated the increase in prime mover speed as the CRPP went through a zero torque coefficient region. The sequence of events employed here were:

1. simultaneously decrease fuel to idle and pitch ratio
2. when pitch ratio equaled -.2, increase fuel to stop the ship

The initial simulation started from a pitch ratio of 1.0 and decreased pitch to -.1.2. At this pitch ratio, the propeller torques were so high that the equivalent of diesel stalling occurred. The change in pitch ratio was modified to go from +1. to -1. This proved to be satisfactory. The time of pitch change was 34.5 seconds. Ship stopping time was 90.5 seconds with a head reach 629.8 ft. The results of this simulation are plotted in figures (6-28) - (6-31). A copy of the program used in sequence (2) is included in Appendix I.



COAST DOWN FROM 31.6 KTS (FIG 6-2)

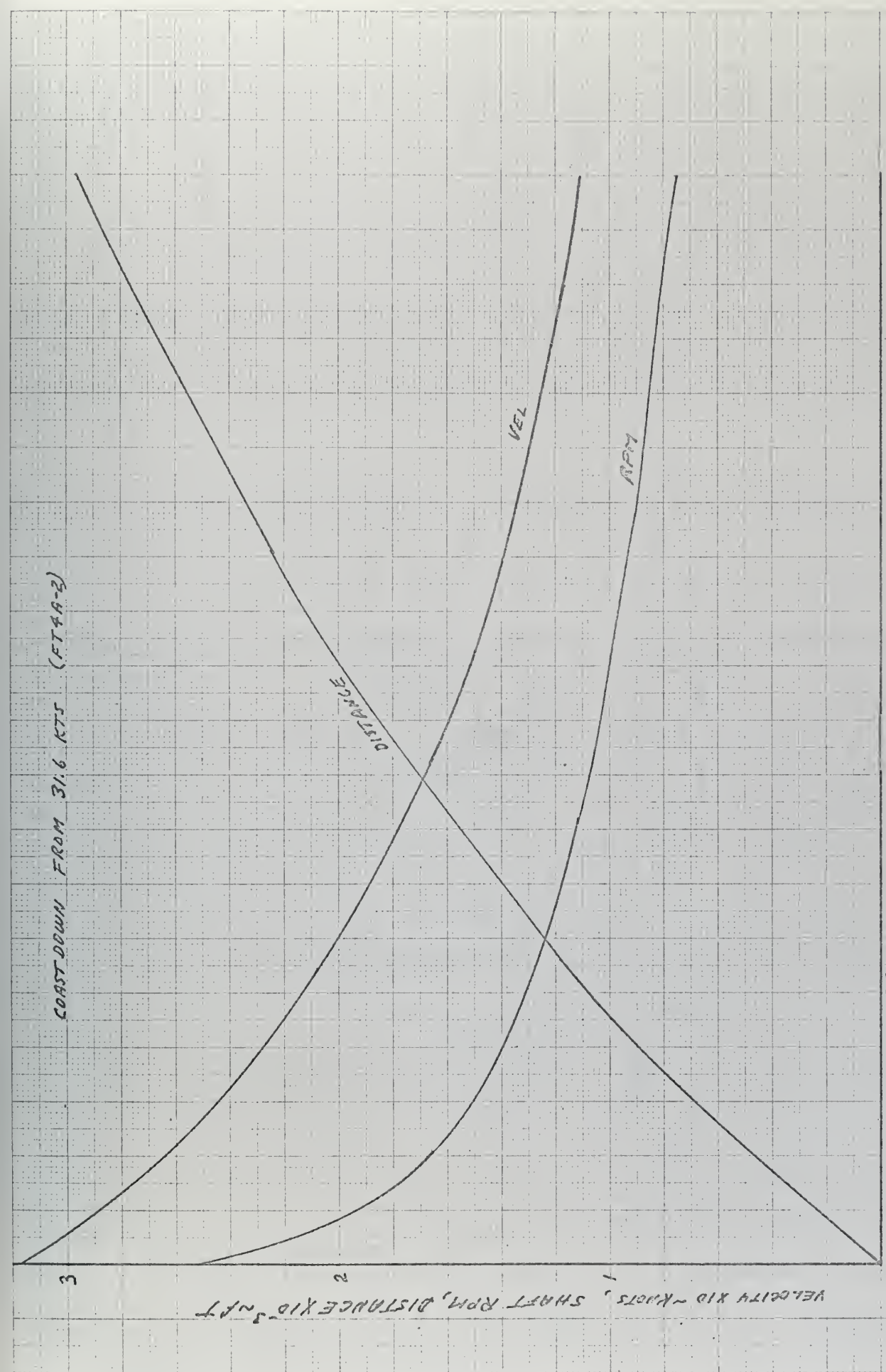
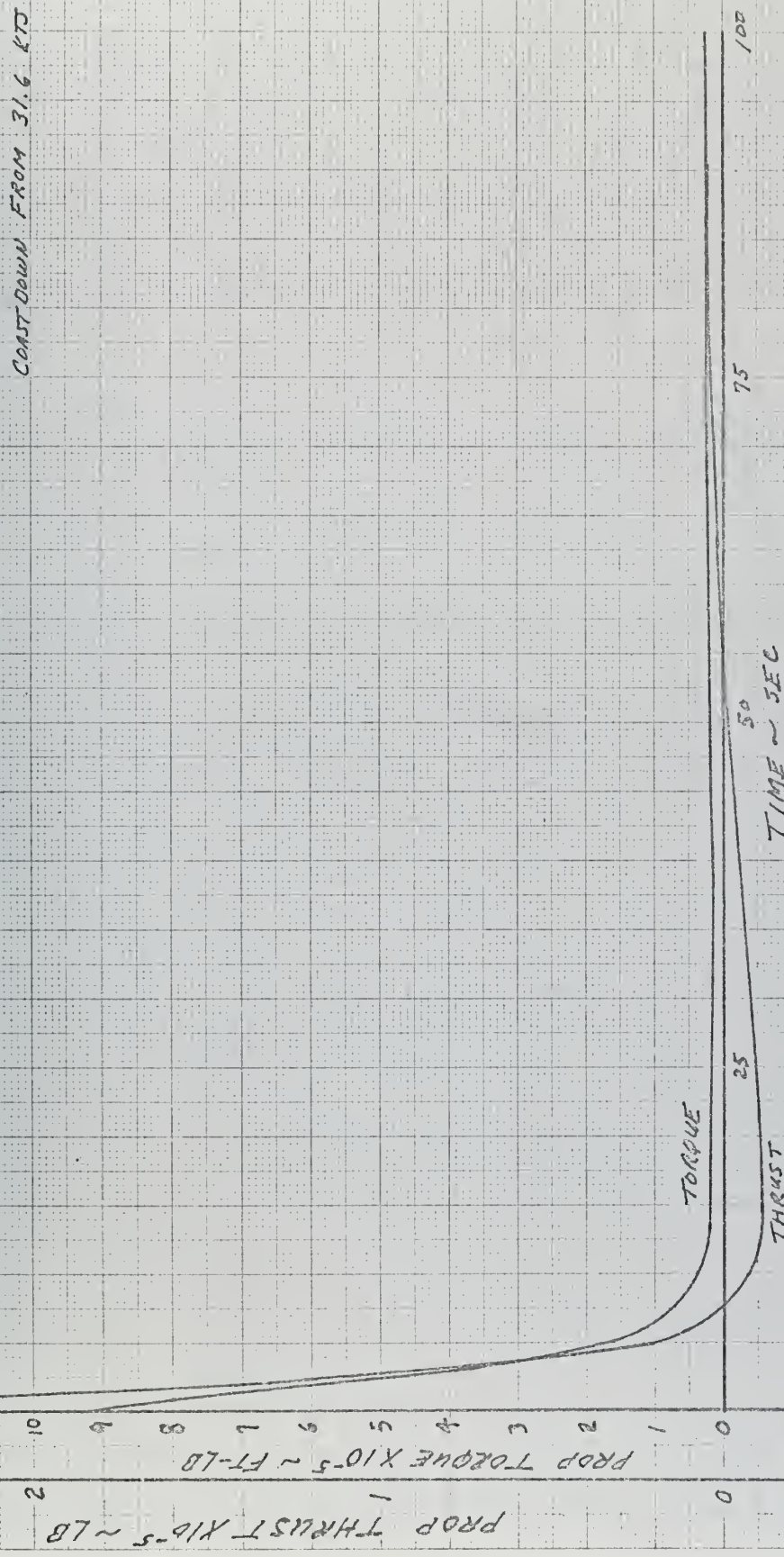
25 50 75 100  
TIME-SEC

FIG (6-2)



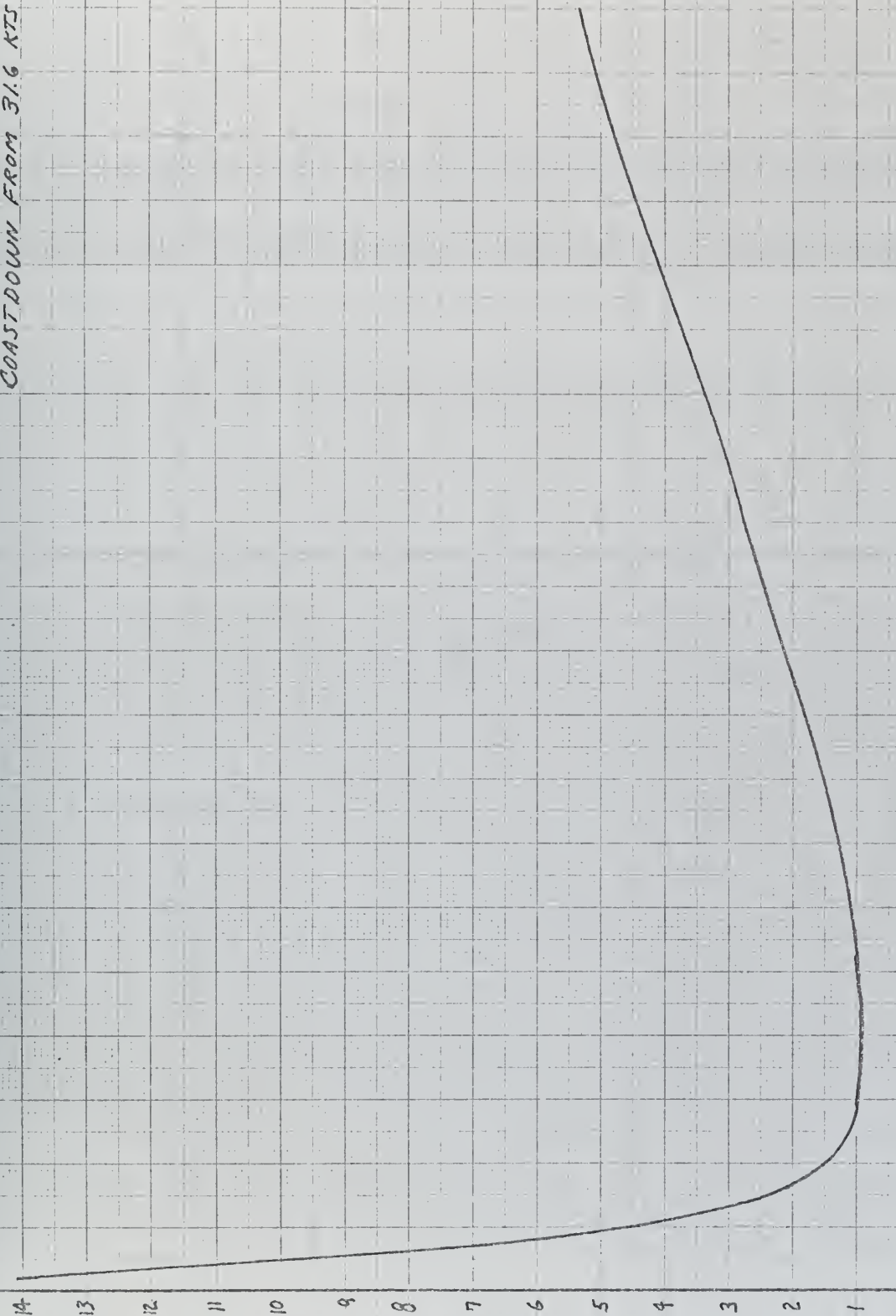
COUNTDOWN FROM 31.6 KTO (FTAG-2)



F16 (6-2)



COASTDOWN FROM 31.6 KTS (FTMA-2)



PROP. TORQUE COEFFICIENT X 10<sup>4</sup>

TIME - SEC

FIG (6-3)

25

15

100

54



COASTDOWN FROM 31.6 KTS (FT44-2)

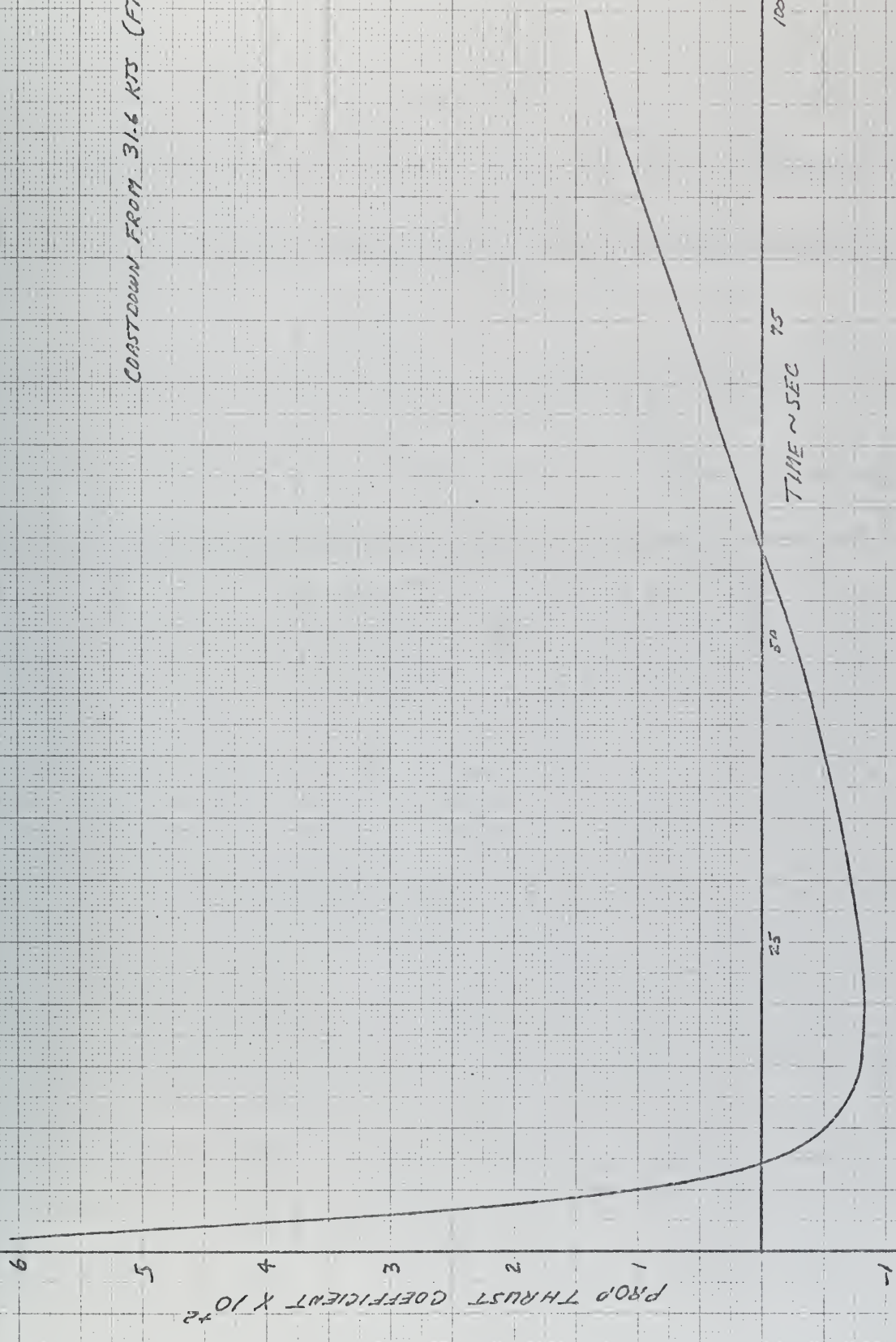


FIG. (6-4)



ACCELERATING FROM 5 KILO (FT4A-2)

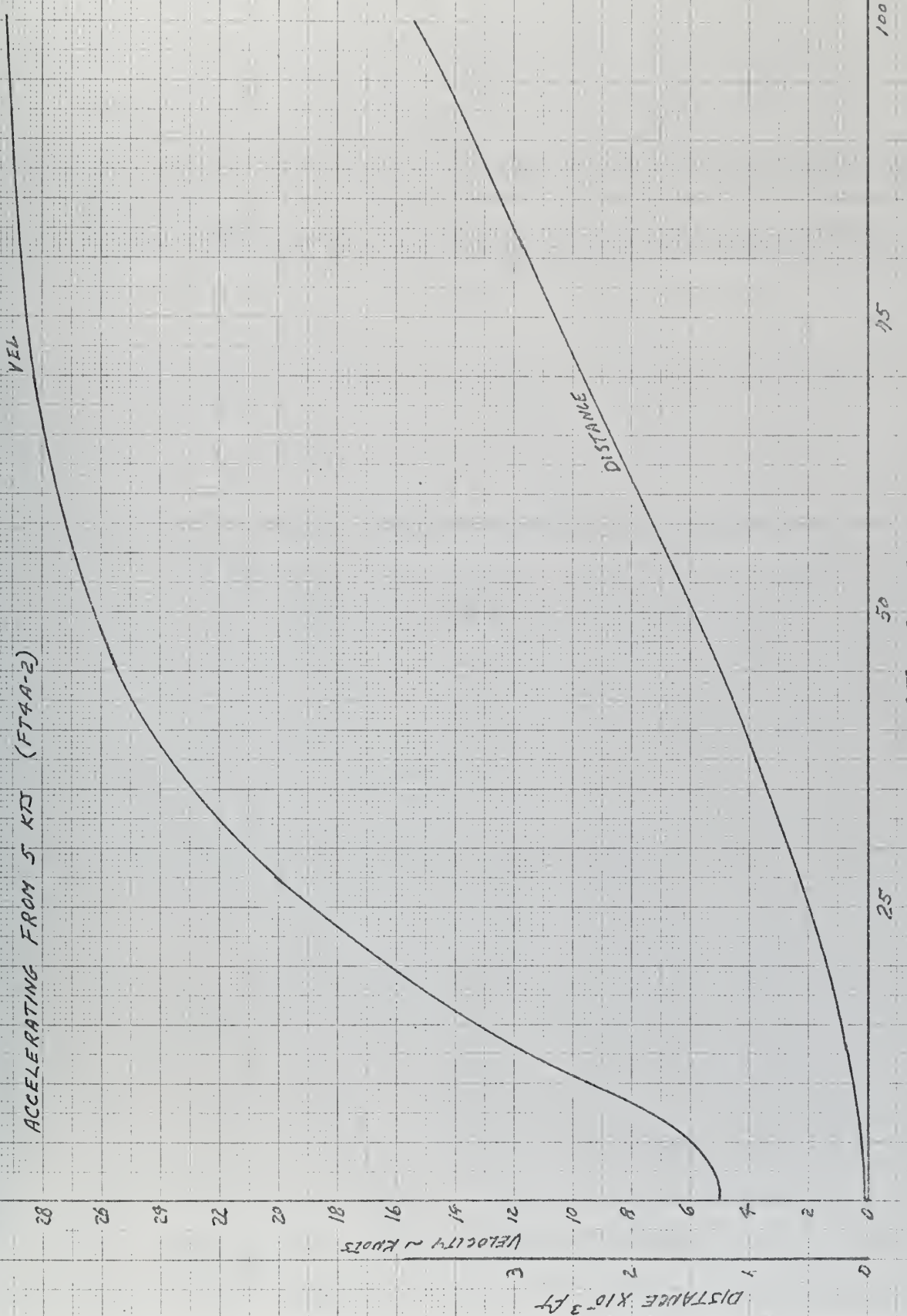


FIG (6-5)



## ACCELERATING FROM 5 KTS (FT-A-2)

POWER TURBINE TORQUE  $\times 10^{-4}$  FT-LBS

5 4 3 2

4

3

2

1

25

50

75

100

TIME SEC  
FIG (6-6)



ACCELERATING FROM 5 KTS. (FIG. 2)

PROP. THRU<sub>5</sub>  $\sim 587 \times 10^{-5}$ TIME  $\sim$  SEC

FIG. (6-7)

100

75

50

25

0

100

75

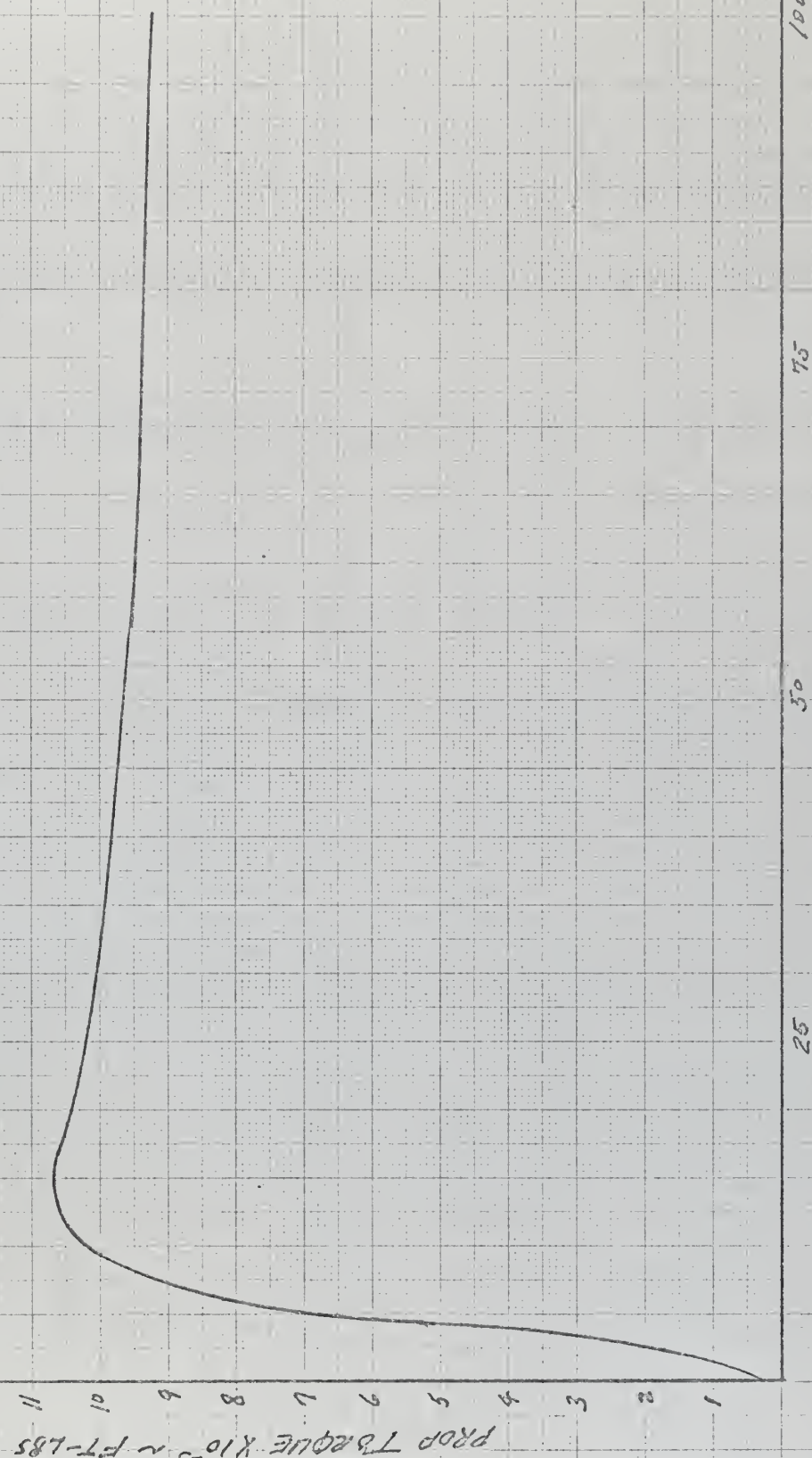
50

25

0



## ACCELERATING FROM 5 KTS (FIG 8-2)





150

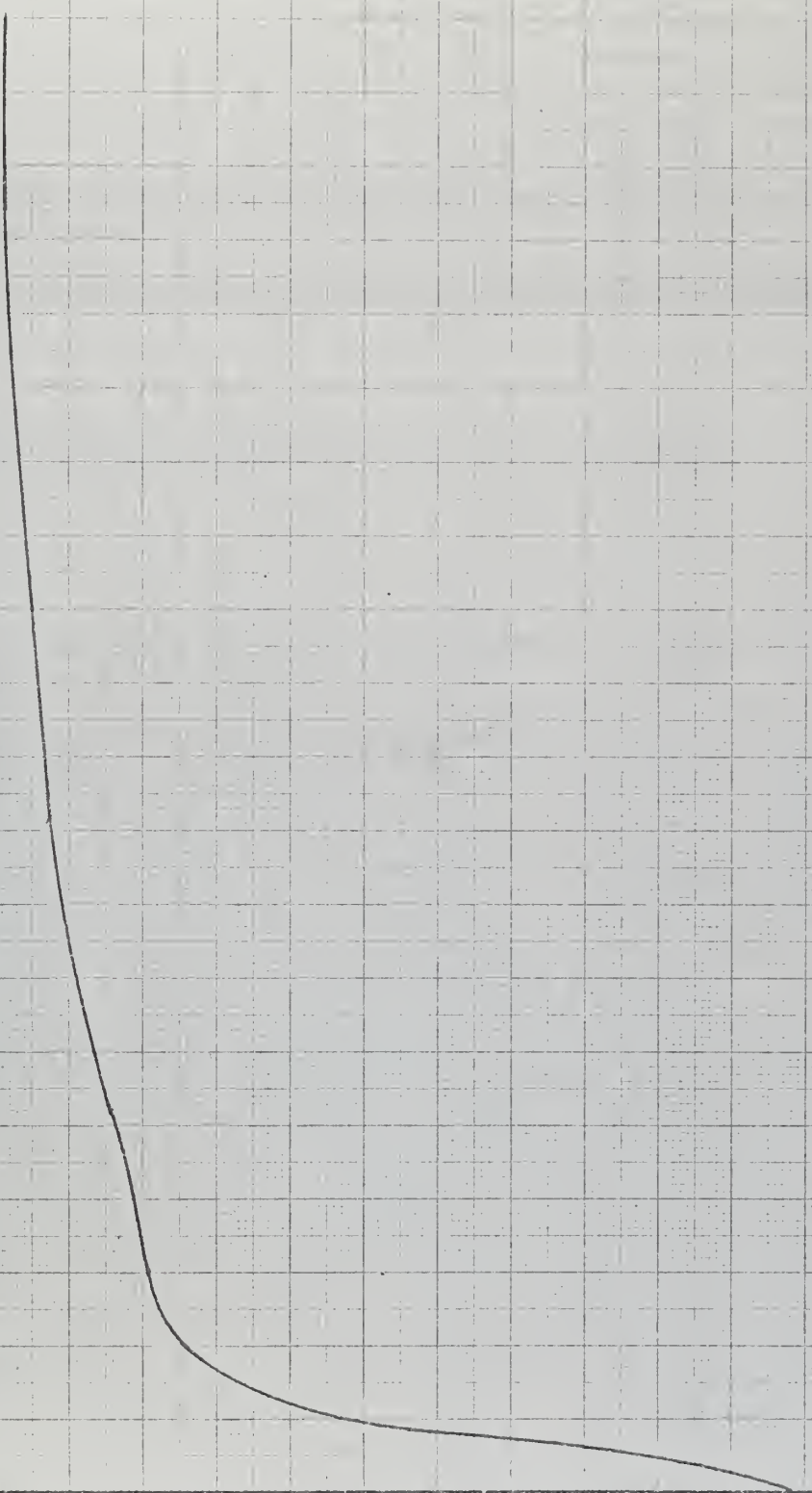
75

50

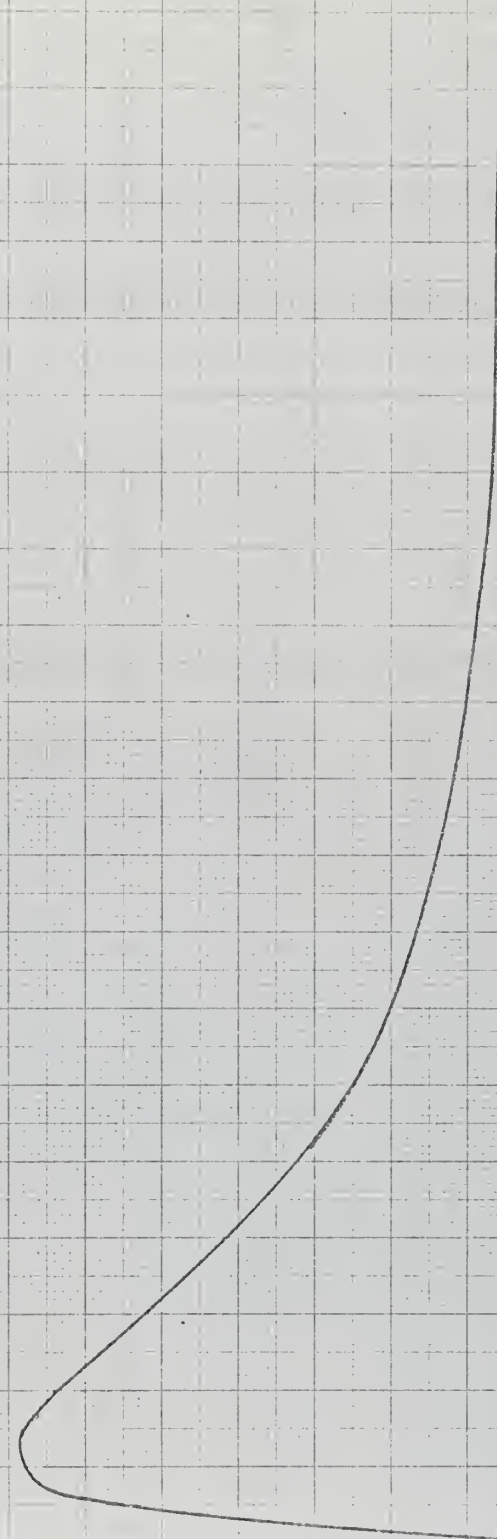
25

TIME ~ SEC  
F1G (6-9)

SHAI-T RPM







PROOF THRUUS T COEFFICIENT X10



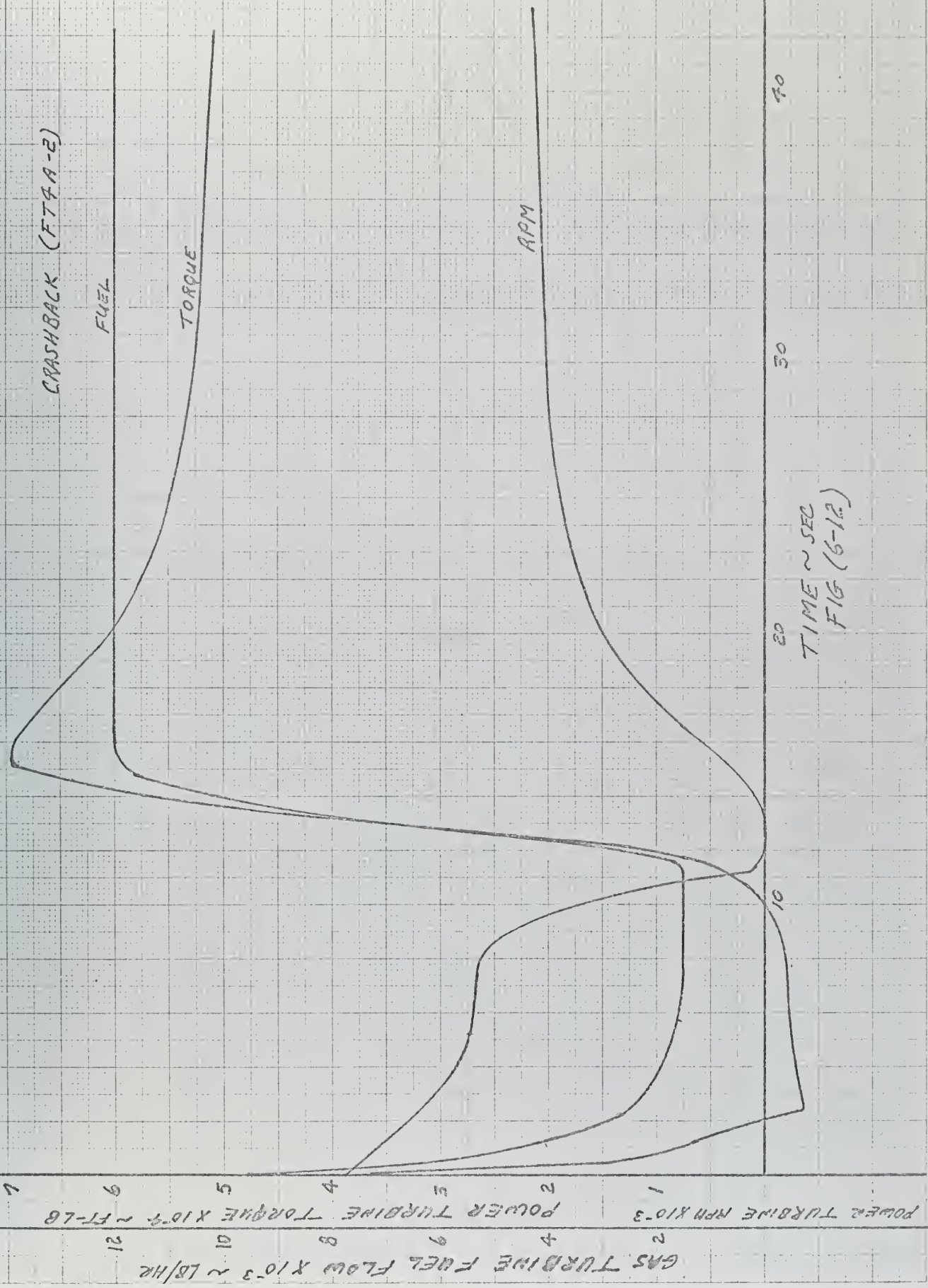
60

56

25

TIME ~ SEC  
F16 (6-1)PROP TORQUE COEFFICIENT  $\times 10^2$ 







CRASH BACK (FT4A-2)

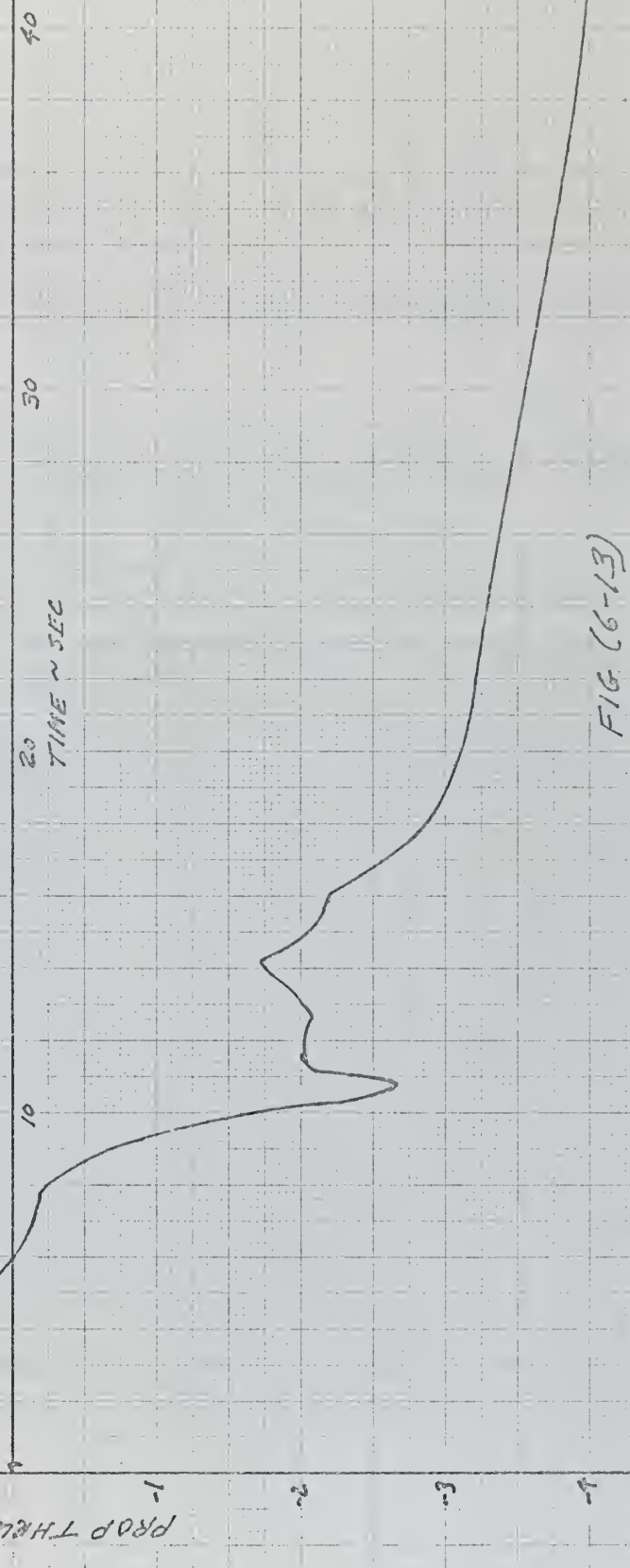


FIG (6-13)



## CRASHBACK (ETRA-2)

DISTANCE

1/2

40

30

20

10

0

TIME ~ 5 SEC  
FIG (6-14)

VELOCITY ~ FT/SEC

DISTANCE  $\times 10^{-2}$  - ft



CRASHBACK (FTTA-2)

10

30

TIME  $\sim$  5 SEC

10

20

0

-1

-2

-3

SHAFT ROTATIONAL VEL  $\sim$  REV/SEC

FIG (6-15)



CRASH BACK (FT4A-2)

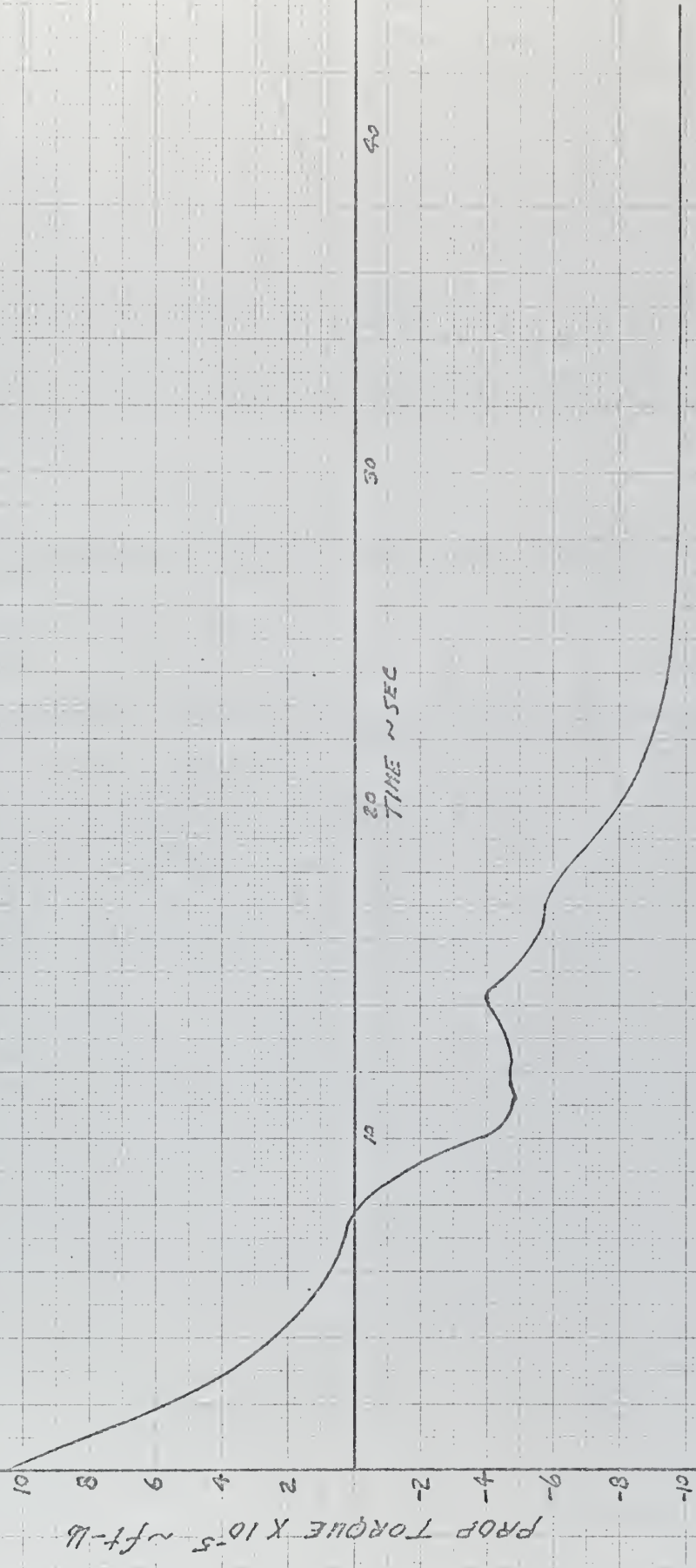


FIG (6-16)



CRASHBACK (FTTA-2)

POWER AND ENERGY  
ABSORBED IN REVERSE  
CLUTCH (FALK TYPE)  
DURING ENGAGEMENT

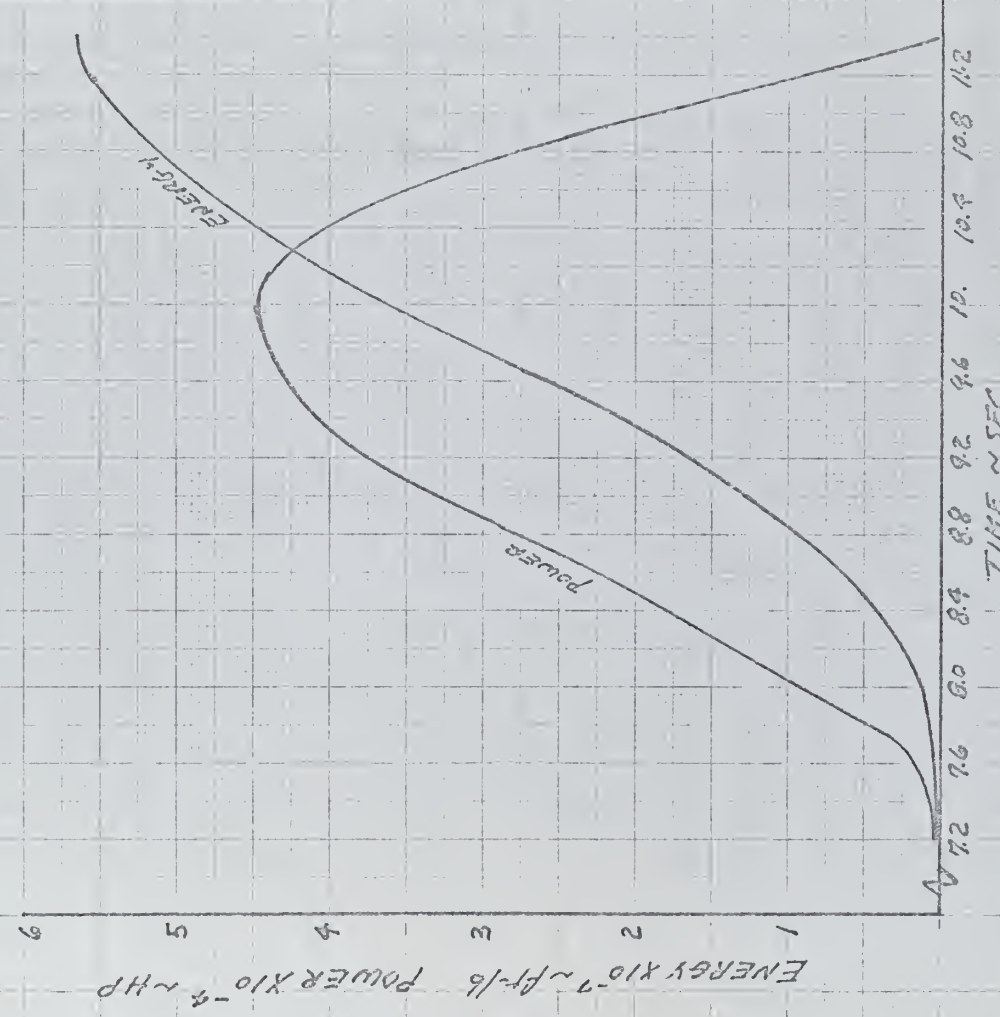


FIG (6-12)



ACCELERATING FROM 15 KTS. (L/M 2500-6 ft CROP)

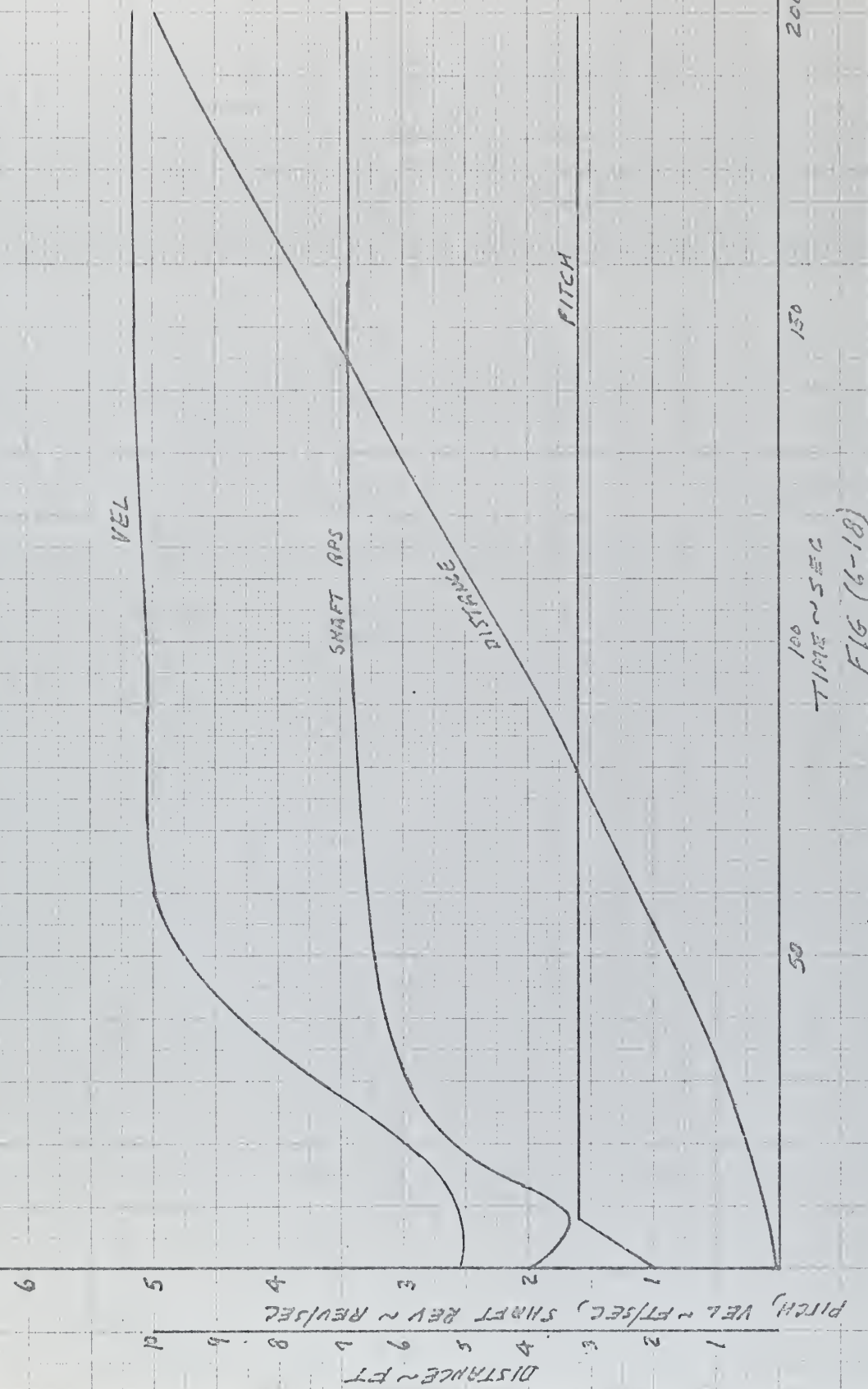
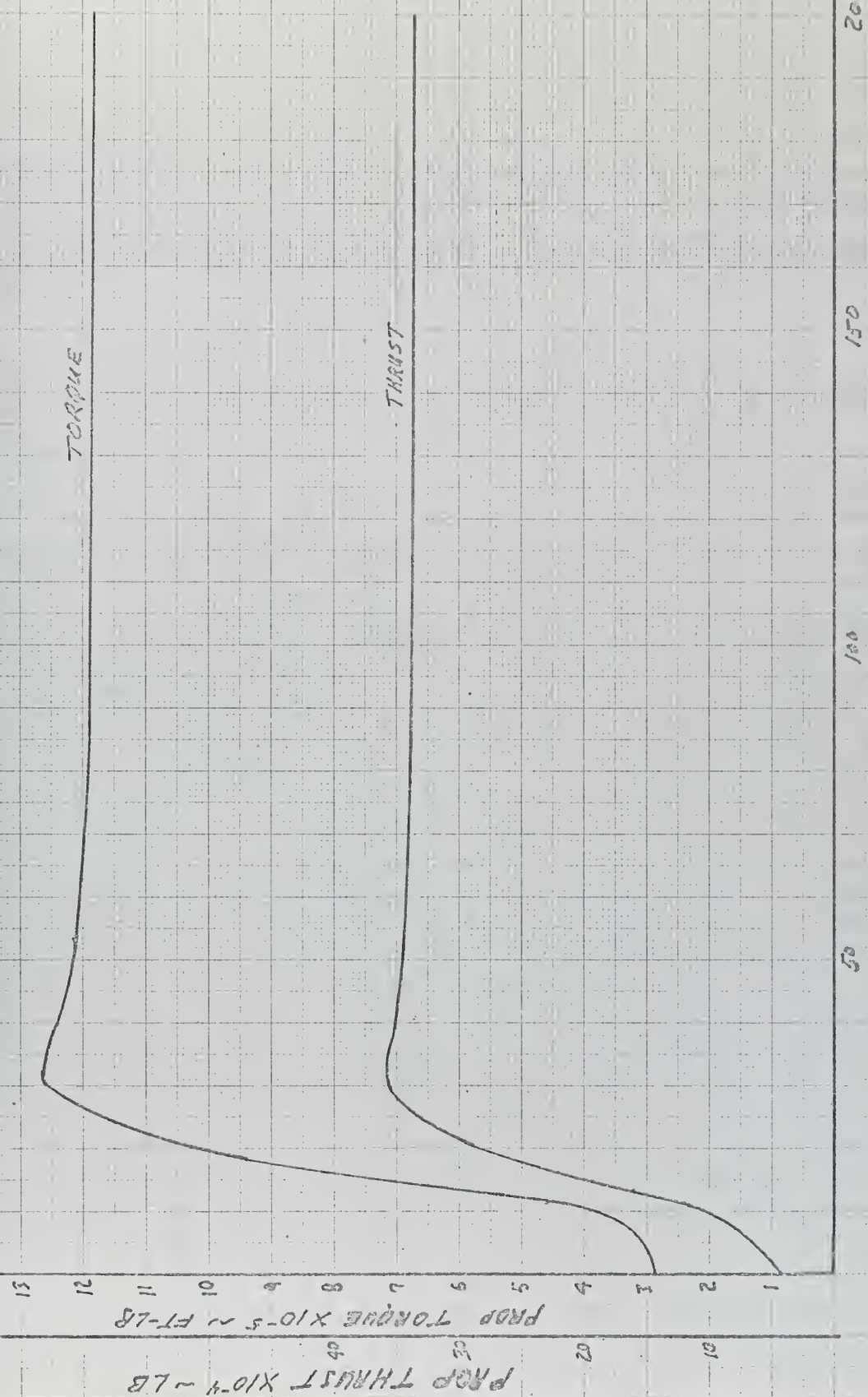


FIG (6-18)

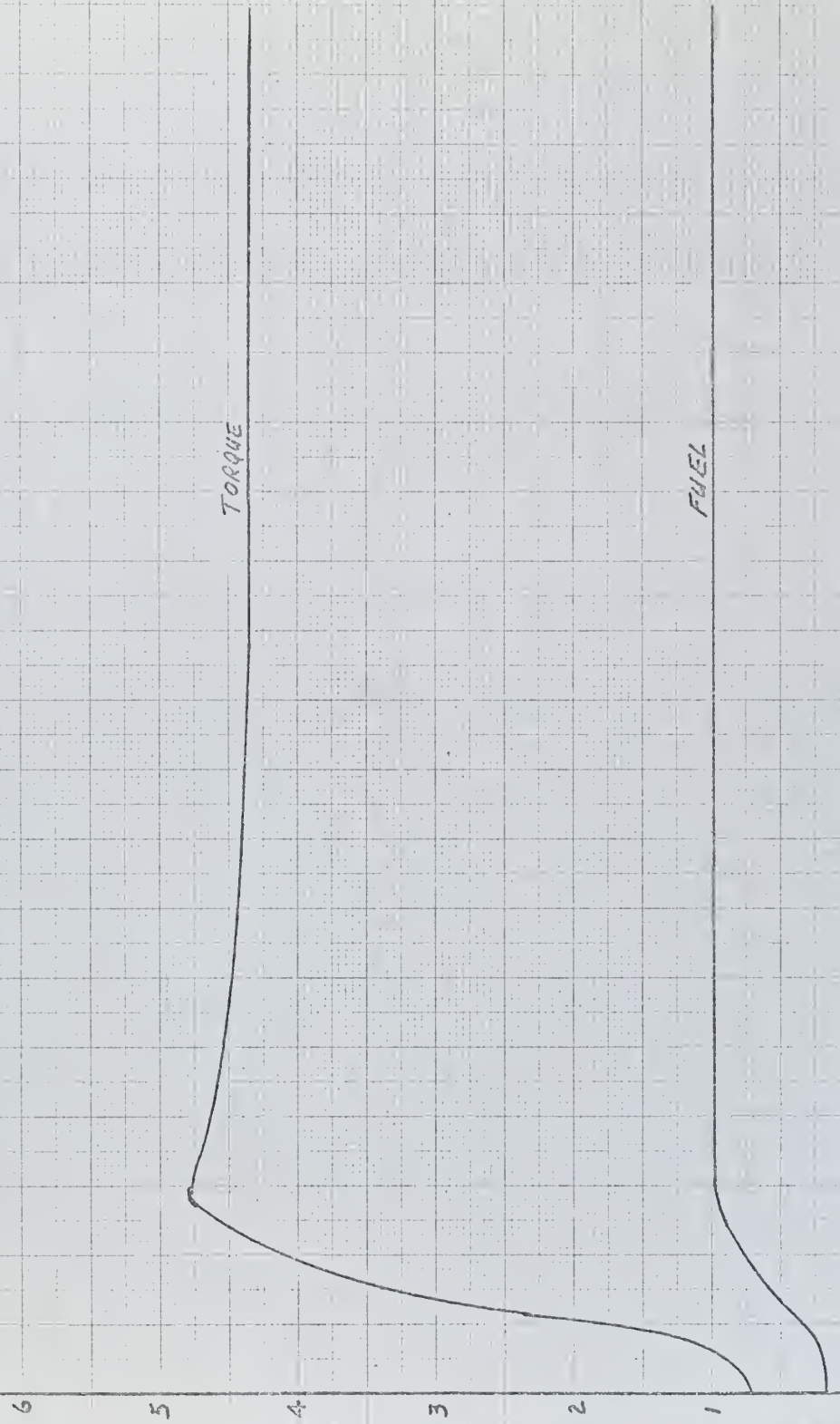


ACCELERATING FROM 15 KTS. (LN2500-N & CAPP)





ACCELERATING FROM 15 KTS (LM 2500-RPM)



10 20 30 40 50 60 70 80 90 100 110 120 130 140 150 160 170 180 190 200

TIME in SEC

FIG (6-20)

GAS TURBINE FUEL FLOW  $\times 10^{-9}$  LB/H, POWER TURBINE TORQUE  $\times 10^{-9}$  LB-FT



## CRASHBACK (LM3500-9 &amp; CRP9)

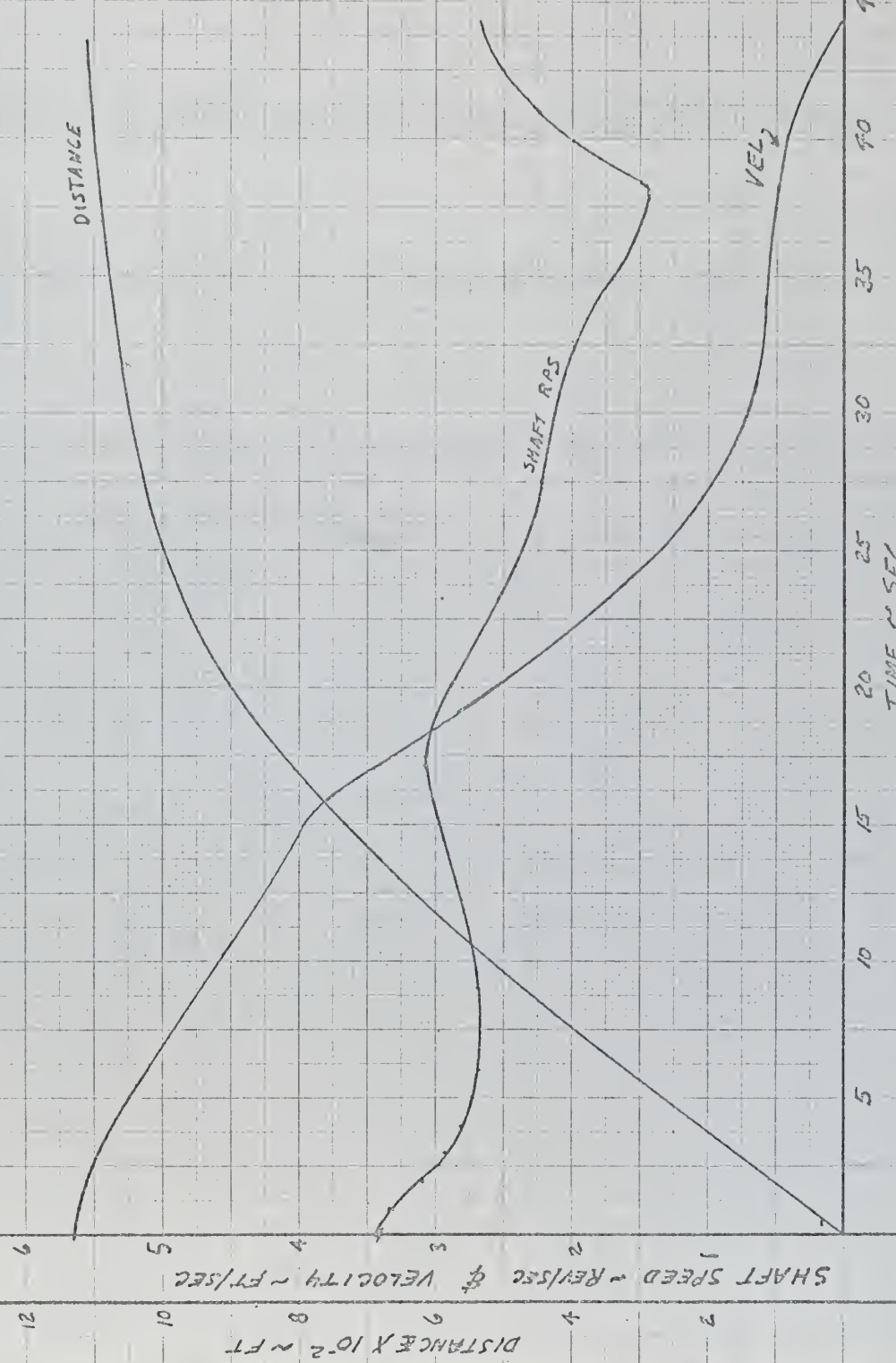


FIG (6-21)



CRASH BACK FROM 30 KTS (LM 2500-A & CPRO)

73

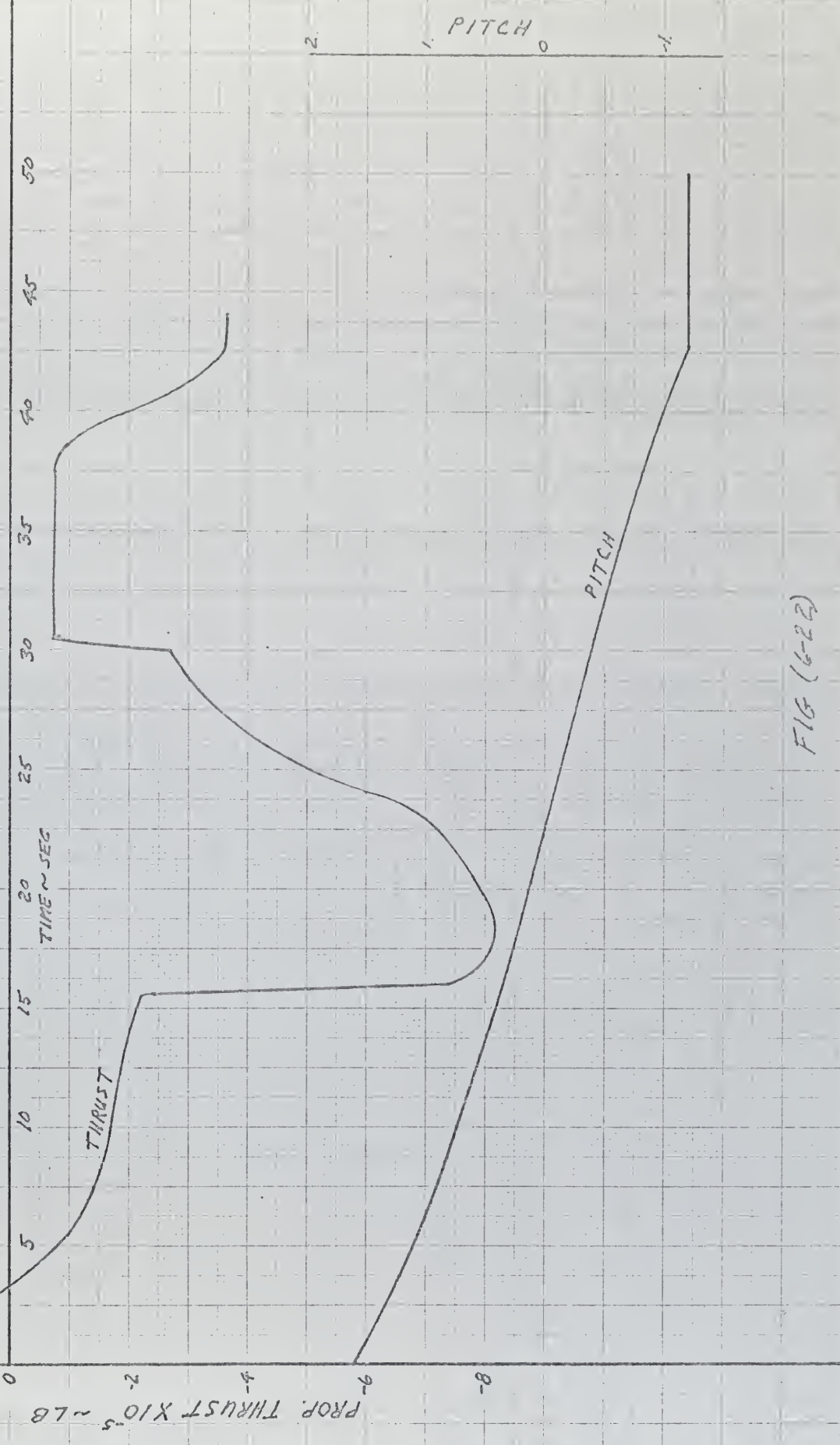
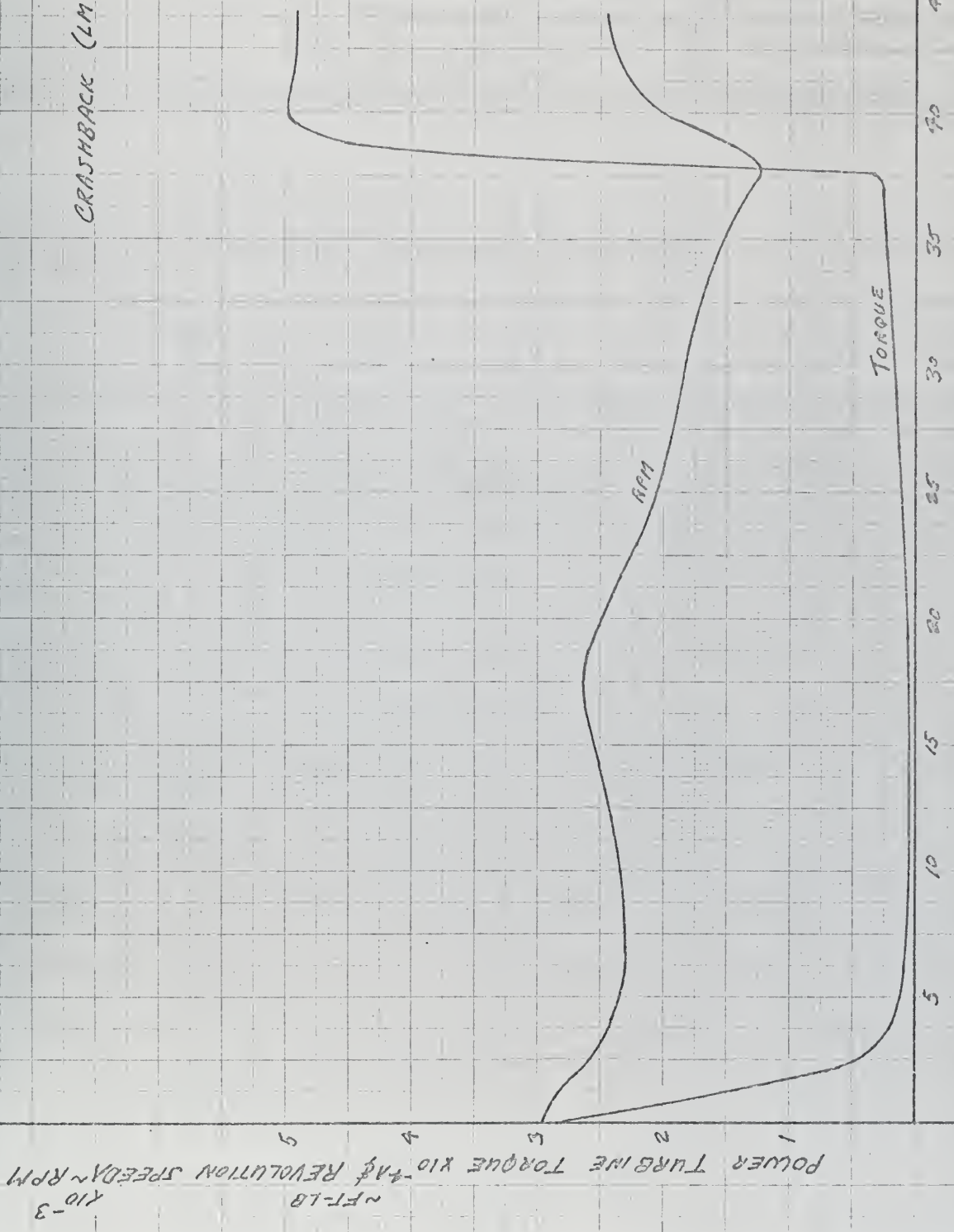


FIG (6-22)



CRASH BACK (2M 2500-A ft CREEP)



F16 (6-23)

POWER TURBINE TORQUE X10<sup>-3</sup> lb-inches  
NFT-18

$\times 10^{-3}$



1.0  
0  
-1.0

PITCH

CRASHBACK (LM 2500-A of Cess)

-1.0

PITCH

12

10

8

6

4

2

PROP TORQ  $\times 10^{-5}$  ~ FT-LB

TORQUE

50  
45  
40  
35  
30  
25  
20  
15  
10  
5

TIME ~ SEC

FIG (6-24)

75



CRASHBACK (KV MAJOR 12)

2.

1.

DISTANCE

VEL

5 10 15 20 25 30 35 40 45 50 55 60 65 70 75 80 85 90 95 100

TIME ~ SEC

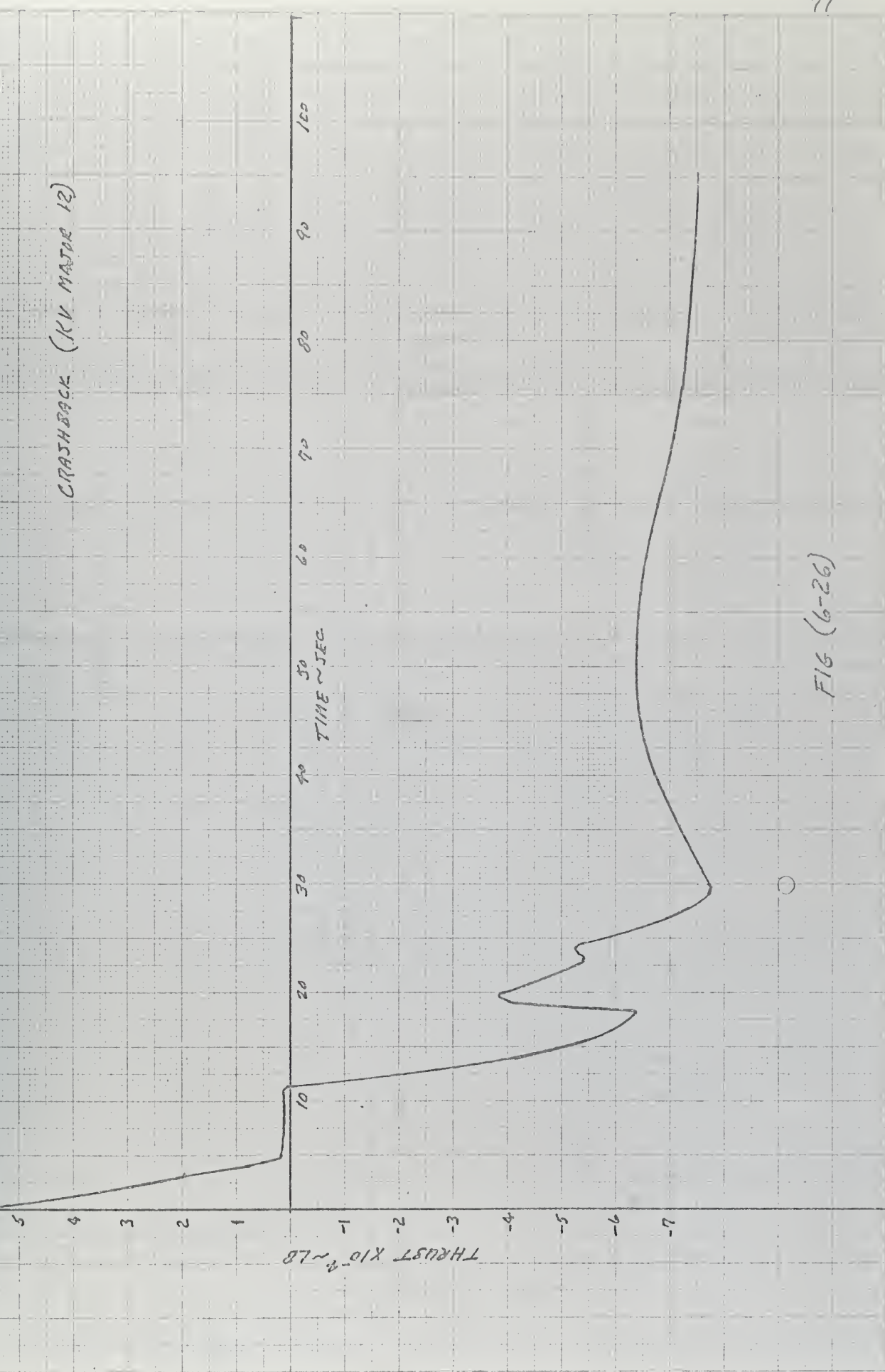
1.

SHAFT POS

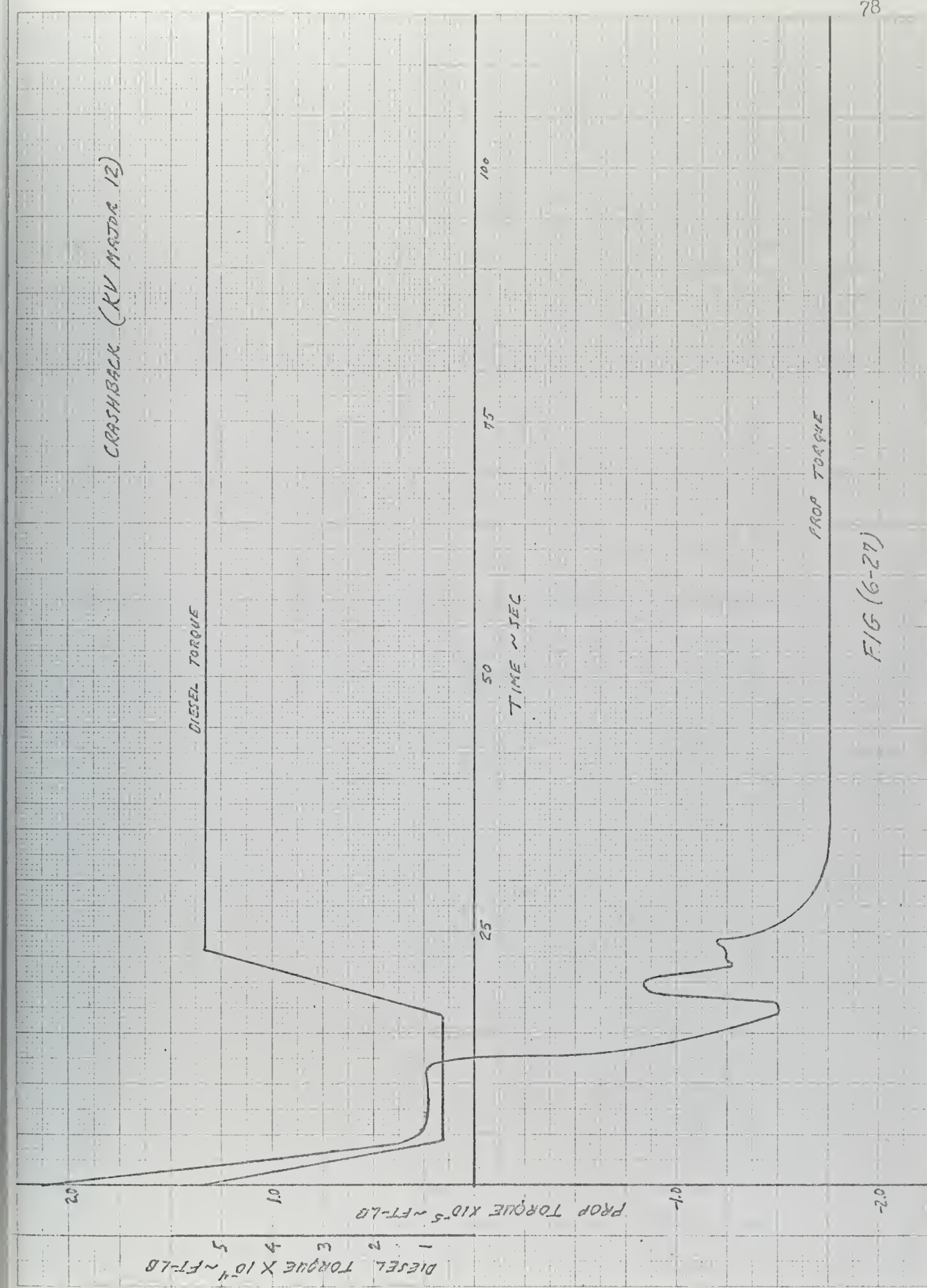
FIG (6-25)

DISTANCE  $\times 10^{-3}$  ft, VELOCITY ~ ft/sec, SHAFT VEL ~ REV/SEC



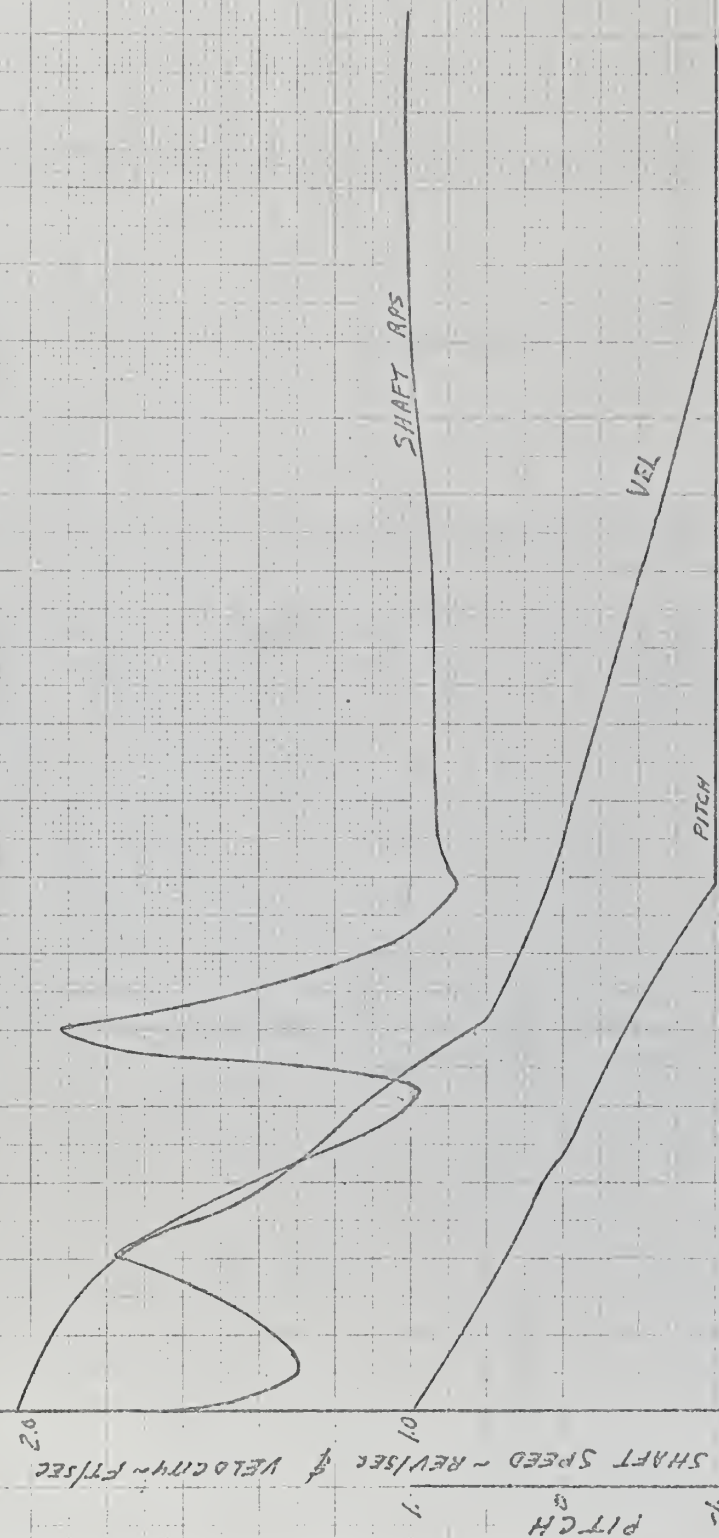








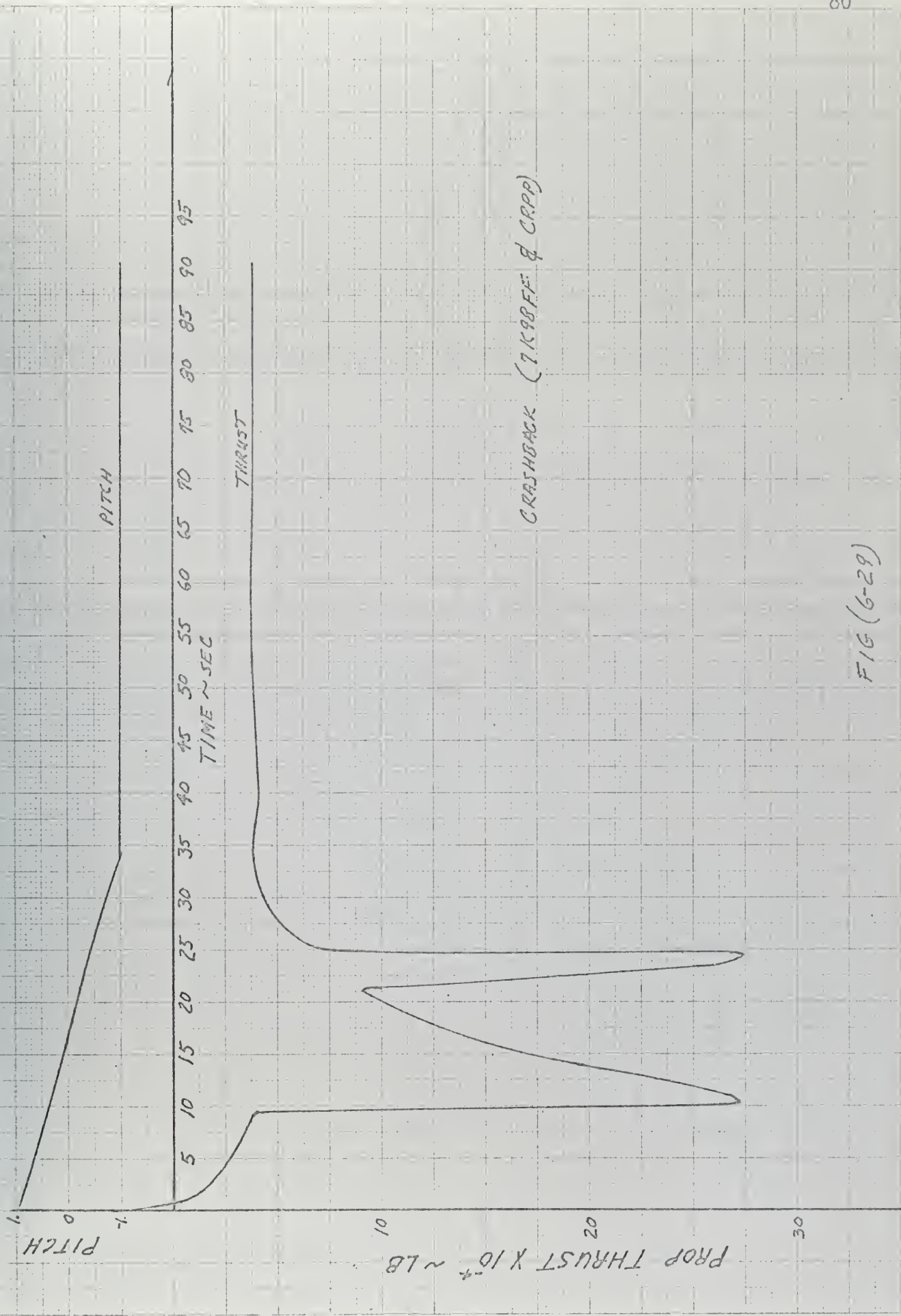
CRASHBACK (7K98FF &amp; CROP)



10    20    30    40    50    60    70    80    90

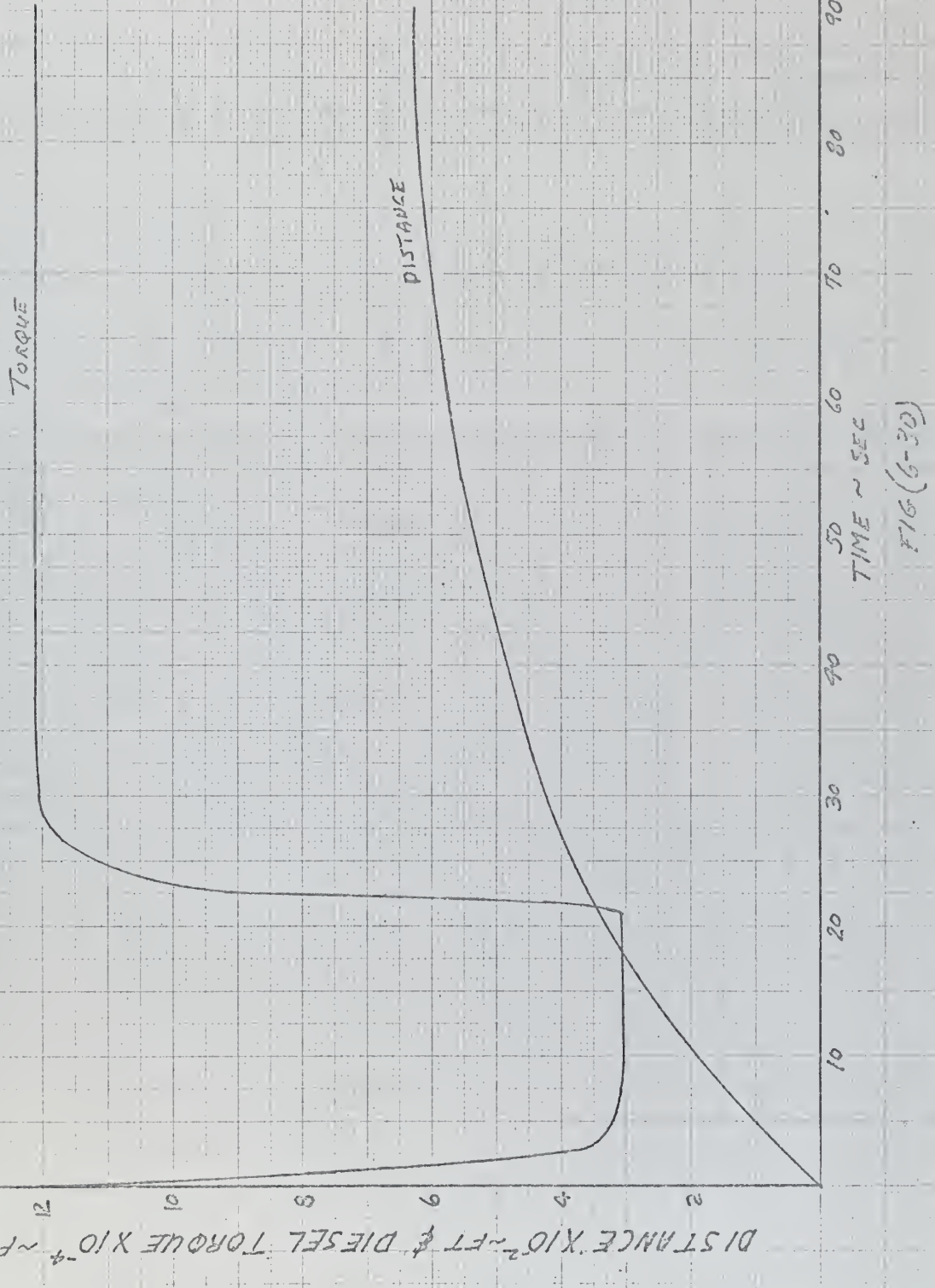
F16 (6-28)







CRASH BACK (7K90FF & C900)





CRASHBACK - (7K98FF & CROP)

82

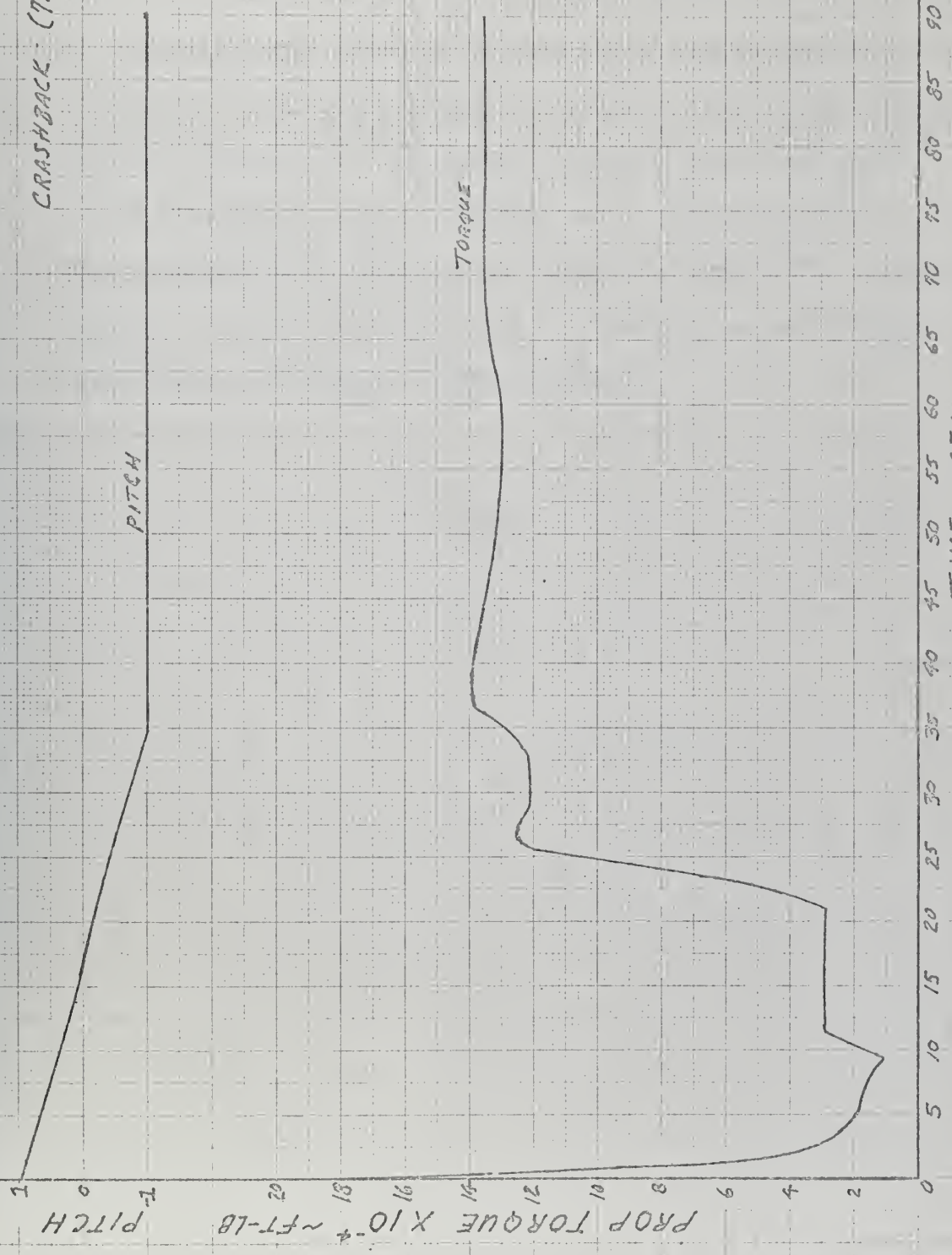


FIG. (6-31)



## 7. CONCLUSIONS

Simple models were found to exist that enable one to model ship propulsion drive trains. Some of the models had to be refined by the addition of time lags, delays, etc. The combination of drive train components must be compatible with the characteristics of each drive train member. The simulations illustrated the importance of proper sequencing of propulsion plant control parameters. Conditions of overspeeding, excess torques, and high energy dissipation rates in clutches can be easily simulated. These simulations can prove to be immensely useful to the control engineer in helping him synthesize a controller that will keep a system within its region of safe operation.



8. RECOMMENDATIONS

1. A study should be taken to determine what is the optimal fuel flow (setting) - pitch ratio combination for a particular prime mover and the CRPP presented here.
2. A model of reversing the B & W 7K98FF should be developed and a crashback simulation of the 7K98FF with a fixed pitch propeller should be performed.
3. A model controller to keep shaft rpm nearly constant while changing pitch ratio on the CRPP could be synthesized for each one of the prime movers.
4. A torque converter model should be developed to be used with the prime movers developed here, and maneuvers should be simulated.



## REFERENCES

- (1) Kiviat, P.J., Digital Computer Simulation: Modeling Concepts, RM-5378-PR (Rand Memorandum), August, 1967; AD 658429.
- (2) Kurzak, K. H., et. al., Propulsion Machinery of the "Koeln" Class Escort Frigates With Special Consideration of Gas Turbine Propulsion, ASME Publication 65-GTP-11.
- (3) Cottington, R.V., The Design of a Digital Three-Term Controller as a Turbojet Engine Speed Governor using Digital Simulation Methods, National Gas Turbine Establishment (Great Britain), Reports and Memoranda No. 3615, November, 1967.
- (4) G. S. Mueller, "Gas Turbine Simulation Using One-Dimensional Flow Relationships," IEE Conference on Industrial Applications of Dynamic Modeling, 16-18 September, 1969, University of Durham; p. 123.
- (5) Marscher, William F., Linear Analysis of Aircraft Gas Turbine Control System Dynamics, Master of Science Thesis, Department of Mechanical Engineering, Massachusetts Institute of Technology, 1960.
- (6) Arthur D. Little, Inc., First Interim Technical Report, Computer Simulation of the Power Conversion System for Nike-X Power Plants DA-49-129-Eng-542
- (7) Saravanamuttoo, H.I.H., Fawke, A. J., "Dynamic Modelling of Gas Turbine Performance," IEE Conference on Industrial Applications of Dynamic Modelling, University of Durham, 16-18 September, 1969, p. 133.
- (8) Saravanamuttoo, H.I.H., Fawke, A.J., Simulation of Gas Turbine Dynamic Performance, ASME Publication 70-GT-23.
- (9) Bichayev, B. P., Analog and Digital Models of Marine Gas-Turbine Units, Shipbuilding Press, Leningrad, 1969, in Russian.
- (10) Lurye, I. Yu, "Mathematical Modeling of a Gas Turbine with the Use of a Real Fuel Apparatus," Sudostroyeniye, No. 12, 1964, pp 24-26, AD 645853.
- (11) Rubis, C. J., "Braking and Reversing Ship Dynamics," Proceedings Second Ship Control Systems Symposium, November 4-6, 1969, sponsored by Naval Research and Development Laboratory (Annapolis, Md.), p. IV-B-2.
- (12) Bodnaruk, A., Rubis, C. J., Acceleration Performance of a Gas Turbine Destroyer Escort, ASME Publication 70-GT-77.



## REFERENCES (Cont'd)

- (13) Rubis, C. J., Transient Response of a 25,000 HP Marine Gas-Turbine Engine, ASME Publication 71-GT-61.
- (14) Woodward, J.B., III, The Diesel Engine: To Drive A Ship, Department of Naval Architecture and Marine Engineering Publication No. 105, January, 1971, University of Michigan.
- (15) Pounder, C. C., Marine Diesel Engines, Newnes-Butterworth, London, pps. 186-258.
- (16) Lewis, J. W., et.al., Digital Computer Simulation of Diesel-Electric Propulsion Systems, Presented during the September 26, 27, & 28 Joint meeting of the Chesapeake & Hampton Roads Section of the Society of Naval Architects and Marine Engineers.
- (17) Garvey, D., Feedback Control Systems Analysis, Paper No. PMCC 71-11, Woodward Governor Company (PMCC is believed to stand for Prime Mover Control Conference, a meeting held annually at the Woodward Governor Company).
- (18) Parker, George, General Discussion and Equations of a Prime Mover, Paper No. PMCC 70-4, Woodward Governor Company (same comments as in previous reference).
- (19) Meulengracht, Per V., High-Powered Marine Diesel Engines, Paper presented in Vancouver, British Columbia, March 2, 1970 to a combined meeting of The Institute of Marine Engineers and the Society of Automotive Engineers.
- (20) Pope, J.A., Lowe, W., "The Development of a Highly-Rated Medium-Speed Diesel Engine of 7000-9000 Horsepower for Marine Propulsion," Transactions, Institute of Marine Engineers, Vol. 78, No. 8, 1966.
- (21) Parker, op. cit., p.2.
- (22) Richardson, W. S., The Friction Clutch Reverse-Reduction Gears for the GTS, ASME Publication 69-GT-5.
- (23) Private correspondence dated April 10, 1972, from J. K. Liu, General Manager, Synchrotorque Division, Philadelphia Gear Corporation.
- (24) Wennberg, P. K., "The Design of the Main Propulsion Machinery Plant Installed in the USCGC Hamilton (WPG-715)," Transactions SNAME, 1966.



## REFERENCES (Cont'd)

- (25) Richardson, W. S. op.cit., p. 5.
- (26) Rowen, W. I., A Comparison of Simulated Gas Turbine Ship Handling Characteristics with Several Different Transmission Systems, ASME Publication 71-GT-65.
- (27) Ibid., p. 7.
- (28) Miniovich, I. Ya., Investigation of Hydrodynamic Characteristics of Screw Propeller Under Conditions of Reversing and Calculation Methods for Backing of Ships, Bureau of Ships Translation No. 697 (translation by Roger & Roger Inc.), originally appearing in Transactions of the Red Banner Central Scientific Research Institute, Issue No. 122, published by the State Union Publishing House of the Shipbuilding Industry, 1958.
- (29) Comstock, John P., ed., Principles of Naval Architecture, The Society of Naval Architects and Marine Engineers, 1967, p. 385.
- (30) Stephanson, T., Propeller Constraints, Ninth International Towing Tank Conference, 1957.
- (31) Baker, Dennis W., Patterson, Clair L., Jr., "Some Recent Developments in Representing Propeller Characteristics," Proceedings Second Ship Control Systems Symposium, November 4-5-6, 1959, pps. AP-A-1 - AP-A-34.
- (32) Van Lammeren, W.P.A., Van Manen, J.D., Oosterveld, M.W.C., The Wageningen B-Screw Series, presented at the Annual Meeting, New York, N.Y., November 12-24, 1969, of the Society of Naval Architects and Marine Engineers.
- (33) Read, C.M.B., "The Control of Gas Turbines Driving Controllable-Pitch Propellers," Proceedings of the First Ship Control Systems Symposium, Vol. I, November 15-17, 1966, held at Annapolis, Maryland.
- (34) Wendel, Alan H., Dunne, James, F., "Dynamic Analysis and Simulation of Ship and Propulsion Plant Maneuvering Performance," Proceedings of the Second Ship Control Systems Symposium, Vol. I, November 4-6, 1969, held at Annapolis, Maryland.
- (35) Harvald, S.V. AA., "Wake and Thrust Deduction at Extreme Propeller Loadings," Publications of the Swedish State Shipbuilding Experimental Tank, No. 61, 1967.
- (36) Miniovich, I. Ya., op. cit, p. 33.



## REFERENCES (Cont'd)

- (37) Rubis, C. J., op. cit., p. IV-B-4.
- (38) Read, C. M. B., op. cit., p. VII-B-8.
- (39) Lewis, et. al., op. cit., p. 10.
- (40) Norrbin, Nils H., "Theory and Observations on the Use of a Mathematical Model for Ship Maneuvering in Deep and Confined Waters," Publications of the Swedish State Shipbuilding Experimental Tank, No. 68.
- (41) Burrill, L. G., Robson, W., "Virtual Mass and Moment of Inertia of Propellers," Transactions North East Coast Institution of Engineers and Shipbuilders, Vol. 78, 1961-62, pps. 325-350.



## APPENDIX A

Gas Turbine Models1. Lurye Model

The following model of a marine gas turbine was proposed by Lurye in Reference (10) in the form of linearized differential equations:

Turbocompressor

$$(T_1 s + 1) \Delta \omega_1 = K_{11} \Delta G_T e^{-sT_1} - K_{12} \Delta \omega_2$$

Free Turbine

$$(T_2 s + 1) \Delta \omega_2 = K_{21} \Delta G_T e^{-sT_2} + K_{22} \Delta \omega_1 - K_\phi \Delta \phi$$

$$T_1 = \frac{J_1}{-\frac{\partial M_T}{\partial \omega_1} + \frac{\partial M_K}{\partial \omega_1}} \quad \dots \text{turbocompressor time constant}$$

$$K_{11} = \frac{\frac{\partial M_{T_1}}{\partial G_T}}{-\frac{\partial M_{T_1}}{\partial \omega_1} + \frac{\partial M_K}{\partial \omega_1}} \quad \dots \text{amplification coefficient of turbocompressor by fuel}$$

$$K_{12} = \frac{\frac{\partial M_K}{\partial \omega_2}}{-\frac{\partial M_{T_1}}{\partial \omega_1} + \frac{\partial M_K}{\partial \omega_1}} \quad \dots \text{load coefficient by the rate of rotation of free turbine}$$

$$T_2 = \frac{J_2}{-\frac{\partial M_2}{\partial \omega_2} + \frac{\partial M_T}{\partial \omega_2}} \quad \dots \text{time constant of free turbine}$$

$$K_{21} = \frac{\frac{\partial M_{T_2}}{\partial G_T}}{-\frac{\partial M_{T_2}}{\partial \omega_2} + \frac{\partial M_T}{\partial \omega_2}} \quad \dots \text{amplification coefficient of free turbine by fuel}$$



## APPENDIX A (Cont'd)

1. (Cont'd)

$$K_{\phi} = \frac{\frac{\partial M_{\phi}}{\partial \phi}}{-\frac{\partial M_{T_2}}{\partial \omega_2} + \frac{\partial M_{T_2}}{\partial \omega_2}} \quad \dots \text{load coefficient by propeller pitch}$$

$$K_{22} = \frac{\frac{\partial M_{T_2}}{\partial \omega_1}}{\frac{\partial M_K}{\partial \omega_1} - \frac{\partial M_{T_2}}{\partial \omega_1}} \quad \dots \text{amplification coefficient by rate of compressor rotation}$$

 $\omega_1$  = turbocompressor rate of rotation $\omega_2$  = free turbine rate of rotation $G_T$  = fuel consumption $\phi$  = propeller pitch $\zeta$  = time lag in combustion chamber $M_{T_1} = f_{T_1}(\omega_1, G_T)$  torque moment of turbocompressor $M_{T_2} = f_{T_2}(\omega_1, \omega_2, G_T)$  torque moment of free turbine $J_1$  = turbocompressor rotational inertia $J_2$  = free turbine rotational inertia $M_{\phi} = f_{\phi}(\omega_2, \phi)$  resistance moment of propeller $M_K = f_K(\omega_1, \omega_2)$  resistance moment of compressor



## APPENDIX A (Cont'd)

2. An Extension of the Saravananuttoo Model

Using the technique proposed by Saravananuttoo in References (7) & (8), the model can be extended to the case where 2-spool gas generator-free turbine combination:

HP Rotor equation

$$\eta_{T_{HP}} W_{HPT} C_{P_{HPT}} (T_4 - T_5) - \frac{1}{\eta_{C_{HP}}} W_{HPC} C_{P_{HPC}} (T_3 - T_2) = I_{HP} \frac{d\left(\frac{N_{HP}^2}{2}\right)}{dt}$$

LP Rotor equation

$$\eta_{T_{LP}} W_{LPT} C_{P_{LPT}} (T_5 - T_6) - \frac{1}{\eta_{C_{LP}}} W_{LPC} C_{P_{LPC}} (T_2 - T_1) = I_{LP} \frac{d\left(\frac{N_{LP}^2}{2}\right)}{dt}$$

Free Turbine equation

$$\eta_{T_{FT}} W_{FT} C_{P_{FT}} (T_6 - T_7) = \frac{d\left(\frac{N_{FT}^2}{2}\right)}{dt}$$

LP-HP Intercompressor Volume

$$W_{HPC} - W_{LPC} = \frac{RT_2}{V_2} \frac{dP_2}{dt}$$

Combustor volume

$$W_{HPT} - W_{HPC} - W_{FB} = \frac{RT_4}{V_4} \frac{dP_4}{dt}$$

Interturbine Volume (LP-HP)

$$W_{LPT} - W_{HPT} = \frac{RT_5}{V_5} \frac{dP_5}{dt}$$

Interturbine Volume (HP-FT)

$$W_{HPT} - W_{FT} = \frac{RT_6}{V_6} \frac{dP_6}{dt}$$



## APPENDIX A (Cont'd)

## 2. (Cont'd)

Combustor

$$T_4 = \frac{W_{fb} HV + C_p W_{HPC} T_3}{C_p (W_{fb} + W_{HPT})}$$

Nomenclature

W = mass flow rate

T = temperature

C<sub>p</sub> = specific heat at constant pressure\eta<sub>t</sub> = turbine over-all efficiency\eta<sub>c</sub> = compressor over-all efficiency

K = gas constant

HV = fuel heating value

V = volume

N = rotational speed

P = pressure

t = time

I = polar moment of inertia

Station Numbering

1 = LP Compressor inlet

2 = HP Compressor inlet

3 = combustor inlet

4 = HP turbine inlet (combustor outlet)

5 = LP turbine inlet

6 = FT inlet

7 = FT outlet



## APPENDIX A (Cont'd)

## 2. (Cont'd)

Subscripts

LPC = low pressure compressor

HPC = high pressure compressor

FB = Combustor

HPT = high pressure turbine

LPT = low pressure turbine

FT = free turbine

HP = HPC-HPT rotor

LP = LPC-LPT rotor



## APPENDIX A (Cont'd)

3. FT4A-2 & LM2500-A Marine Gas Turbines

Figure (A-1) is the power-speed curve for constant SFC values. The torque-speed characteristics shown in figure (A-2) can be derived from this curve. Figure (A-3) and (A-4) are the corresponding curves for the LM2500-A. Figures (A-2) and (A-4) show examples of the linear approximations for constant fuel rate values used to approximate the gas turbines' characteristics. For intermediate values of fuel rate, linear interpolation was used. The subroutines used for the FT4A-2 and the LM2500-A are included in the rear of this appendix.

A sketch of the FT4A-2 with a JFC 25-28 fuel controller is shown in Figure (A-5). A controller similar to the JFC 25-28 is the JFC 25-7 shown in figure (A-6). This controller is typical of the non-linear systems engineers are often asked to model.



SEA LEVEL

 $T_{AMBIENT} = 59^{\circ}\text{F}$ 

BASED ON LIQUID FUEL LHV = 18,500 BTU/LB

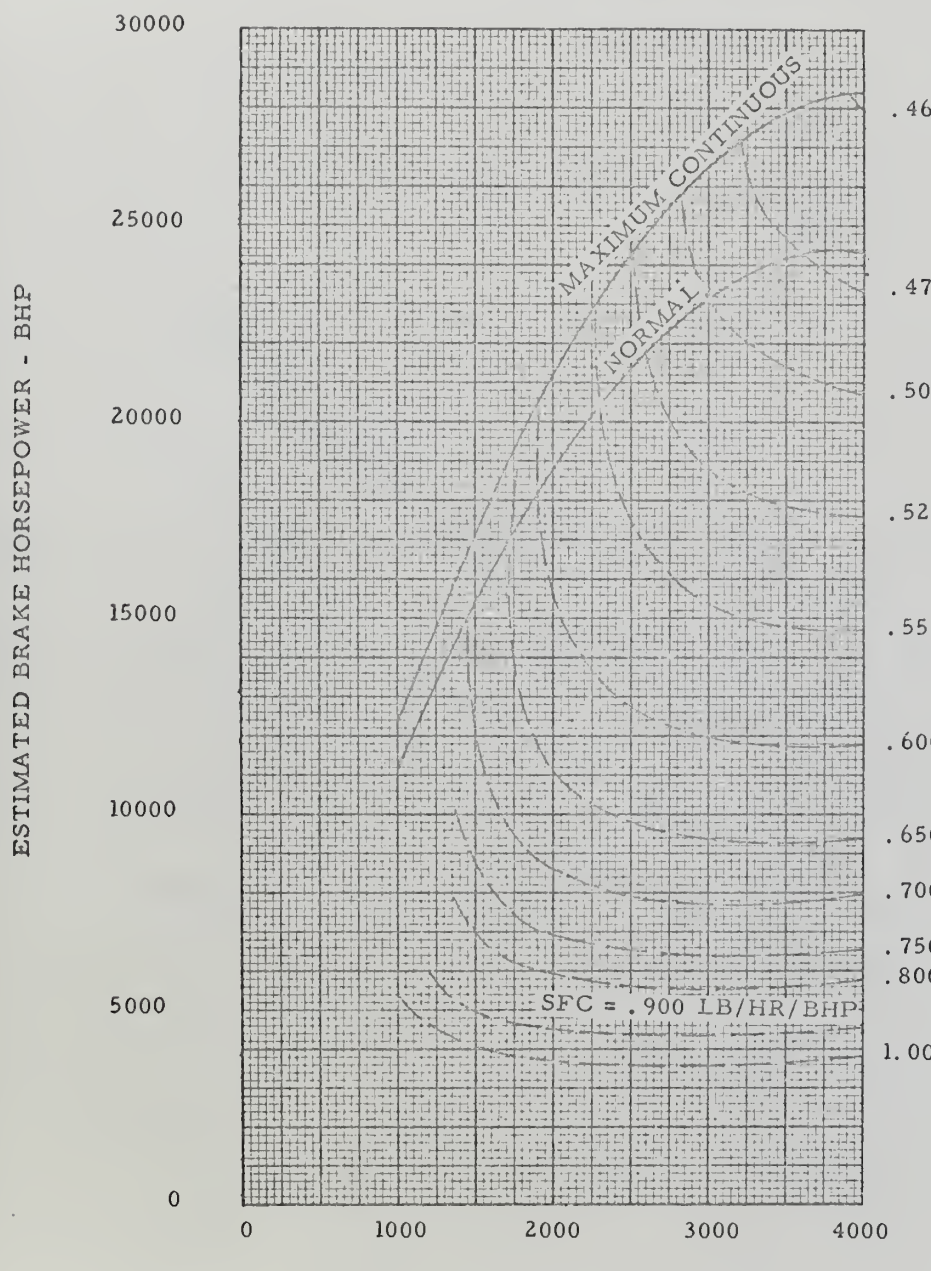


Fig. (A-1)



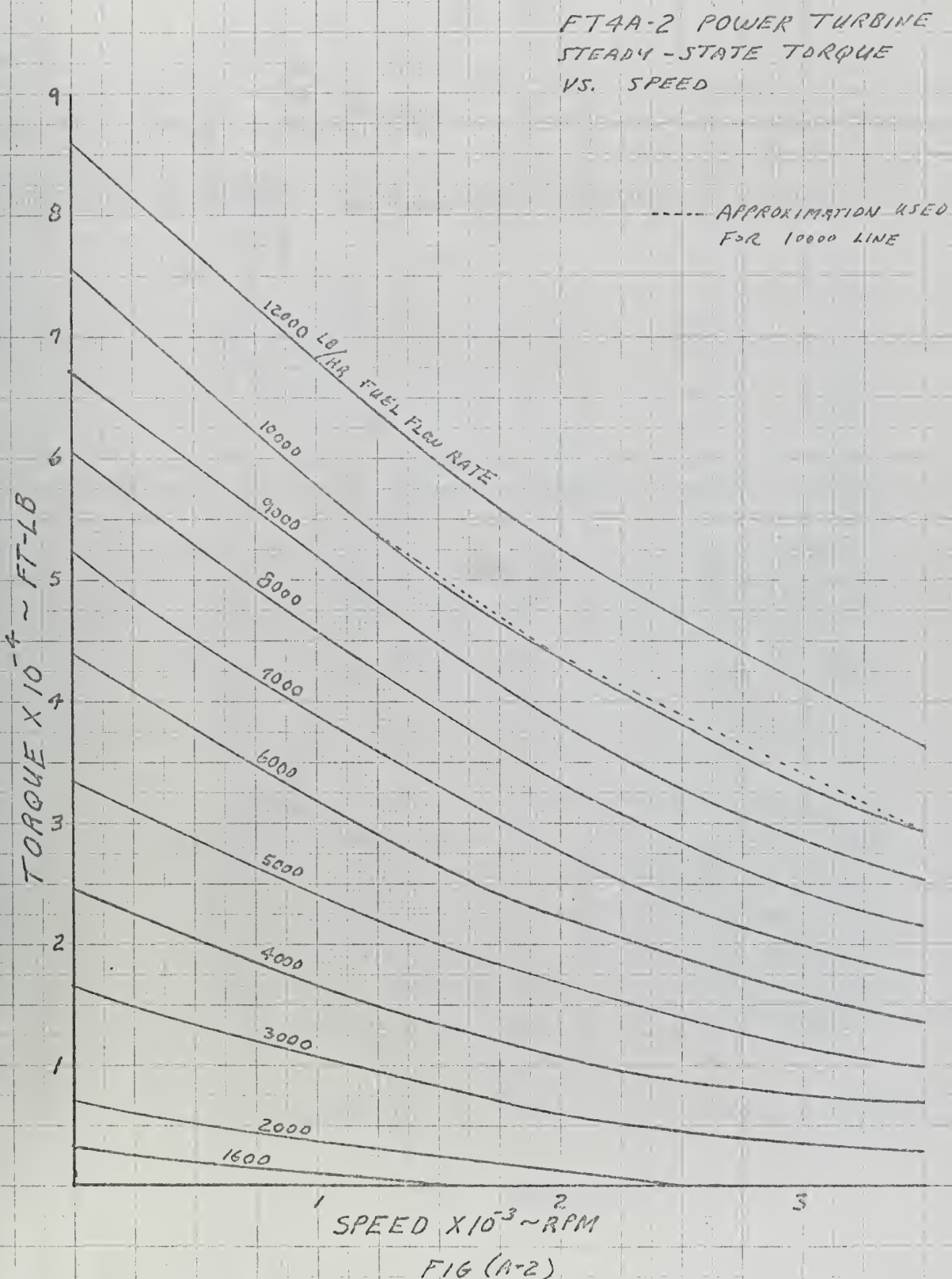
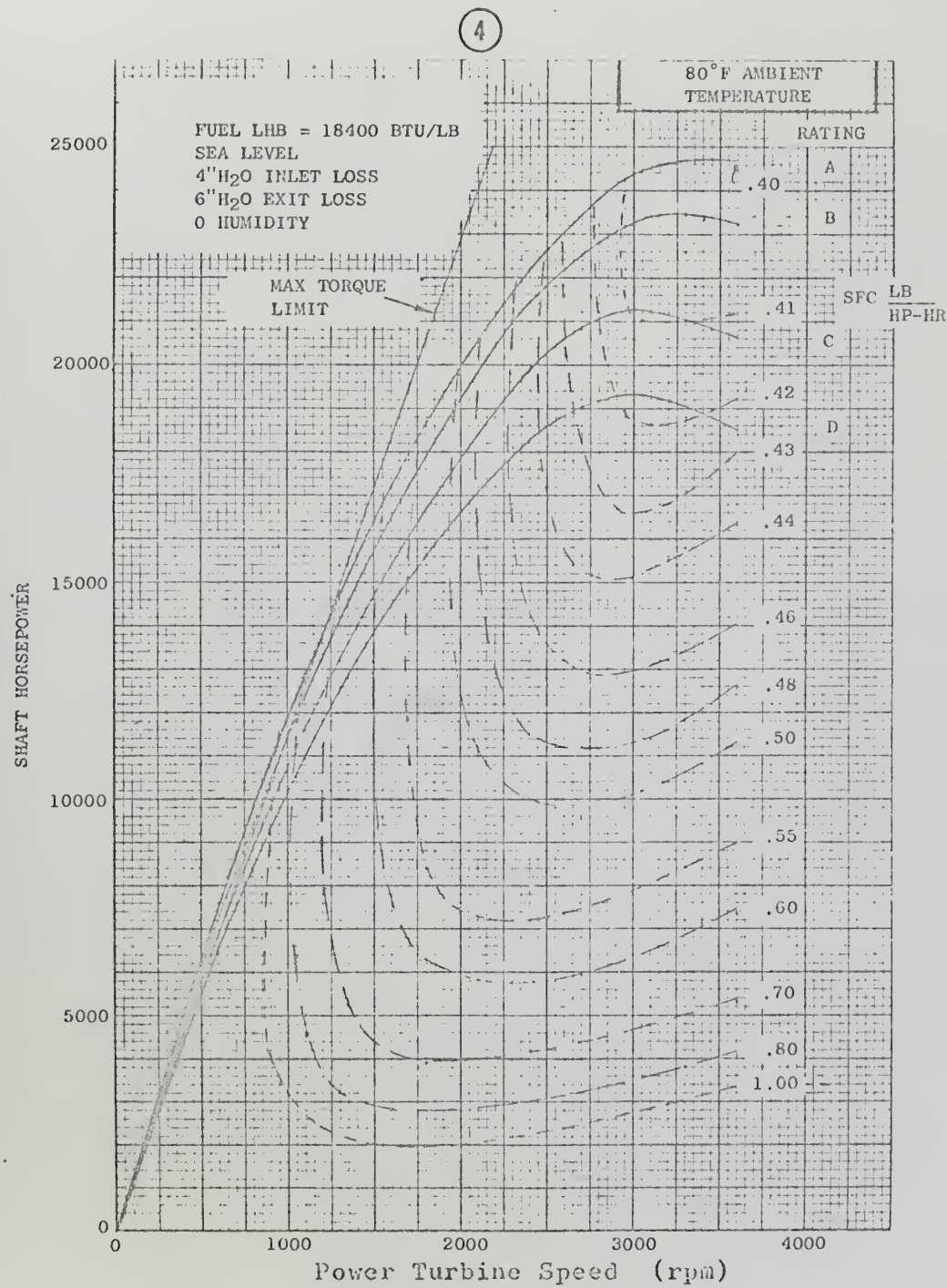


FIG (A-2)





SHAFT HORSEPOWER vs. POWER TURBINE SPEED FOR LM2500-A

Fig. (A-3)



L113500-A POWER TURBINE  
STEADY-STATE TORQUE  
VS. SPEED

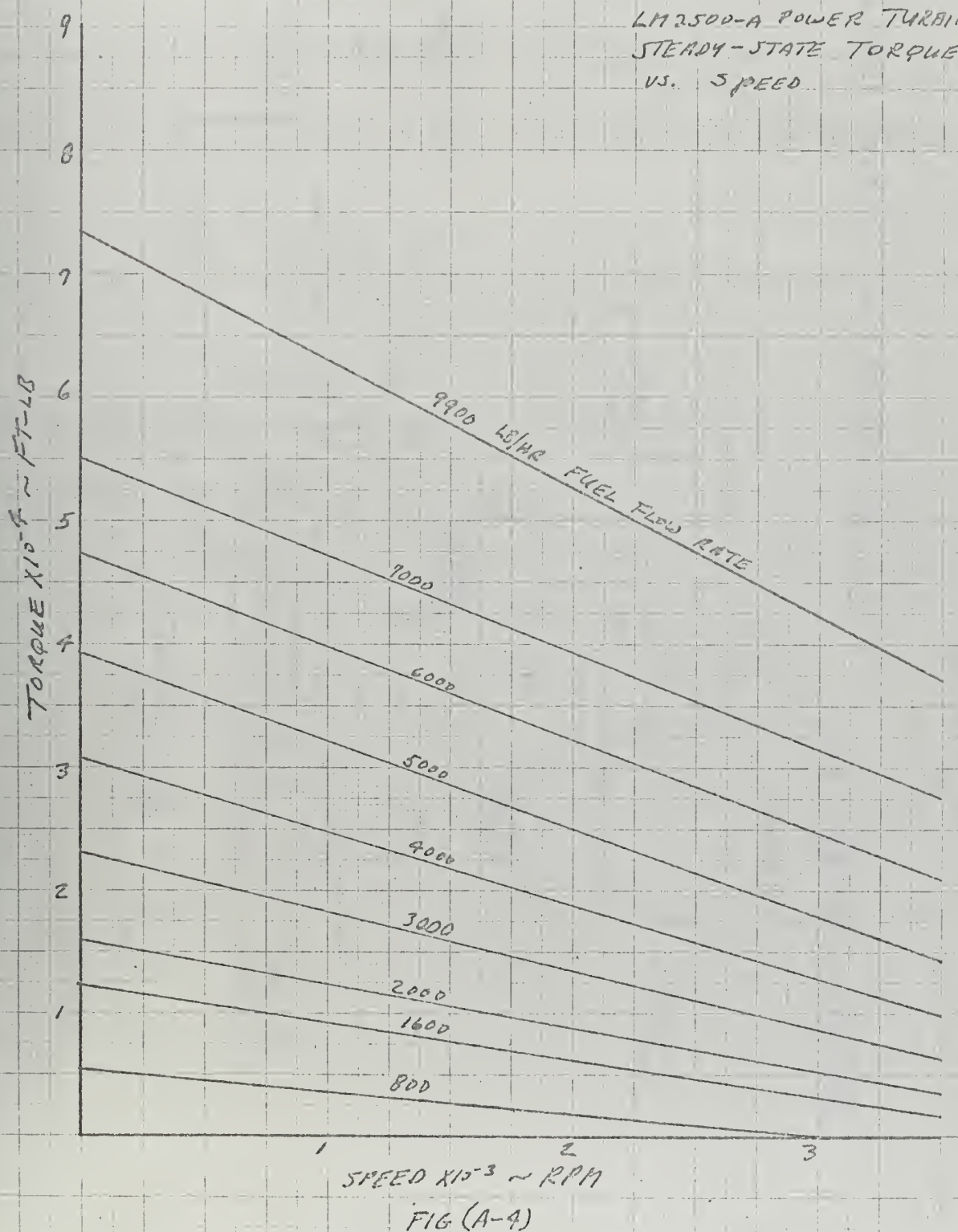


FIG (A-9)



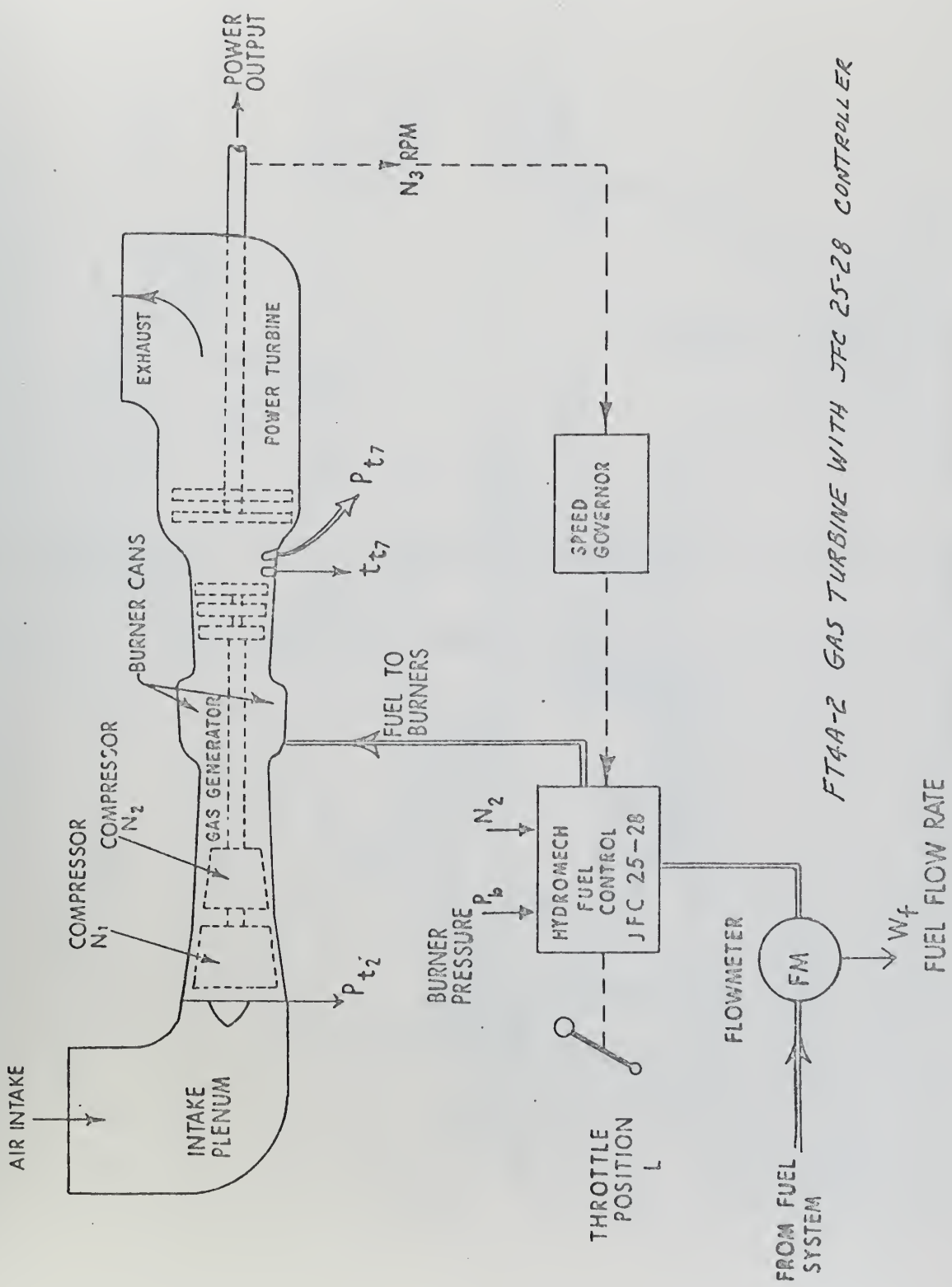


Fig. (A-5)



**JFC 25-7 FUEL CONTROL HAMILTON STANDARD**

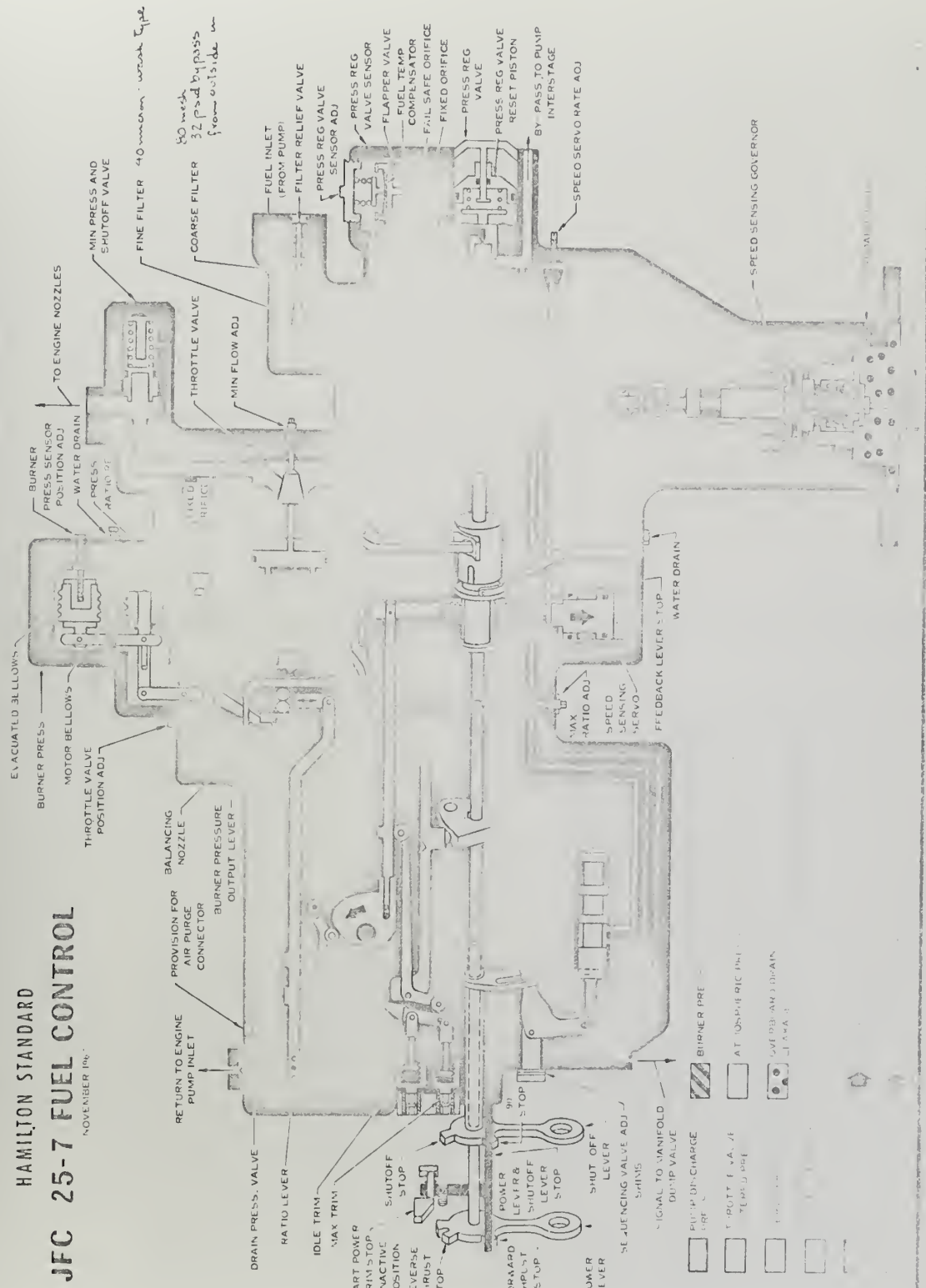


Fig. 6 (A and C)



C SUBROUTINE FT4A2 (AN3,WF,Q3)  
 C THIS SUBROUTINE COMPUTES FREE TURBINE TORQUE AS A FUNCTION OF  
 C FUEL RATE AND INITIAL N3 SPEED  
 C FUEL RATES MUST BE LIMITED BETWEEN 1600 LB/HR AND 12000 LB/HR.  
 C INPUTS ARE POWER TURBINE SPEED (AN3) IN RPM AND FUEL RATE (WF).  
 C OUTPUT IS POWER TURBINE TORQUE IN FT-LBS.  
 C NOTE: FOR HIGH SPEEDS AND LOW FUEL RATES, THIS PROGRAM WILL  
 C GIVE NEGATIVE TORQUES. A WINDAGE TORQUE MUST BE INCLUDED IN  
 C THE MAIN PROGRAM.

```

    IF(WF.LE.2000.)GOTO40
    IF(WF.LE.3000.)GOTO41
    IF(WF.LE.4000.)GOTO42
    IF(WF.LE.5000.)GOTO43
    IF(WF.LE.6000.)GOTO44
    IF(WF.LE.7000.)GOTO45
    IF(WF.LE.8000.)GOTO46
    IF(WF.LE.9000.)GOTO47
    IF(WF.LE.10000.)GOTO48
    GOTO49
  40  QWE2=-3.*AN3+7000.
    QWF16=-2.05*AN3+3250.
    Q3=QWF16+((WF-1600.)*.0025)*(QWF2-QWF16)
    RETURN
  41  CALL WF3(AN3,QWF3)
    QWF2=-3.*AN3+7000.
    Q3=QWF2+((WF-2000.)*.001*(QWF3-QWF2))
    RETURN
  42  CALL WF4(AN3,QWF4)
    CALL WF3(AN3,QWF3)
    Q3=QWF3+((WF-3000.)*.001*(QWF4-QWF3))
    RETURN
  43  CALL WF5(AN3,QWF5)
    CALL WF4(AN3,QWF4)
    Q3=QWF4+((WF-4000.)*.001*(QWF5-QWF4))
    RETURN
  44  CALL WF6(AN3,QWF6)
  
```



```

CALL WF5 (AN3,QWF5)
Q3=QWF5+((WF-5000.)*.001*(QWF6-QWF5))
RETURN

45 CALL WF7 (AN3,QWF7)
CALL WF6 (AN3,QWF6)
Q3=QWF5+((WF-6000.)*.001*(QWF7-QWF6))
RETURN

46 CALL WF8 (AN3,QWF8)
CALL WF7 (AN3,QWF7)
Q3=QWF7+((WF-7000.)*.001*(QWF8-QWF7))
RETURN

47 CALL WF9 (AN3,QWF9)
CALL WF8 (AN3,QWF8)
Q3=QWF3+((WF-8000.)*.001*(QWF9-QWF8))
RETURN

48 CALL WF10 (AN3,QWF10)
CALL WF9 (AN3,QWF9)
Q3=QWF9+((WF-9000.)*.001*(QWF10-QWF9))
RETURN

49 CALL WF12 (AN3,QWF12)
CALL WF10 (AN3,QWF10)
Q3=QWF10+((WF-10000.)*.0005*(QWF12-QWF10))
RETURN

END
SUBROUTINE WF3 (AN3,QWF3)
IF (AN3.LE.2000.) GOT3C
QWF3=-2.*AN3+10000.
RETURN

30 QWF3=-5.*25*AN3+16500.
RETURN

END
SUBROUTINE WF4 (AN3,QWF4)
IF (AN3.LE.1000.) GOT4C
IF (AN3.LE.2000.) GOT41
QWF4=-2.*67*AN3+15930.
RETURN

```



```

40 QWF4=-8.*AN3+24000.
RETURN
41 QWF4=-5.*7*AN3+22000.
RETURN
END
SUBROUTINE WF5 (AN3, QWF5)
IF (AN3.LE.1000.) GOT05C
IF (AN3.LE.2250.) GOT051
QWF5=-4.*AN3+24000.
RETURN
50 QWF5=-9.*3*AN3+33500.
RETURN
51 QWF5=-7.*36*AN3+24000.
RETURN
END
SUBROUTINE WF6 (AN3, QWF6)
IF (AN3.LE.1000.) GOT06C
IF (AN3.LE.2250.) GOT061
QWF6=-5.*36*AN3+32500.
RETURN
56 QWF6=-12.*45*AN3+44000.
RETURN
61 QWF6=-9.*45*AN3+41500.
RETURN
END
SUBROUTINE WF7(AN3, QWF7)
IF (AN3.LE.1250.) GOT06C
IF (AN3.LE.2000.) GOT061
QWF7=-5.*8*AN3+41300.
RETURN
60 QWF7=-15.*35*AN3+5500C.
RETURN
61 QWF7=-10.*3*AN3+49100.
RETURN
END
SUBROUTINE WF8 (AN3, QWF8)

```



```

IF (AN3.LE.1750.) GOTO 80
IF (AN3.LE.2500.) GOTO 81
QWF8=-7.2*AN3+46500.
RETURN
80  QWF8=-13.73*AN3+60500.
     RETURN
81  QWF9=-10.4*AN3+54500.
     RETURN
END
SUBROUTINE WF9(AN3, QWF9)
IF (AN3.LE.1750.) GOTO 91
IF (AN3.LE.3000.) GOTO 92
QWF9=-7*AN3+49980.
RETURN
91  QWF9=-14.45*AN3+67000.
     RETURN
92  QWF9=-10.15*AN3+59480.
     RETURN
END
SUBROUTINE WF10 (AN3, QWF10)
IF (AN3.LE.1250.) GOTO 101
IF (AN3.LE.2000.) GOTO 102
QWF10=-9.67*AN3+62830.
RETURN
101 QWF10=-17.2*AN3+75500.
     RETURN
102 QWF10=-14.*AN3+71500.
     RETURN
END
SUBROUTINE WF12(AN3, QWF12)
IF (AN3.LE.2000.) GOTO 103
QWF12=-10.8*AN3+74300.
RETURN
103 QWF12=-16.54*AN3+86000.
     RETURN
END

```



SUBROUTINE LM250 (RPM,WF,TORQ,A08,A16,A2,A3,A4,A5,A6,A7,A99)  
THIS SUBROUTINE CALCULATES FREE TURBINE TORQUE AS A FUNCTION OF  
RPM AND FUEL FLOW  
MINIMUM FUEL RATE IS 800 LP/HR  
MAXIMUM FUEL RATE ALLOWABLE IS 9900 LB/HR  
ENTERING ARGUMENTS FOR THIS SUBROUTINE ARE FUEL RATE (WF)  
AND POWER TURBINE RPM (RPM) OUTPUT IS POWER TURBINE TORQUE IN  
FT-LBS  
SEARCH TO BRACKET WF AND THEN PROCEED TO FUEL SUBROUTINES  
IF(WF .EQ. 800.) GOTO15  
IF(WF .LE. 1600.) GOTO16  
IF(WF .LE. 2000.) GOTO17  
IF(WF .LE. 3000.) GOTO18  
IF(WF .LE. 4000.) GOTO10  
IF(WF .LE. 5000.) GOTO 11  
IF(WF .LE. 6000.) GOTO12  
IF(WF .LE. 7000.) GOTO13  
IF(WF .LE. 9900.) GOTO14  
15 TORQ=-1.965\*RPM+5500.  
RETURN  
16 CALL LWF08 (RPM,A08)  
CALL LWF16 (RPM,A16)  
TORQ=A08+(WF-800.)\*.00125\*(A16-A08)  
RETURN  
17 CALL LWF2 (RPM,A2)  
CALL LWF16 (RPM,A16)  
TORQ=A16+(WF-1600.)\*.0025\*(A2-A16)  
RETURN  
18 CALL LWF3 (RPM,A3)  
CALL LWF2 (RPM,A2)  
TORQ=A2+(WF-2000.)\*.001\*(A3-A2)  
RETURN  
10 CALL LWF4 (RPM,A4)  
CALL LWF3 (RPM,A3)  
TORQ=A3+(WF-3000.)\*.001\*(A4-A3)  
RETURN  
11 CALL LWF5 (RPM,A5)  
CALL LWF4 (RPM,A4)  
TORQ=A4+(WF-4000.)\*.001\*(A5-A4)  
RETURN  
12 CALL LWF6 (RPM,A6)  
CALL LWF5 (RPM,A5)  
TORQ=A5+(WF-5000.)\*.001\*(A6-A5)  
RETURN  
13 CALL LWF7 (RPM,A7)  
CALL LWF6 (RPM,A6)  
TORQ=A6+(WF-6000.)\*.001\*(A7-A6)  
RETURN  
14 CALL LWF99 (RPM,A99)  
CALL LWF7 (RPM,A7)  
TORQ=A7+(WF-7000.)\*.0003448\*(A99-A7)  
RETURN  
END  
SUBROUTINE LWF08 (RPM,A08)  
A08=-1.965\*RPM+5500.  
RETURN



PAGE 2

```
END
SUBROUTINE LWF16 (RPM,A16)
A16=-2.94*RPM+12500.
RETURN
END
SUBROUTINE LWF2 (RPM,A2)
A2=-3.48*RPM+16150.
RETURN
END
SUBROUTINE LWF3 (RPM,A3)
A3=-4.77*RPM+23250.
RETURN
END
SUBROUTINE LWF4 (RPM,A4)
A4=-5.933*RPM+30800.
RETURN
END
SUBROUTINE LWF5 (RPM,A5)
A5=-7.133*RPM+39500.
RETURN
END
SUBROUTINE LWF6 (RPM,A6)
A6=-7.5*RPM+47500.
RETURN
END
SUBROUTINE LWF7 (RPM,A7)
A7=-8.*RPM+55300.
RETURN
END
SUBROUTINE LWF99 (RPM,A99)
A99=-10.15*RPM+73600.
RETURN
END
```



## APPENDIX B

Diesel Particulars1. Burmeister and Wain 7K98FF

Test-bed results of the B & W 7K98FF are shown in Figure (B-1). From this figure, it was possible to derive the ideal diesel power-speed curves for constant fuel settings; this is shown in figure (B-2). The torque-speed characteristics, figure (B-3), are in turn derived from figure (B-2). The "FF" at the end of the designation of this engine denotes that this diesel is intended for direct drive, i.e., no reduction gears. Other technical data is presented below:

continuous service rating 24500 metric BHP @ 100 rpm

maximum continuous service rating 26600 metric BHP @ 103 rpm

Length 45' 2"

Breadth 16' 2"

Height 43' 2"

The computer program used to model the diesel is included at the end of this appendix.

2. Mirrless KV Major 12

A cutaway drawing and technical specifications of this engine is shown in figure (B-4). The "12" at the end of the designation indicates the number of cylinders. Figure (B-5) shows the fuel map for this engine. Using this fuel map and the elementary diesel equation discussed in section 2, it was possible to obtain the approximately Linear torque-fuel setting characteristics shown in figure (B-6). The relationship obtained from figure (B-6) is



## APPENDIX B (Cont'd)

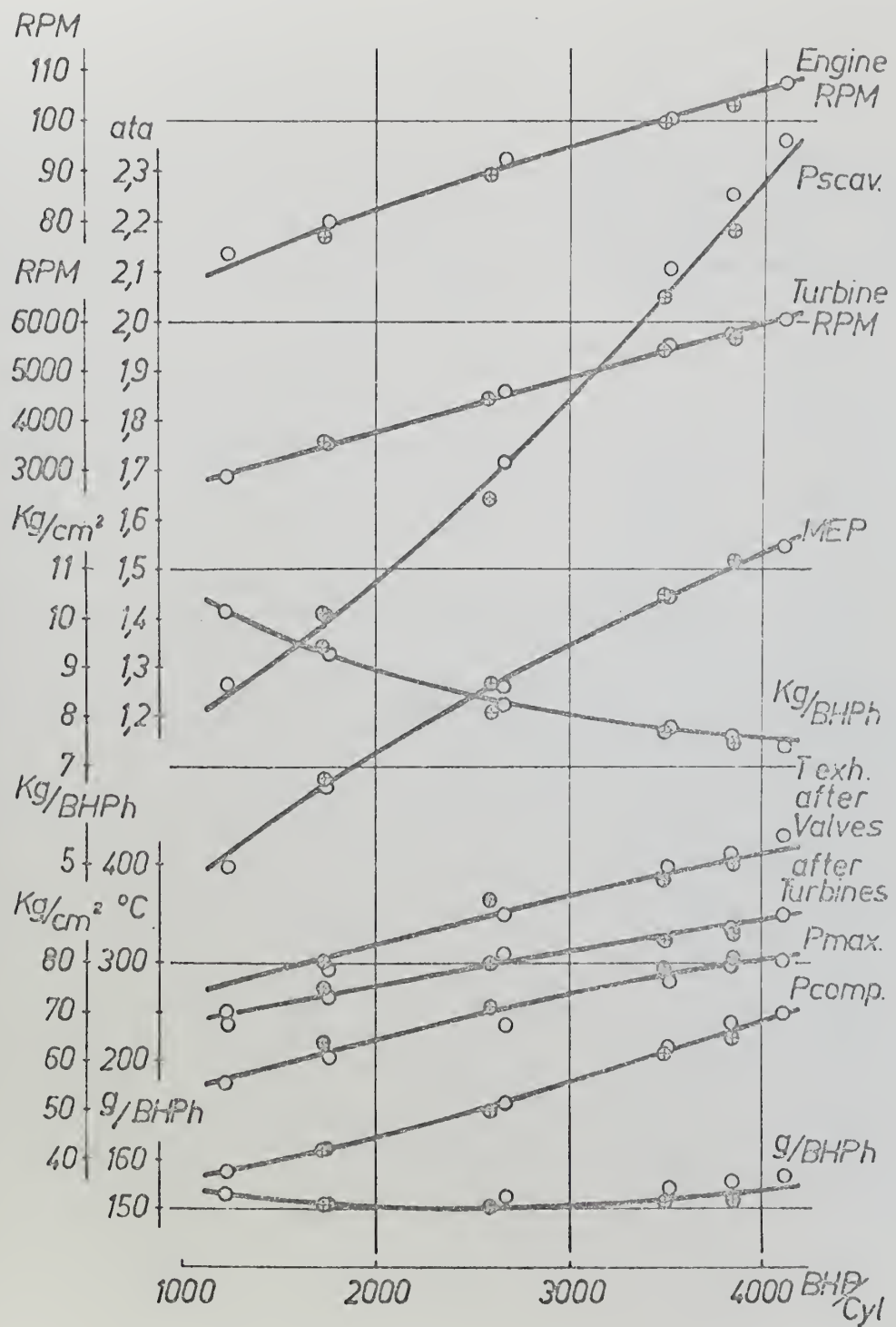
2. (Cont'd)

$$T = 550z$$

*z* = fuel setting in percent

*T* = torque in ft-lbs





TEST BDD RESULTS OF B&amp;W 7K98FF

Fig. (B-1)



IDEALIZED POWER-SPEED  
CURVES FOR 13 G.W. 7KG/PF  
LOW SPEED DIESEL FOR CONSTANT  
VALUES OF FUEL SETTING.

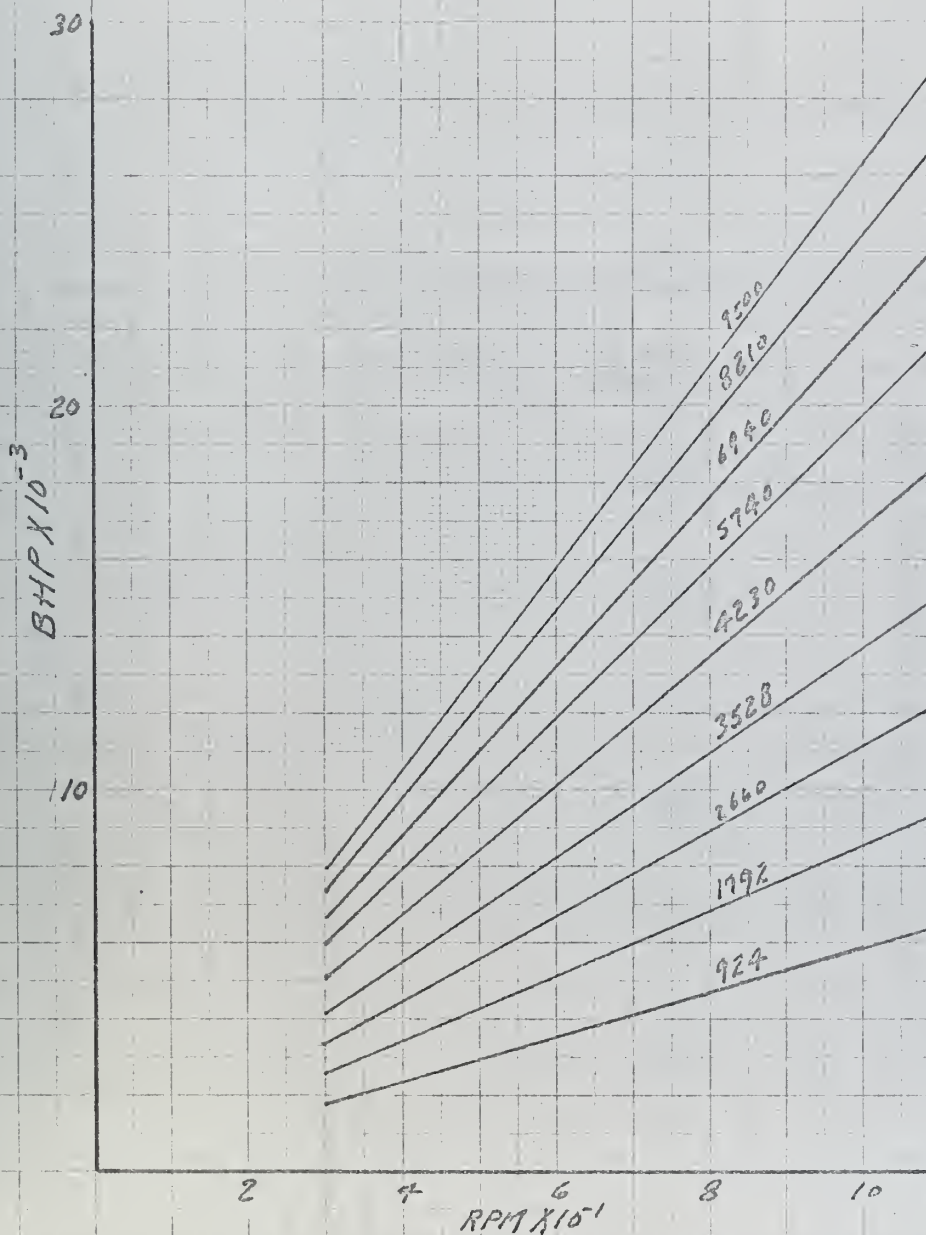


FIGURE (B-2)



IDEALIZED TORQUE-SPEED  
CURVES FOR B&W 7K98FF  
LOW SPEED DIESEL FOR CONSTANT  
VALUES OF FUEL SETTING.

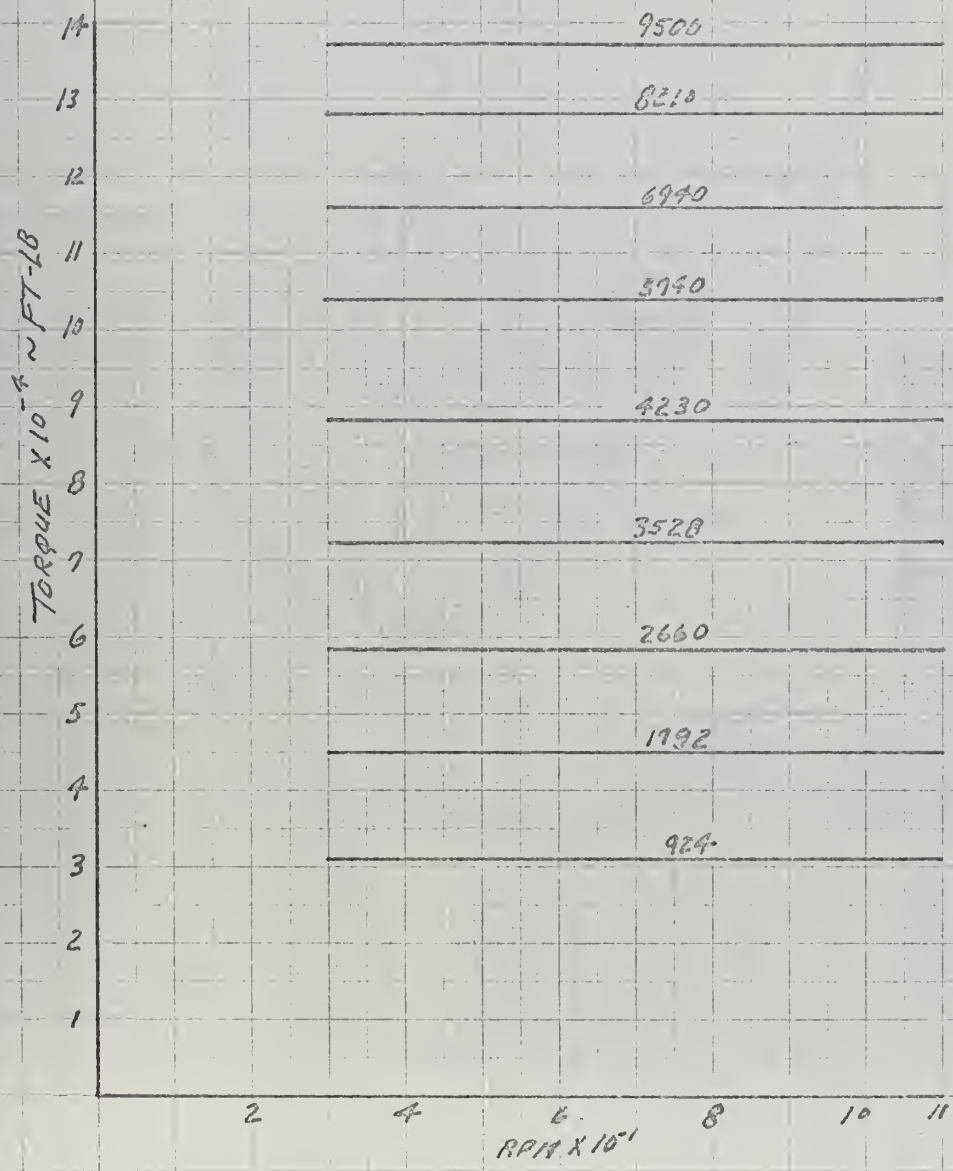


FIG (B-3)





## Technical Specification

No. of cylinders	6, 7, 8 and 9 in-line
12, 14, 16 and 18	
Vee-form	
Bore	15" (381 mm)
Stroke	18" (457 mm)
Compression ratio	11.35 to 1
Maximum continuous r.p.m.	525
Lubricating oil flow rate	approx. 3.45 galls BHP/hr (15.5 litres/cv/hr)
Lubricating oil engine inlet temperature	155°F (68.5°C)
Lubricating oil engine outlet temperature	175°F (79°C)
Lubricating oil drain tank capacity—	approx. 500 gallons (2270 litres)
in-line engines	
Lubricating oil drain tank capacity—	approx. 600 gallons (2730 litres)
vee engines	
Fresh and salt water pump flow rates	5.4 gals/BHP/hr (24.2 litres/cv/hr)
70 ft. head (21.33m)	
Jacket water heat dissipation	800 BTUS BHP/hr (202 kcal/BHP/hr)
Lubricating oil heat dissipation	360 BTUS BHP/hr (88.2 kcal/BHP/hr)
Air charge cooler heat dissipation	610 BTUS BHP/hr (153 kcal/BHP/hr)
Engine cooling water inlet temperature	165°F (74°C)
Engine cooling water outlet temperature	180°F (82°C)
Exhaust gas mass flow	13.25 lb BHP-hr (5.95 kg cv-hr)
Exhaust temperature after turbo-	10.5° (36°C)
charger	at 220 p.s.i.
Fuel consumption—based on operation on fuel having a net calorific value of 18,000 B.t.u./lb	435 lb BHP hr (150 gm cv hr)
Starting air pressure	400 p.s.i. (28 kg/cm <sup>2</sup> )
Thermal efficiency (based on Class A fuel, net calorific value 18,400 BTUs/lb)	41.5%

## KV MAJOR UNI-DIRECTIONAL ENGINE

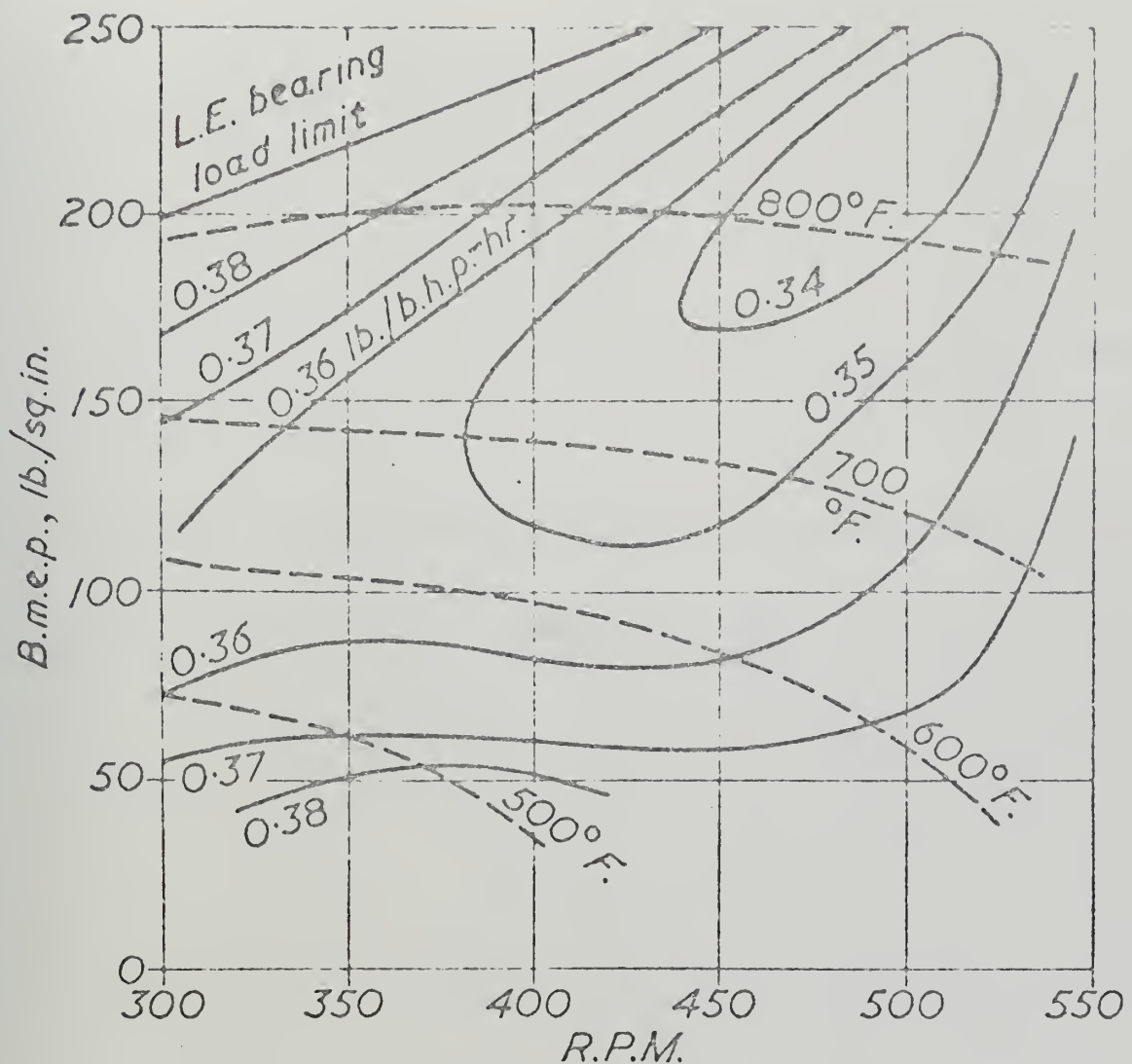
For complete information see separate sheet in pocket inside back cover.

### KEY TO MAIN COMPONENTS

1—Admittent to turbocharger	18—Crankcase leather	40—Exhaust valves rocker transfer link
2—Cylinders water outlet	17—Cylinders	55—Exhaust valves push rod
3—Cylinders	18—Cylinders	56—Exhaust valves push rod
4—Cylinder block bolts	19—Cylinders	57—Exhaust valves seat
5—Heavy fuel manifold	20—Injector nozzle cooling pipes	58—Exhaust valves seat
6—Valve gear lubricating oil manifold	21—Exhaust valves	59—Exhaust valves seat
7—Charge air cooler	22—Exhaust valves	60—Exhaust valves seat
8—Valve gear lubricating oil manifold	23—Exhaust valves	61—Exhaust valves seat
9—Valve gear lubricating oil regulator	24—Exhaust valves	62—Exhaust valves seat
10—Sea water outlet	25—Exhaust valves	63—Exhaust valves seat
11—Sea water inlet	26—Exhaust valves	64—Exhaust valves seat
12—Lubricating oil outlet	27—Exhaust valves	65—Exhaust valves seat
13—Starting air inlet	28—Exhaust valves	66—Exhaust valves seat
14—Air inlet manifold	29—Exhaust valves	67—Exhaust valves seat
15—Fuel pump	30—Exhaust valves	68—Exhaust valves seat
16—Fuel pump	31—Exhaust valves	69—Exhaust valves seat
17—Fuel pump	32—Intake cam follower	70—Exhaust valves seat
18—Glycerine centrifugal lubricating oil by-pass line	33—Intake cam follower	71—Exhaust valves seat
19—Injector nozzle cooling pipes	34—Exhaust cam follower	72—Exhaust valves seat
20—Exhaust valves	35—Exhaust cam follower	73—Exhaust valves seat
21—Exhaust valves	36—Pump cooling oil return valve	74—Exhaust valves seat
22—Exhaust valves	37—Pump bearing and piston	75—Exhaust valves seat
23—Exhaust valve rotor	38—Pump bearing and piston	76—Exhaust valves seat
24—Shaft valve	39—Pump bearing and piston	77—Exhaust valves seat
25—Fuel injection	40—Pump bearing and piston	78—Exhaust valves seat
26—Cylinder head and end tube	41—Pump bearing and piston	79—Exhaust valves seat
27—Fuel pump	42—Pump bearing and piston	80—Exhaust valves seat
28—Fuel pump	43—Pump bearing and piston	81—Exhaust valves seat
29—Fuel pump	44—Column	82—Exhaust valves seat
30—Exhaust valves	45—Crankcase	83—Exhaust valves seat
31—Pump rod bearing and guide	46—Main bearing cap	84—Exhaust valves seat
32—Intake cam follower	47—Connecting rod	85—Exhaust valves seat
33—Intake cam follower	48—Exhaust cam follower	86—Exhaust valves seat
34—Exhaust cam follower	49—Exhaust cam follower	87—Exhaust valves seat
35—Exhaust cam follower	50—Upward exhaust ducts	88—Exhaust valves seat
36—Pump cooling oil return valve	51—Rocking valve outlet	89—Exhaust valves seat
37—Pump bearing and piston	52—Water inlet to head	90—Exhaust valves seat
38—Pump bearing and piston	53—Pressure relief valve	91—Exhaust valves seat
39—Pump bearing and piston	54—Main air filter	92—Exhaust valves seat
40—Pump bearing and piston	55—Fuel pump	93—Exhaust valves seat
41—Pump bearing and piston	56—Fuel pump	94—Exhaust valves seat
42—Pump bearing and piston	57—Fuel pump	95—Exhaust valves seat
43—Pump bearing and piston	58—Fuel pump	96—Exhaust valves seat
44—Pump bearing and piston	59—Fuel pump	97—Exhaust valves seat
45—Crankcase	60—Exhaust valves seat	

CUTAWAY OF KV MAJOR ENGINE (E<sub>100</sub>)





FUEL MAP FOR KV MAJOR 12

Fig. (B-5)



TORQUE VS. FUEL SETTING  
FOR KV MAJOR 12

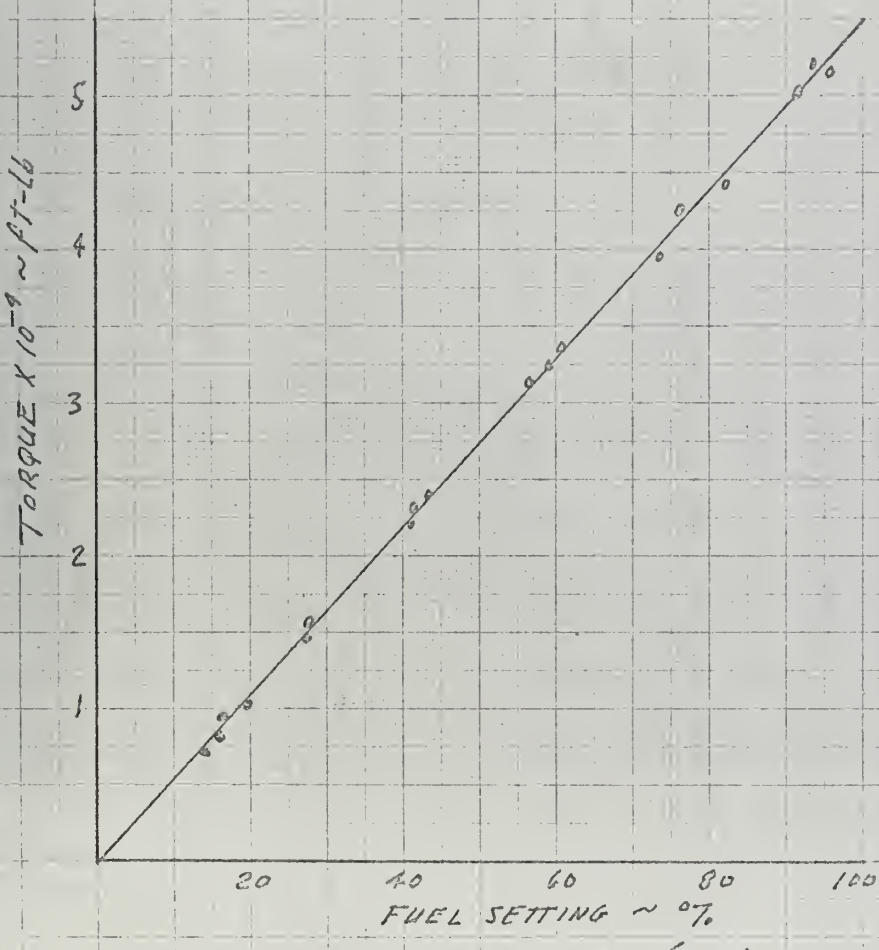


FIGURE (B-6)



SUBROUTINE BURME (WF,TORQ)  
 THIS SUBROUTINE COMPUTES B&W 7K98FF DIESEL TORQUE AS A FUNCTION  
 FUEL SETTING.

FUEL SETTING (WF) MUST BE LIMITED BETWEEN 924. AND 9500.

```

C INPUT TO THIS PROGRAM IS FUEL SETTING (WF); OUTPUT IS TORQUE
C (TORQ) IN FT-LBS
C
  IF(WF .EQ. 924.)GO TO 7
  IF(WF .LE. 172.)GO TO 8
  IF(WF .LE. 2650.)GO TO 9
  IF(WF.LE.3528.)GOTO 10
  IF(WF.LE.4230.)GOTO 11
  IF(WF.LE.5720.)GOTO 12
  IF(WF.LE.6940.)GOTO 13
  IF(WF.LE.8210.)GOTO 14
  IF(WF.LE.9500.)GOTO 15
  TORQ=31100.

 7  RETURN
 8  TORQ=31100.+(WF-924.)*16.
 9  TORQ=45000.+(WF-1792.)*15.55
  RETURN
10  TORQ=53500.+(WF-2660.)*16.2
  RETURN
11  TORQ=72600.+(WF-3528.)*22.9
  RETURN
12  TORQ=88700.+(WF-4230.)*10.35
  RETURN
13  TORQ=104100.+(WF-5740.)*9.92
  RETURN
14  TORQ=116000.+(WF-6940.)*9.67
  RETURN
15  TORQ=128300.+(WF-8210.)*7.375
  RETURN
END

```



## APPENDIX C

Clutches

Figures (C-1) and (C-2), which were provided by the Philadelphia Gear Company, describe the operation of quill shaft version of the firm's synchroclutch. Additional useful information provided by Philadelphia Gear Is:

Inertia ..... Input -174 lb-ft<sup>2</sup>  
Output -110 lb-ft<sup>2</sup>

torsional stiffness\*..... Approx. 270 million in-lb/Rad

Figures (C-3) and (C-4), which were provided by the Koppers Co., describe the operation of the BLH-Dynetic clutches.

\* For information purposes only



## SYNCHROCLUTCH - CROSS SECTION

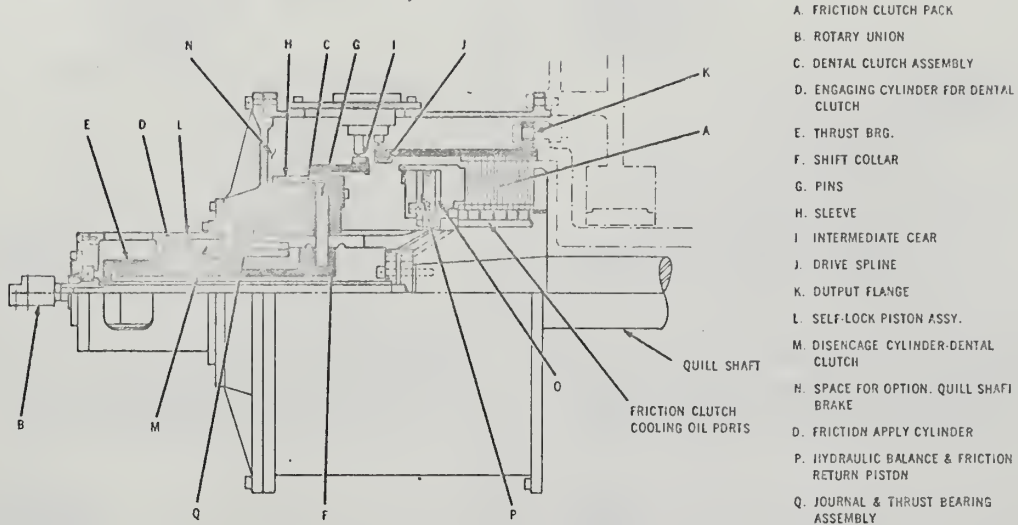


FIG. 2 CROSS SECTION OF TYPICAL SYNCHROCLUTCH (QUILL SHAFT VERSION)

## DESCRIPTION AND OPERATION

The new Philadelphia SYNCHROCLUTCH consists of a friction clutch in parallel with a positive drive dental clutch. The friction clutch synchronizes the driving and driven shafts, after which the dental clutch is engaged to provide a positive drive. The dental clutch features fully crowned, nitrided gears for maximum capacity for a given diameter. The friction clutch is of the multi-disc type with positive oil circulation for long life and heat removal. The friction clutch has ample capacity to absorb thermal loads imposed by the synchronizing cycle—even very high loads encountered when reversing large marine gears in the 40,000 plus HP range. In addition, dead shaft pickup is possible in large marine propulsion systems. This permits the prime mover to be run at speed in port for auxiliaries; such as generators, while retaining the ability to get underway instantly by clutching in the propeller.

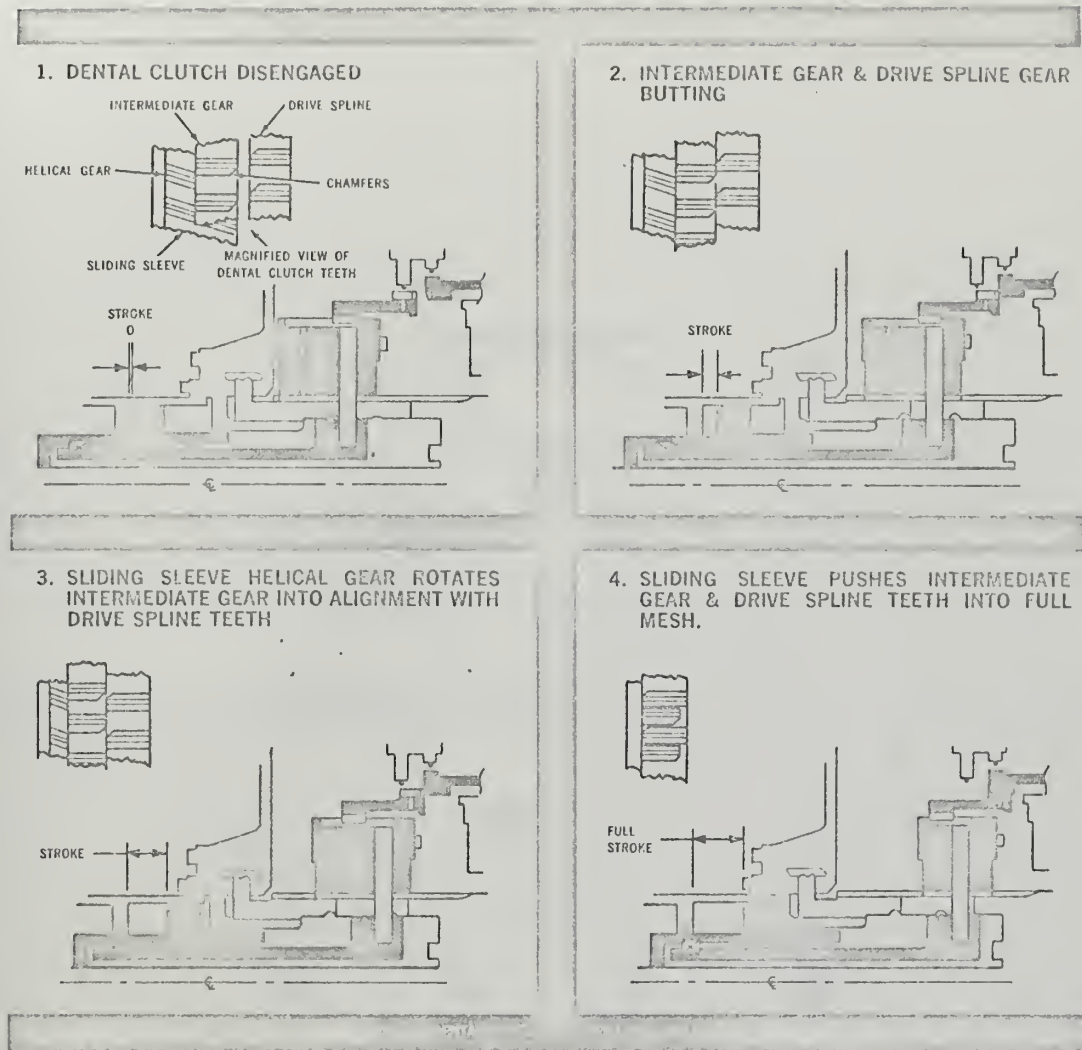
The dental clutch features a unique helical gear element which automatically aligns the teeth of the dental clutch prior to engagement. This feature is illustrated in Fig. 3. The clutch may be actuated hydraulically or pneumatically, using low pressure air (100 psi) or oil (150 psi). The synchronizing action is controlled by a transistorized differential speed control using non-contacting magnetic pick-ups for speed indication and position readout. Once engaged, the dental clutch does not require power to remain in mesh, thus eliminating dependence on electrical or hydraulic power for continued torque transmission.

External jacking is provided for emergency manual engagement and disengagement of the dental clutch.

Referring to Fig. 2, the friction clutch (a) is first engaged to force the driving and driven shafts into synchronism. The clutch is clamped by admitting oil (or air) to the piston through the rotary union (b). After the driving and driven shafts have reached a speed differential of approximately  $\frac{1}{2}\%$ , the transistorized speed control signals for dental clutch (c), engagement by admitting oil (or air) pressure to the engaging side of the dental clutch piston (d). The piston transmits the thrust through a heavy duty thrust bearing (e), to the rotating shift collar (f), which is connected through large pins (g), to the sleeve (h), of the dental clutch. The sleeve carries with it the intermediate gear (i), and meshes with the drive spline (j), on the output flange (k), in the manner illustrated in Fig. 2. A self-locking piston (l) on the dental clutch prevents piston back-off under torque reversal. This action is shown in Fig. 3. To disengage, pressure is admitted to the reverse side (m) of the dental clutch piston, which pulls the dental elements out of engagement as shown in Fig. 3. The friction clutch may then be de-energized to permit the driving and driven shafts to rotate relative to each other. Where desired, a quill shaft brake (n) may be incorporated into the clutch to stop the quill shaft from rotating, due to residual drag torque within the friction clutch. This feature requires no additional length.

Fig. (C-1)





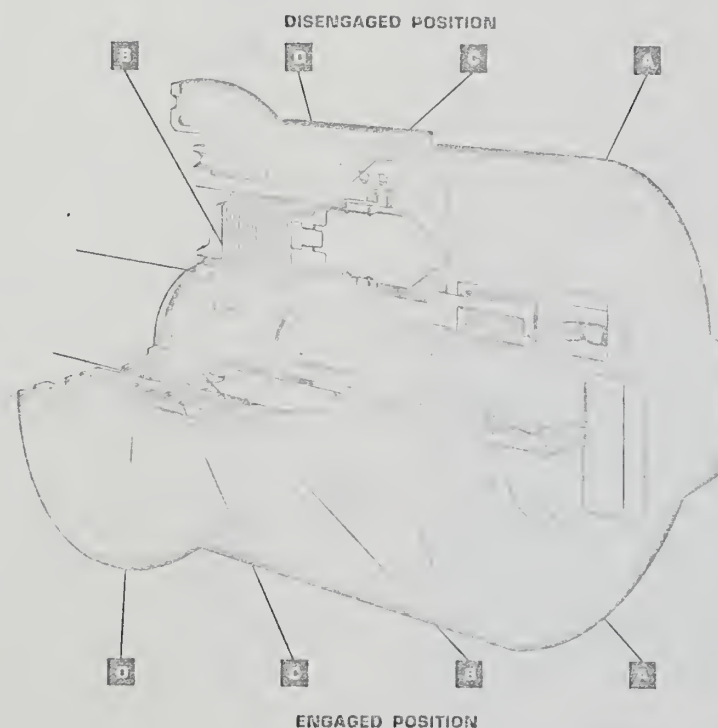
## SPECIFICATIONS

1. SPEED DIFFERENTIAL (INPUT/OUTPUT).	UP TO 100% OF RATED SPEED.
2. ACTUATION FLUID.	OIL @ 150 PSI. (SPECIAL-AIR @ 100 PSI.)
3. FRICTION MATERIAL.	PGC, FS001 GRADE RC1.
4. STEEL DISC MATERIAL.	HARDENED STEEL, HIGH CARBON, GROUND.
5. ROTATING PARTS.	FORGED STEEL, HEAT TREATED AND DYNAMICALLY BALANCED.
6. DENTAL CLUTCH MEMBERS.	NITRIDED STEEL.
7. DENTAL CLUTCH TEETH.	CROWNED, CHAMFERED ON ENTRY SIDE.
8. ROTARY UNION.	EXTERNAL-UNIT CONSTRUCTION.
9. ACCESSIBILITY.	ALL CLUTCH MEMBERS REMOVABLE WITHOUT REMOVING HUB OR QUILL SHAFT.
10. DIRECTION OF ROTATION.	CW OR CCW.
11. PERMISSIBLE AXIAL MOTION OF OUTPUT FLANGE CONNECTION.	$\pm 1/8$ " STANDARD.
12. PERMISSIBLE RADIAL RUNOUT AT OUTPUT FLANGE.	.015 TIR ON 500 SIZE AND LARGER. .010 TIR ON 120 SIZE.
13. ELECTRICAL POWER REQUIREMENTS FOR CONTROLS.	115V, AC 50/60 HZ, 50 WATTS.
14. CLUTCH ENGAGEABLE AT STANDSTILL.	YES.
15. EMERGENCY MANUAL CLUTCH OPERATION.	YES.

OPERATION AND SPECIFICATION OF SYNCHROCLUTCH

Fig. (C-2)





#### FUNDAMENTAL DESIGN

All BLH-Dynetic Clutches are of the same basic design, modified as necessary to meet a wide variety of application conditions.

The forces developed during engagement are completely self-contained, and produce no thrust loads on the shafts or clutch housing. After engagement, power is transmitted through hardened and nitrided coupling teeth in positive mesh, with no loss due to slippage. Hydraulic pressure is required only during the actual engaging or disengaging cycle. The parts are held in their final positions by spring loaded detents, or mechanical locks, as necessary.

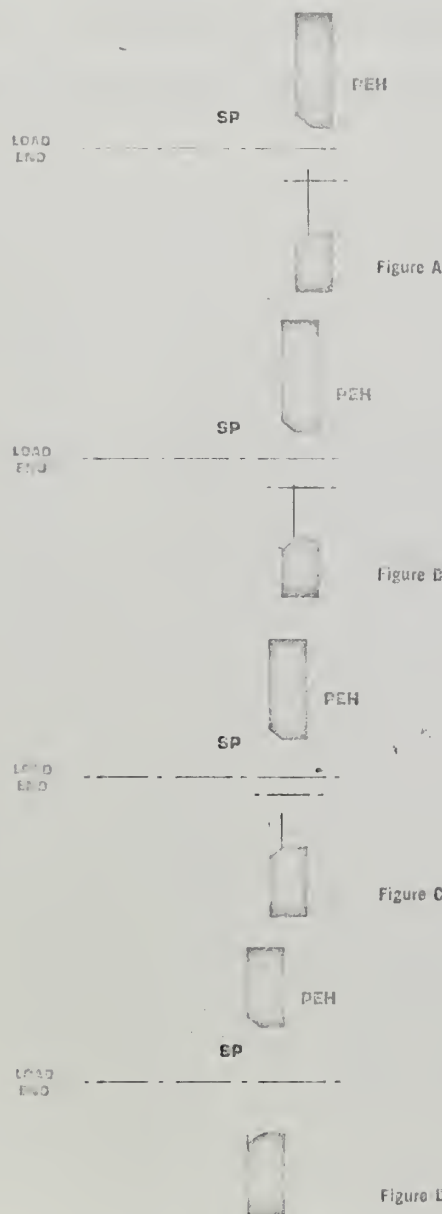
#### MAJOR COMPONENTS

- A** **Operating Cylinder**—to provide the axial force necessary to engage or disengage the clutch. Actuation is usually hydraulic using lubricating oil as the fluid, but pneumatic operation is also available.
- B** **Friction Discs**—to develop friction torque necessary to synchronize the shaft speeds. These discs are cooled by a continuous flow of lubricating oil.
- C** **Transition Torque Control**—spring loaded pins key with lugs in the load end hub to transmit torque during the transition from friction to gear tooth drive, and to align gear teeth prior to engagement.
- D** **Gear Coupling**—to transmit power after engagement is complete and accommodate shaft misalignment, if present.

#### DESCRIPTION OF BLH DYNAMIC CLUTCH

Fig. (C-3)





The heart of the synchronizing mechanism is the cluster of synchronizing pins (SP) which cooperate with the holes in the power end hub (PEH) through which they project to control engagement as indicated by the diagrams at the left.

As engagement begins the actuating piston moves the power end hub and its connected parts toward the load end hub. Through detent action, an initial friction torque is developed which swings the small diameters of the synchronizing pins against the sides of their respective holes in the power end hub, as in Figure A.

Continued pressure brings the cam surfaces of the synchronizing pins into contact with those of the power end hub, thereby transmitting full piston pressure to the friction disc pack as in Figure B. The friction torque so developed acts to synchronize shaft speeds. The geometry of the assembly is such that the parts remain in the position shown as long as slipping occurs in the friction discs.

Slipping stops at the friction discs when the shaft speeds synchronize. This unbalances the forces and permits the power end hub to advance over the synchronizing pins as in Figure C. At the same time, spring loaded pins are moved into spaces between lugs in the end of the load end hub, acting as loose keys to control torque until the coupling teeth engage.

As the synchronizing pins become aligned with their mating holes as in Figure D, the cam surfaces separate, removing the axial force on the friction disc pack. This permits the spring loaded pins to contact the sides of their lugs, maintaining synchronism of shaft speeds and aligning the coupling teeth for engagement as the piston completes its travel.

With completion of engagement the hydraulic pressure is cut off, and the assembly transmits power as a simple gear-type coupling.

During disengagement the piston moves the parts away from the load end hub, disengaging the spring-loaded pins from their lugs before the coupling teeth disengage, and securing the assembly in the final position to prevent dynamic unbalance.

#### OPERATION OF BLH DYNAMIC CLUTCH

Fig. (C-4)



## APPENDIX D

Propeller Subroutines

This appendix contains the computer programs used to model the B4-70 (P/D = 1.) propeller and Read's CRPP, both of which are discussed in Section 4. Included in this appendix is the program described in Section 5.4 that computes shaft friction.



SUBROUTINE PRPLR(VA,SRPS,CT,CQ)  
 THIS SUBROUTINE COMPUTES THRUST AND TORQUE COEFFICIENTS FOR  
 34-70 PROPELLER HAVING A PITCH RATIOIC CF 1.  
 ENTERING ARGUMENTS ARE PRPELLER SPEED OF ADVANCE (VA) AND  
 PROPELLER ROTATION RATE (SRPS). OUTPUTS ARE THRUST AND TORQUE  
 COEFFICIENTS, CT AND CQ RESPECTIVELY.  
  
 CT=T/(.5\*RH0\*(3.14/4.)\*(D\*\*2)\*(VA\*\*2+.7\*SRPS\*(D\*\*2)))  
 CQ=Q/(.5\*RH0\*(3.14/4.)\*(D\*\*3)\*(VA\*\*2+.7\*SRPS\*(D\*\*2)))  
  
 RHO=FLUID DENSITY  
 VA=PROPELLER SPEED OF ADVANCE  
 SRPS=PROPELLER ROTATION RATE  
 D=PROPELLER DIAMETER  
 T=THRUST  
 C=TORQUE  
 IF(SRPS .EQ. 0. .AND. VA .GT. 0.) GC TO 10  
 IF(SRPS .EQ. 0. .AND. VA .LT. 0.) GO TO 11  
 B=ATAN(VA/(33.\*SRPS))  
 IF(SRPS .LT. 0.) B=B+3.14  
 IF(B .LT. 0.) B=B+6.28  
 GC TO 12  
 10 B=1.57  
 GC TO 12  
 11 B=4.71  
 12 CONTINUE  
 CT=.025350+.17820\*COS(B)-.74777\*SIN(B)+.014674\*COS(2.\*B)-.013822\*S  
 1\*IN(2.\*B)+.028054\*COS(3.\*B)+.100777\*SIN(3.\*B)-.016328\*COS(4.\*B)-.011  
 2318\*SIN(4.\*B)-.053041\*COS(5.\*B)+.047186\*SIN(5.\*B)+.00060605\*COS(6.  
 3.\*B)+.010666\*SIN(6.\*B)+.036823\*COS(7.\*B)-.0090239\*SIN(7.\*B)-.002542  
 49\*COS(8.\*B)-.0078452\*SIN(8.\*B)-.017680\*COS(9.\*B)+.023941\*SIN(9.\*B)  
 5+.\*0027331\*COS(10.\*B)+.0080787\*SIN(10.\*B)+.021436\*COS(11.\*B)  
 CQ=.024645+.26718\*COS(B)-1.1081\*SIN(B)+.016056\*COS(2.\*B)+.0015909\*  
 1\*SIN(2.\*B)+.065822\*COS(3.\*B)+.15455\*SIN(3.\*B)-.022497\*COS(4.\*B)-.02  
 20601\*SIN(4.\*B)-.078062\*COS(5.\*B)+.085343\*SIN(5.\*B)+.0024126\*COS(6.  
 3.\*B)+.0087856\*SIN(6.\*B)+.061475\*COS(7.\*B)-.031327\*SIN(7.\*B)-.016065



```
4*COS(8.*B)-.0096650*SIN(8.*B)-.033291*COS(9.*B)+.04319*SIN(9.*B)+.
5012311*COS(10.*B)+.012453*SIN(10.*B)
CG=.1*CG
RETURN
END
```



PAGE 1

05/03/

SUBROUTINE CRPP (J,CQ,CT,AP1,AP8,BP1,BP8,AM8,AM1,BM8,BM1,AM4,BM4,A  
2M2,BM2,AM0,BM0,AP4,BP4,PD)

CRPP COMPUTES MODIFIED THRUST AND TORQUE COEFFICIENTS FOR A GIVEN  
VALUE OF MODIFIED ADVANCE COEFFICIENT AND PITCH DIAMETER RATIO.

PROPELLOR DATA IS TAKEN FROM DYNAMIC ANALYSIS AND SIMULATION  
OF SHIP AND PROPULSION PLANT MANUVERING PERFORMANCE BY WENDEL  
AND DUNNE APPEARING IN PROCEEDINGS OF THE SECOND SHIP CONTROL  
SYSTEMS SYMPOSIUM.

MODIFIED ADVANCE COEFF.....J=VA/SQRT(VA\*\*2+(N\*D)\*\*2)

MODIFIED THRUST COEFF...CT=T/(RHO\*(D\*\*2)\*(VA\*\*2+(N\*D)\*\*2))

MODIFIED TORQUE COEFF...CQ=Q/(RHO\*(D\*\*3)\*(VA\*\*2+(N\*D)\*\*2))

RHO=DENSITY OF WATER

D=PROPELLOR DIAMETER

VA=PROPELLOR SPEED OF ADVANCE

N=PROPELLOR ROTATION RATE

T=THRUST

Q=TORQUE

PITCH DIAMETER RATIOS ARE LIMITED BETWEEN +1.6 TO -1.2  
ENTERING ARGUMENTS ARE MODIFIED ADVANCE COEFFICIENT (J) AND  
PITCH DIAMETER RATIO (PD)

OUTPUTS ARE CQ AND CT

REAL J

IF(J.LE.-.8)GOTO10

IF(J.LE.-.4)GOTO11

IF(J.LE.-.2)GOTO12

IF(J.LE.0.)GOTO13

IF(J.LE..4)GOTO14

IF(J.LE. .8)GOTO15

CALL PLUS1 (PD,AP1,BP1)

CALL PLUS8 (PD,AP8,BP8)

F=(J-.8)\*5.

CQ=AP8+F\*(AP1-AP8)

CT=BP8+F\*(BP1-BP8)

RETURN

10 CALL M10NE (PD,AM1,BM1)

CALL MIN8 (PD,AM8,BM8)

F=(J+1.)\*5.

CQ=AM1+F\*(AM8-AM1)

CT=BM1+F\*(BM8-BM1)

RETURN

11 CALL MIN4 (PD,AM4,BM4)

CALL MIN8 (PD,AM8,BM8)

F=(J+.8)\*5.

CQ=AM8+F\*(AM4-AM8)

CT=BM8+F\*(BM4-BM8)

RETURN

12 CALL MIN2 (PD,AM2,BM2)

CALL MIN4 (PD,AM4,BM4)



PAGE 2

```

F=(J+.4)*5.
CQ=AM4+F*(AM2-AM4)
CT=BM4+F*(BM2-BM4)
RETURN
13 CALL ZERO (PD,AM0,BM0)
CALL MIN2 (PD,AM2,BM2)
F=(J+.2)*5.
CQ=AM2+F*(AM0-AM2)
CT=BM2+F*(BM0-BM2)
RETURN
14 CALL PLUS4 (PD,AP4,BP4)
CALL ZERO (PD,AM0,BM0)
F=J*2.5
CQ=AM0+F*(AP4-AM0)
CT=BM0+F*(BP4-BM0)
RETURN
15 CALL PLUS8 (PD,AP8,BP8)
CALL PLUS4 (PD,AP4,BP4)
F=(J-.4)*2.5
CQ=AP4+F*(AP8-AP4)
CT=BP4+F*(BP8-BP4)
RETURN
END
SUBROUTINE PLUS1 (PD,AP1,BP1)
IF(PD.GE. .63)GOTO10
AP1=-.477*PD-.015
GOTO11
10 AP1=.00516*PD-.049
11 BP1=-.4
RETURN
END
SUBROUTINE PLUS8 (PD,AP8,BP8)
IF(PD.GE. .35)GOTO10
AP8=-.06*PD
GOTO11
10 AP8=.026*PD-.03
11 IF(PD.LT.-.4)GOTO12
IF(PD.GT. .4) GOTO13
BP8=.085*PD-.275
RETURN
12 BP8=.165*PD-.243
RETURN
13 BP8=.243*PD-.3382
RETURN
END
SUBROUTINE PLUS4 (PD,AP4,BP4)
IF(PD.GT. .4)GOTO10
IF(PD.LT. -.4)GOTO11
AP4=.015
GOTO12
10 AP4=.0848*PD-.019
GOTO12
11 AP4=-.123*PD-.0325
12 IF(PD.LT. -.4)GOTO13
IF(PD .GT. .4) GOTO14
BP4=.245*PD-.9

```



PAGE 3

```
      RETURN
13  BP4=.37*PD-.04
      RETURN
14  BP4=.415*PD-.158
      RETURN
      END
      SUBROUTINE ZERO (PD,AM0,BM0)
      IF(PD.LT.-.4)GOTO10
      IF(PD.GT. .4)GOTO11
      AM0=.0125
      GOTO12
10  AM0=-.125*PD-.0375
      GOTO12
11  AM0=.1092*PD-.0311
12  IF(PD.LT.-.625)GOTO13
      IF(PD.GT. .425)GOTO14
      BM0=.310*PD+.020
      RETURN
13  BM0=.53*PD+.1575
      RETURN
14  BM0=.53*PD-.0732
      RETURN
      END
      SUBROUTINE MIN2 (PD,AM2,BM2)
      IF(PD .GT. .045)GOTO10
      IF(PD .LT. -.0475)GOTO11
      AM2=.0125
      GOTO12
10  AM2=.123*PD-.043
      GOTO12
11  AM2=-.132*PD-.05
      GOTO12
12  IF(PD .LT. -.625)GOTO13
      IF(PD .GT. .425)GOTO14
      BM2=.310*PD+.02
      RETURN
13  BM2=.53*PD+.1575
      RETURN
14  BM2=.53*PD-.0732
      RETURN
      END
      SUBROUTINE MIN4 (PD,AM4,BM4)
      IF(PD.LT.-.425)GOTO10
      IF(PD.GT. .275)GOTO11
      AM4=.006
      GOTO12
10  AM4=-.0925*PD-.0335
      GOTO12
11  AM4=.0725*PD-.014
12  IF(PD .GT. .88) GOTO13
      IF(PD .LT. -.36)GOTO14
      BM4=.184*PD+.076
      RETURN
13  BM4=.5*PD-.202
      RETURN
14  BM4=.4*PD+.145
```



```
RETURN
END
SUBROUTINE MIN8 (PD,AM8,BM8)
IF(PD .LT. -.55)GOTO10
AM8=.07*PD
GOTO13
10 AM8=-.028*PD-.054
13 IF(PD .LT. -.45)GOTO11
  IF(PD .GT. .42) GOTO12
  BM8=.09*PD+.2760
  RETURN
11 BM8=.21*PD+.33
  RETURN
12 BM8=.283*PD+.1652
  RETURN
END
SUBROUTINE M1ONE (PD,AM1,BM1)
AM1=.064*PD-.018
IF(PD .GT. .6)GOTO11
IF(PD .LE. .400)GOTO10
BM1=-.88*PD+.743
RETURN
10 BM1=.391
  RETURN
11 BM1=.215
  RETURN
END
```



PAGE 1

```
SUBROUTINE SHAFT (SN,QF)
THIS SUBROUTINE COMPUTES SHAFT FRICTION

ENTERING ARGUMENT IS SHAFT ROTATION RATE (SN) IN REV PER SECOND
OUTPUT IS FRICTION TORQUE (QF) IN FT-LBS

SN=ABS(SN)
IF(SN.LE..417)GOTO10
QF=SN*6000.
RETURN
10 QF=2500.
RETURN
END
```



## APPENDIX E

Ship Dynamics1. Ship Propulsion Equations

The ship propulsion equations with no external forces or rudder movement are the two first-order, non-linear, differential equations given below:

$$m \frac{dv}{dt} = T - R \quad (\text{thrust equation})$$

$$\frac{dn}{dt} = Q_D - Q_F - Q_p \quad (\text{torque equation})$$

$v$  = ship velocity (ft/sec)

$T$  = thrust (lbs)

$R$  = resistance (lbs)

$m$  = mass of ship plus 10% ( $\frac{\text{lb}\cdot\text{sec}^2}{\text{ft}}$ )

$I$  = rotational inertia of drive shaft ( $\text{lb}\cdot\text{ft}\cdot\text{sec}^2$ )

$Q_D$  = prime mover drive torque on propeller (lb-ft)

$Q_F$  = shaft friction torque (lb-ft)

$Q_p$  = propeller torque (lb-ft)

$n$  = propeller angular speed (rev/sec)

The two equations are coupled through the propeller terms  $T$  and  $Q_p$ . The equations were solved simultaneously on an IBM 1130 computer using a fourth order Runge-Kutta integration technique.

2. Sign Convention

The sign convention used here is that propeller angular speed,  $n$ , and velocity,  $v$ , are defined as positive for forward ship motion. Torques are considered positive when acting in the direction of



## APPENDIX E (Cont'd)

## 2. (Cont'd)

positive  $n$ ; thrusts are considered positive in the direction of positive  $v$ .

3. Ship Displacement

For all simulations, a ship with a displacement of 4000 tons was used. In the equations of motion, 10% of this figure was included to account for entrained water.



## APPENDIX F

FT4A-2 Drive Train1. Digital Simulation of an FT4A-2 Forward Drive Train

Figure (F-1) is a sketch of a drive train powered by two FT4A-2 marine gas turbines that was used in the simulations. Except for the propeller the drive train is basically the same used by Rubis in Reference (11). The reduction gear ratios relate propeller speed and torque to power turbine speed and torque.

The drive train moment of inertia was assumed to be the same as Rubis', viz.,  $2.88 \times 10^5$  lb-ft-sec<sup>2</sup> (referred to propeller shaft).

It should be noted that at high speeds and low fuel rates, the FT4A-2 gas turbine subroutine will yield negative torques. A statement was made in the main program to ignore this and substitute instead a linear windage torque of the form,

$$Q = -2N + 3000 \text{ (ft-lb)}$$

N = Free Turbine Speed (RPM)

For the crashback simulation, a Falk clutch whose torque capacity is

$$Q_c = 5687.5 \quad P_{\text{net}}$$

where

$P_{\text{net}}$  = net air pressure acting on shoes

was used (cf. section 3.2). A supply air pressure of 200 psi was assumed. The criteria for clutch disengagement was the same used by Rubis in Reference (11): whenever the propeller torque "seen" by the clutch exceeded clutch torque, clutch disengagement was



## APPENDIX F (Cont'd)

## 1. (Cont'd)

was assumed to have taken place instantaneously. For the crash-back simulation, the equation for forward clutch disengagement torque was

$$Q_c = 5687.5 (195-30t-4N^2) \text{ (ft-lb)}$$

$t$  = time (sec)

$N$  = propeller shaft rotation rate (rev/sec)

The propeller torque opposing the forward clutch was

$$Q_{pc} = \frac{Q_p}{K_3} = \frac{Q_p}{4.3197}$$

$K_3$  = reduction gear ratio (see fig. (F-1))

$Q_p$  = propeller torque ft-lbs

During reverse clutch engagement, reverse clutch torque is given by

$$Q_{CR} = 5687.5 (5t-5-4n^2) \text{ (ft-lb)}$$

$t$  = time (sec)

$n$  = propeller shaft rotation rate (rev/sec)

The open drive train is defined to exist whenever the quantity  $(5t-5-4n^2)$  is negative; if this occurs,  $Q_{CR}$  is set to a zero value obviating a negative value for clutch torque. A slip speed across the clutch exists during reverse clutch engagement and this is given by

$$N_{slip} = K_3 N - \left( - \frac{N_3}{K_1 K_2} \right)$$

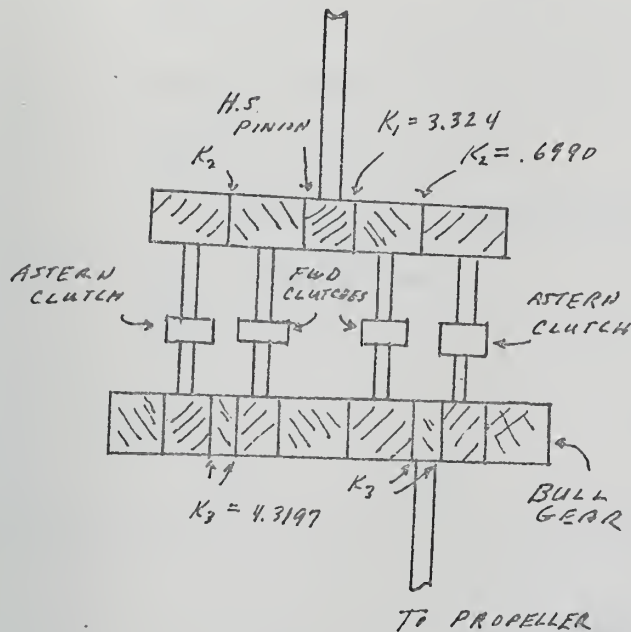
$N$  = propeller rotation rate (rpm)

$N_3$  = power turbine speed (rpm)



ONLY ONE GAS TURBINE SHOWN

To GAS TURBINE (FT4A-2)



#### DRIVE TRAIN MOMENT OF INERTIAS

GOING AHEAD	$2.88 \times 10^5$	16-ft-sec <sup>2</sup>	(REFERRED TO PROPELLOR SHAFT)
GOING ASTERN	$2.36 \times 10^5$	16-ft-sec <sup>2</sup>	(REFERRED TO PROPELLOR SHAFT)
WITH CLUTCHES OPEN:			
GAS TURBO. END	$1.05 \times 10^3$	16-ft-sec <sup>2</sup>	(REFERRED TO GAS TURB. SHAFT)
PROP END	$.71 \times 10^5$	16-ft-sec <sup>2</sup>	(REFERRED TO PROP SHAFT)

FT4A-2 DRIVE TRAIN ARRANGEMENT

FIG (F-1)



## APPENDIX F (Cont'd)

## 1. (Cont'd)

$K_1, K_2, K_3$ , = reduction gear ratios

The product of  $N_{\text{slip}}$  and  $Q_{\text{CR}}$  is the power dissipated in the clutch, and the integral of power over time is a measure of the energy absorbed in the clutch.

Reverse clutch engagement was assumed to exist the instant  $N_{\text{slip}}$  equaled zero.



## APPENDIX G

LM2500-A Drive Train1. Digital Simulation of an LM2500-A Powered Drive Train

Figure (G-1) is a sketch of the drive train powered by two LM2500-A marine gas turbines with a controllable reversible pitch propeller (CRPP). A popular control strategy is to increase speed by first increasing propeller pitch while keeping shaft rotation rate constant; once full pitch is attained, shaft rotation rate is increased.(24) A proportional-integral controller of the form

$$\frac{W_F}{RPM} = 5 + \frac{2.5}{s}$$

$W_F$  = fuel rate (lb/hr)

RPM = (ordered shaft RPM)-(Actual Shaft RPM) (RPM)

$s$  = differential operator

was used in one simulation to keep shaft rotation rate constant while increasing pitch.

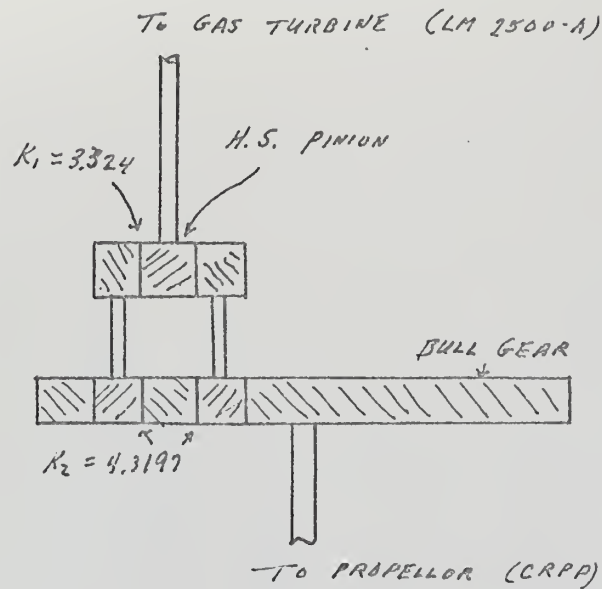
As in the FT4A-2 subroutine, the LM2500-A subroutine will also yield negative torques for high power turbine RPM and low fuel rates. These torques were also ignored and a windage torque expressed by

$$Q_W = -1.965 N + 5500 \text{ (ft-lb)}$$

$N$  = power turbine speed (RPM)



ONLY ONE GAS TURBINE SHOWN



DRIVE TRAIN MOMENT OF INERTIA

$2.5 \times 10^5$  LB-FT-SEC<sup>2</sup> (REFERRED TO PROPELLOR SHAFT)

LM2500-A DRIVE TRAIN ARRANGEMENT

FIG (G-1)



SUBROUTINE EGSIM  
 STOPPING THE SHIP WITH THE FT4A-2  
 COMMNCN T, DT, Y(20),DY(20),STIME,FTIME,NEWDT  
 VA=.96\*Y(2)  
 CALL PRPLR ( VA,CT,CQ )  
 DENOM=VA\*\*2+(33.0\*Y(1))\*\*2  
 COMPUTE PROPELLOR TORQUE Y(5)  
 Y(5)=262.5\*DENO\*CT  
 COMPUTE PROPELLOR THRUST  
 Y(6)=171.5\*DENO\*CT  
 PROPELLOR THROUST IS REDUCED BY THRUST DEDUCTION FACTOR  
 Y(6)=Y(6)\*.98  
 ETA IS REDUCTION GEAR EFFICIENCY AS A FUNTION OF SHAFT SPEED  
 ETA=.75+.22\*(1.0-EXP(-ABS(Y(1))/1.04))  
 Y(7) IS FUEL FLOW AS A FUNTION OF TIME FOR THIS MANEUVER  
 Y(7)=1600.+2600.\*(T-11.119)  
 IF(Y(7)>6T,12000.,Y(7)=12000.  
 RT IS SHIP RESISTANCE AS A FUNTION OF SHIP'S SPEED  
 RT=104.8\*(Y(2))\*\*2  
 SHAFT COMPUTES SHAFT FRICTION  
 SN=Y(1)  
 CALL SHAFT (SN, QF)  
 AN3=600.25\*(-Y(1))  
 Y(9) IS POWER TURPINE SPEED IN RPM  
 Y(9)=AN3  
 WF=Y(7)  
 FT4A2 COMPUTES GAS TURBINE TORQUE  
 CALL FT4A2 ( AN3,WF, C3 )  
 IF( Q3 > LT, 0. ) Q3=-2.\*AN3+3000.  
 Q3=Q3-2165.2  
 DELAY=.3+.7\*(1.-EXP(-.4\*(T-11.119)))  
 Q3=Q3\*DELAY  
 Q3=Q3+2165.2  
 Y(8) IS POWER TURBINE TORQUE DIVIDED BY 100  
 Y(8)=Q3\*.01  
 QD IS GAS TURBINE TORQUE MODIFIED BY REDUCTION GEAR FACTOR



```

QD=-29.1*Q3*ETA
C Y(1) IS SHAFT SPEED IN RPS
C FY(1)=(QD-QE-Y(5))*6.75E-7
C Y(2) IS SHIP'S VELOCITY IN FPS
C CY(2)=(Y(6)-RT)*3.33E-6
C Y(3) IS DISTANCE TRAVELED BY SHIP
C DY(3)=Y(2)
C Y(4) IS SHIP'S VELOCITY IN KNOTS
C Y(4)=.591*Y(2)
C Y(19) IS THRUST COEFFICIENT
C Y(19)=CT
C Y(20) IS TORQUE COEFFICIENT
C Y(20)=CO
C IF(Y(2).LE.0.)FTIME=T
C IF(T.GT.16.)DT=.4
C RETURN
C END

```



C SUBROUTINE EOSIM  
C ACCELERATING FROM 5 KNOTS WITH THE FT4A-2  
COMMON T, DT, Y(20), DY(20), STIME, FTIME, NEWDT  
VA=.96\*Y(2)  
CALL PRPLR (VA,CT,CQ)  
DENOM=VA\*\*2+(33.\*Y(1))\*\*2  
C COMPUTE PROPELLOR TORQUE Y(5)  
Y(5)=262.5\*DENO\*CQ  
C COMPUTE PROPELLOR THRUST  
Y(6)=171.5\*DENO\*CT  
C PROPELLOR THRUST IS REDUCED BY THRUST DEDUCTION FACTOR  
Y(6)=Y(6)\*.98  
C ETA IS REDUCTION GEAR EFFICIENCY AS A FUNCTION OF SHAFT SPEED  
ETA=.75+.22\*(1.0-EXP(-Y(1)/1.04))  
C Y(7) IS FUEL FLOW A A FUNCTION OF TIME FOR THIS MANEUVER  
Y(7)=2500.+(-EXP(-T))\*9500.  
C RT IS SHIP RESISTANCE AS A FUNCTION OF SHIP'S SPEED  
RT=104.8\*(Y(2))\*\*2  
C SHAFT COMPUTES SHAFT FRICTION  
SN=Y(1)  
CALL SHAFT (SN,QF)  
AN3=861.\*Y(1)  
WF=Y(7)  
C FT4A2 COMPUTES POWER TURBINE TORQUE  
CALL FT4A2 (AN3,WF,Q3)  
DELAY=.3+.7\*(1.-EXP(-.4\*T))  
Q3=Q3-814.  
Q3=Q3\*DELAY  
Q3=Q3+814.  
C Y(9) IS POWER TURBINE TORQUE  
Y(9)=Q3  
C QD IS POWER TURBINE TORQUE MODIFIED BY REDUCTION GEAR FACTOR  
QD=28.72\*Q3\*ETA  
C Y(1) IS SHAFT SPEED IN RPS  
DY(1)=(QD-QF-Y(5))\*5.54E-7  
C Y(8) IS SHAFT SPEED IN RPM DIVIDED BY 100.  
Y(8)=.6\*Y(1)  
C Y(2) IS SHIP'S VELOCITY IN FPS  
DY(2)=(Y(6)-RT)\*3.33E-6  
C Y(3) IS DISTANCE TRAVELED BY SHIP  
DY(3)=Y(2)  
C Y(4) IS SHIP'S VELOCITY IN KNOTS  
Y(4)=.591\*Y(2)  
C Y(16) IS PROPELLOR THRUST COEFFICIENT  
Y(16)=CT  
C Y(17) IS PROPELLOR TORQUE COEFFICIENT  
Y(17)=CQ  
IF(T .GT. 10.)DT=1.  
RETURN  
END



```

SUBROUTINE EQSIM
C STOPPING THE SHIP WITH THE FT4A-2
COMMON T, DT,Y(20),DY(20),STIME,FTIME,NEWDOT
VA=.96*Y(2)
CALL PRPLR (VA,CT,CQ)
DENOM=VA**2+(33.*Y(1))**2
C COMPUTE PROPELLOR TORQUE Y(5)
Y(5)=262.5*DENOM*CQ
C COMPUTE PROPELLOR THRUST
Y(6)=171.5*DENOM*CT
C PROPELLOR THRUST IS REDUCED BY THRUST DEDUCTION FACTOR
Y(6)=Y(6)*.98
C ETA IS REDUCTION GEAR EFFICIENCY AS A FUNTION OF SHAFT SPEED
ETA=.75+.22*(1.0-EXP(-ABS(Y(1))/1.04))
C Y(7) IS FUEL FLOW AS A FUNCTION OF TIME FOR THIS MANUVER
Y(7)=1600.+2600.*(T-11.119)
IF(Y(7) .GT. 12000.)Y(7)=12000.
C RT IS SHIP RESISTANCE AS A FUNTION OF SHIP'S SPEED
RT=104.8*(Y(2))**2
C SHAFT COMPUTES SHAFT FRICTION
SN=Y(1)
CALL SHAFT (SN,QF)
AN3=600.25*(-Y(1))
C Y(9) IS POWER TURBINE SPEED IN RPM
Y(9)=AN3
WF=Y(7)
C FT4A2 COMPUTES GAS TURBINE TORQUE
CALL FT4A2 (AN3,WF,Q3)
IF(Q3 .LT. 0.)Q3=-2.*AN3+3000.
Q3=Q3-2165.2
DELAY=.3+.7*(1.-EXP(-.4*(T-11.119)))
Q3=Q3*DELAY
Q3=Q3+2165.2
C Y(8) IS POWER TURBINE TORQUE DIVIDED BY 100
Y(8)=Q3*.01
C QD IS GAS TURBINE TORQUE MODIFIED BY REDUCTION GEAR FACTOR
QD=-20.1*Q3*ETA
C Y(1) IS SHAFT SPEED IN RPS
DY(1)=(QD-QF-Y(5))*6.75E-7
C Y(2) IS SHIP'S VELOCITY IN FPS
DY(2)=(Y(6)-RT)*3.33E-6
C Y(3) IS DISTANCE TRAVELED BY SHIP
DY(3)=Y(2)
C Y(4) IS SHIP'S VELOCITY IN KNOTS
Y(4)=.591*Y(2)
C Y(19) IS THRUST COEFFICIENT
Y(19)=CT
C Y(20) IS TORQUE COEFFICIENT
Y(20)=CQ
IF(Y(2).LE. 0.)FTIME=T
IF(T .GT. 16.)DT=.4
RETURN
END

```



```

SUBROUTINE EQSIM
REAL J
COMMON T,DT,Y(20),DY(20),STIME,FTIME,NEWDT
C Y(1) IS SHAFT SPEED IN RPS
C Y(2) IS SHIP'S SPEED IN FPS
C Y(3) IS A PI CONTROLLER PARAMETER
C Y(4) IS DISTANCE TRAVELED BY SHIP
C Y(5) IS PITCH DIAMETER RATIO FOR CRPP
C Y(6) IS FUEL FLOW IN LB/HR
C Y(7) IS POWER TURBINE SPEED IN RPM
C Y(8) IS HYDRAULIC FLUID FLOW TO CRPP IN GAL/SEC
C Y(9) IS PROPELLER TORQUE
C Y(10) IS PROPELLER THRUST
C Y(11) IS LM2500 POWER TURBINE TORQUE
C VA=.96*Y(2)
DENOM=VA*VA+Y(1)*Y(1)*225.
J=VA/SQRT(DENOM)
Y(8)=1.+4.35*Y(1)
DY(5)=-.0528-.0100*Y(5)*Y(5)*Y(8)
IF(Y(5)<0. LT. -1.2)Y(5)=-1.2
PD=Y(5)
CALL CRPP (J,CQ,CT,AP1,AP8,BP1,BP8,AV8,AM1,BM8,BM1,AM4,BM4,A
2M2,BM2,AMC,BM0,AP4,BP4,PD)
C Y(12) IS PROPELLER TORQUE COEFFICIENT
C Y(13) IS PROPELLER THRUST COEFFICIENT
Y(12)=CQ
Y(13)=CT
Y(9)=6720.*DENOM*Y(12)
Y(10)=448.*DENOM*Y(13)
C THRUST IS REDUCED BY THRUST DEDUCTION FACTOR
Y(10)=.99*Y(10)
C RT IS SHIP RESISTANCE IN LBS AS A FUNCTION OF SHIP'S SPEED
C RT=104.8*Y(2)*Y(2)
C SHAFT COMPUTES SHAFT FRICTION AS A FUNCTION OF SHAFT SPEED
C SN=Y(1)
CALL SHAFT (SN,QF)

```



```

C CALL SHAFT (SN, QF)
C RPM IS POWER TURBINE SPEED
C RPM=861.*Y(1)
C WF=Y(6)
C LN250 COMPUTES POWER TURBINE TORQUE AS A FUNCTION OF WF AND RPM
C CALL LN250 (RPM,WF,TORQ,A08,A16,A2,A3,A4,A5,A6,A7,A99)
C IF(TORQ .LT. 0.)TORQ=-1.965*RPM+5500.
C Y(11)=TORQ
C QD IS GAS TURBINE TORQUE MODIFIED BY PREDUCTION GEAR FACTOR
C ETA=.75+.22*(1.0-EXP(-Y(1)/1.04))
C QD=28.72*Y(11)*ETA
C DY(1)=(QD-QF-Y(9))*6.37E-7
C DY(2)=(Y(10)-RT)*3.33E-6
C RPSO IS ORDERED SHAFT ROTATION RATE IN REV/SEC
C RPSO=2.06
C IF(Y(5) .EQ. 1.6)RPSO=3.06
C Y(7)=RPSO-Y(1)
C DY(3)=300.*Y(7)
C Y(6)=Y(3)+2.4*Y(7)
C THE FOLLOWING IF STATEMENTS LIMIT FUEL FLOW BETWEEN 800 LB/HR
C AND 9900 LB/HR
C IF(Y(6) .GT. 9900.)Y(6)=9900.
C IF(Y(6) .LT. 800.)Y(6)=800.
C DY(4)=Y(2)
C RETURN
C END

```



SUBROUTINE EOSIM  
INCREASING SPEED FROM 15 KNOTS TO 30 KNOTS

REAL J  
COMMON T, DT, Y(20), DY(20), STIME, FTIME, NEWDT

C Y(1) IS SHAFT SPEED IN RPS  
C Y(2) IS SHIP'S SPEED IN FPS  
C Y(3) IS A PI CONTROLLER PARAMETER  
C Y(4) IS DISTANCE TRAVELED BY SHIP  
C Y(5) IS PITCH DIAMETER RATIO FCR CRPP  
C Y(6) IS FUEL FLOW IN LB/HR  
C Y(7) IS FRRCR BETWEEN ORDERED SHAFT RPM AND ACTUAL SHAFT RPM  
C Y(8) IS HYDRAULIC FLUID FLCH TC CRPP IN GAL/SEC  
C Y(9) IS PROPELLOR TORQUE  
C Y(10) IS PROPELLOR THRUST  
C Y(11) IS LN2500 POWER TURBINE TORQUE  
C  
VA=.96\*Y(2)  
DENOM=VA\*VA+Y(1)\*Y(1)\*225.  
J=VA/SQRT(DENOM)  
Y(8)=1.0+.435\*Y(1)  
DY(5)=.0528+.0109\*Y(5)\*Y(5)\*Y(8)  
IF(Y(5)>1.6)Y(5)=1.6  
PD=Y(5)  
CALL CRPP (J,CQ,CT,AP1,AP8,BP1,BP8,AM8,AM1,BM8,BM1,AM4,BM4,A  
2M2,RM2,AM0,BM0,AP4,BP4,PD)  
Y(12) IS PROPELLOR TORQUE COEFFICIENT  
Y(13) IS PROPELLOR THRUST COEFFICIENT  
Y(12)=CQ  
Y(13)=CT  
Y(9)=6720.\*DENOM\*Y(12)  
Y(10)=448.\*DENOM\*Y(13)  
C THRUST IS REDUCED BY THRUST DEDUCTION FACTOR  
Y(10)=.98\*Y(10)  
C RT IS SHIP RESISTANCE IN LBS AS A FUNCTION OF SHIP'S SPEED  
RT=104.3\*Y(2)\*Y(2)  
C SHAFT COMPUTES SHAFT FRICTION AS A FUNCTION OF SHAFT SPEED  
SN=Y(1)



```

C RPM IS POWER TURBINE SPEED
C RPM=861.*Y(1)
Y(7)=RPM
WF=Y(6)
C LN250 COMPUTES POWER TURBINE TORGUE AS A FUNCTION CF WF AND RPM
CALL LM250 (RPM,WF,TORG,A08,A16,A2,A3,A4,A5,A6,A7,A99)
IF(TORQ .LT. 0.)TORQ=-1.965*RPM+5500.
Y(11)=TORG
C QC IS GAS TURBINE TORQUE MODIFIED BY REDUCTION GEAR FACTCR
ETA=.75+.22*(1.0-EXP(-Y(1)/1.04))
OD=28.72*Y(11)*ETA
DY(1)=(CD-CF-Y(9))*6.37E-7
DY(2)=(Y(10)-RT)*3.33E-6
IF(Y(5) .LE. -.8)FTIME=T
Y(6)=800C.+9100.*EXP(-T)
DY(4)=Y(2)
IF(T .GT. 4.5)DT=.5
IF(Y(2) .LE. 0.)FTIME=T
RETURN
END

```

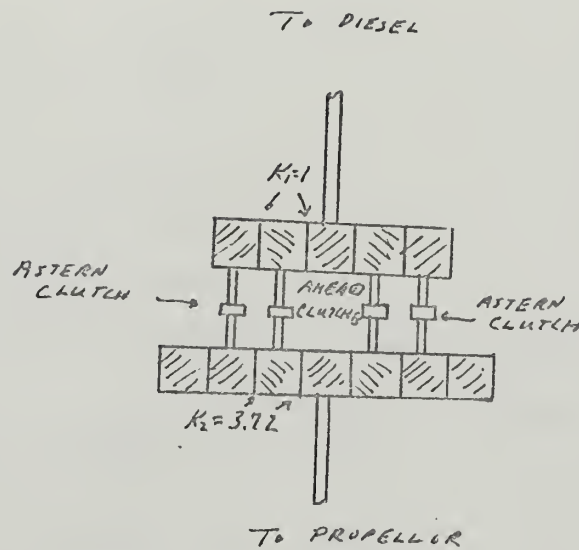


## APPENDIX H

KV Major 12 Drive Train

Figure (H-1) is a sketch of the drive train used for simulation. The WR<sup>2</sup> of the engine-flywheel was provided by the Hawker-Siddeley Co.





## MOMENTS OF INERTIA

DIESEL &amp; FLYWHEEL

712 16-Ft-SEC<sup>2</sup>

TOTAL DRIVE TRAIN

18.45 X 10<sup>3</sup> 16-Ft-SEC<sup>2</sup>

WITH CLUTCHES OPEN:

REFERRED TO DIESEL SHAFT

DIESEL END

720 16-Ft-SEC<sup>2</sup>

PROPELLOR END

8.645 X 10<sup>3</sup> 16-Ft-SEC<sup>2</sup>

REFERRED TO PROP SHAFT

REFERRED TO DIESEL SHAFT

REFERRED TO PROP SHAFT

KV MAJOR 12 DRIVE TRAIN ARRANGEMENT

FIG (H-1)



SUBROUTINE EQSIM

C COASTDOWN AND OPEN CLUTCHING WITH THE MIRRLESS ENGINE

C COMMON T, DT, Y(20), DY(20) , STIME, FTIME, NEWDT

C Y(1) IS SHAFT SPEED IN RPS

C Y(2) IS SHIP'S SPEED IN FPS

C Y(3) IS DISTANCE TRAVELED IN FT

C Y(4) IS PROPELLOR THRUST

C Y(5) IS PROPELLOR TORQUE

VA=.96\*Y(2)

CALL PRPLR (VA,CT,CQ)

DENOM=VA\*\*2 + (33.\*Y(1))\*\*2

C COMPUTE PROPELLOR TORQUE

Y(5)=262.5\*DENOM\*CQ

C COMPUTE PROPELLOR THRUST

Y(4)=171.5\*DENOM\*CT

C PROPELLOR THRUST IS REDUCED BY THRUST DEDUCTION FACTOR

Y(4)=.98\*Y(4)

C ETA IS REDUCTION GEAR EFFICIENCY AS A FUNCTION OF SHAFT SPEED

ETA=.75+.22\*(1.0-EXP(-Y(1)/1.04))

C Y(6) IS SHIP'S SPEED IN KNOTS

Y(6)=.591\*Y(2)

C Y(7) IS FUEL SETTING IN PER CENT

Y(7)=97.8-20.\*T

IF(Y(7) .LE. 12.3)Y(7)=12.3

C TORQ COMPUTES MIRRLESS DIESEL TORQUE AS A FUNCTION OF

C FUEL SETTING

TORQ=550.\*Y(7)

C RT IS SHIP RESISTANCE AS A FUNCTION OF SHIP'S SPEED

RT=104.8\*Y(2)\*\*2

C SHAFT COMPUTES SHAFT FRICTION

SN=Y(1)

CALL SHAFT (SN,QF)

C Y(8) IS DIESEL TORQUE

Y(8)=TORQ

C QD IS DIESEL TORQ MODIFIED BY REDUCTION GEAR

QD=3.72\*TORQ\*ETA

DY(1)=(QD-Y(5))\*8.64E-6

DY(2)=(Y(4)-RT)\*3.33E-6

DY(3)=Y(2)

C QCF IS FORWARD CLUTCH TORQUE

QCF=60000.\*EXP(-T/5.0)

C QSLK IS PROPELLOR TORQUE AS SEEN BY CLUTCH

OSLK=Y(5)/3.72

IF(ABS(QCF) .LT. ABS(OSLK))FTIME=T

Y(9)=QCF

Y(10)=OSLK

RETURN

END



```

SUBROUTINE EQSIM
C MIRRLESS ENGINE
C OPEN-CLUTCH--RECLUTCHING PHASE
C COMMON T,DT,Y(20),DY(20),STIME,FTIME,NEWDT
C Y(1) IS SHAFT SPEED IN RPS
C Y(2) IS SHIP'S VELOCITY IN FPS
C Y(3) IS DISTANCE TRAVELED BY SHIP IN FEET
C Y(4) IS ENGINE SPEED IN RPS
C Y(5) IS CLUTCH ABSORBED ENERGY
C Y(6) IS PROPELLOR THRUST
C Y(7) IS FUEL SETTING IN PER CENT
C Y(8) IS SHAFT SPEED IN RPM
C Y(9) IS DIESEL TORQUE
C Y(10) IS CLUTCH SLIP SPEED
C Y(11) IS REVERSE CLUTCH TORQUE
C Y(12) IS POWER ABSORBED BY REVERSE CLUTCH
C Y(13) IS PROPELLOR TORQUE
VA=.96*Y(2)
CALL PRPLR(VA,CT,CQ)
DENOM=VA*VA+(33.*Y(1))**2
Y(13)=262.5*DENOM*CQ
Y(6)=171.5*DENOM*CT
C RT IS SHIP RESISTANCE AS A FUNCTION OF SHIP'S SPEED
RT=104.8*Y(2)*Y(2)
C SHAFT COMPUTES SHAFT FRICTION
SN=Y(1)
CALL SHAFT(SN,QF)
RPM=Y(4)*60.
Y(7)=97.8-20.*((T-11.199)
IF(Y(7) .LE. 12.3)Y(7)=12.3
TORQ=550.*Y(7)
Y(9)= TORQ
C TORQ COMPUTES MIRRLESS DIESEL TORQUE AS A FUNCTION
C OF FUEL SETTING
C ETA IS REDUCTION GEAR EFFICIENCY AS A FUNCTION OF SHAFT SPEED
ETA=.75+.22*(1.0-EXP(-Y(1)/1.04))
C CLCRT IS CLUTCH REVERSE TORQUE
CLCRT=60000.*((1.-EXP((-T+11.199)/5.))
DY(1)=-CLCRT*6.85E-5-.921E-5*QF-1.842E-5*Y(13)
DY(2)=(Y(6)-RT)*3.33E-6
DY(3)=Y(2)
DY(4)=(TORQ-CLCRT)*2.21E-4
Y(10)=(3.72*Y(1)-(-RPM))*60.
Y(12)=Y(10)*CLCRT*1.904E-4
DY(5)=550.*Y(12)
Y(8)=60.*Y(1)
C Y(14) IS SHIP'S SPEED IN KNOTS
Y(14)=.591*Y(2)
IF(Y(10) .LE. 0.)FTIME=T
RETURN
END

```



```

SUBROUTINE EQSIM
C STOPPING THE SHIP WITH MIRRLESS
COMMON T,DT,Y(20),DY(20),STIME, FTIME, NEWDT
C Y(1) IS SHAFT SPEED IN RPS
C Y(2) IS SHIP'S VELOCITY IN FPS
C Y(3) IS DISTANCE TRAVELED IN FT
C Y(4) IS PROPELLOR TORQUE
C Y(5) IS PROPELLOR THRUST
C Y(6) IS FUEL SETTING IN PER CENT
VA=.96*Y(2)
CALL PRPLR (VA,CT,CQ)
DENOM=VA*VA+(33.*Y(1))**2
Y(4)=262.5*DENOM*CQ
Y(5)=171.5*DENOM*CT
C RT IS SHIP RESISTANCE
RT=104.8*Y(2)*Y(2)
C SHAFT COMPUTES SHAFT FRICTION
SN=Y(1)
CALL SHAFT (SN,CF)
C ETA IS REDUCTION GEAR EFFICIENCY AS A FUNCTION OF SHAFT SPEED
ETA=.75+.22*(1.0-EXP(-ABS(Y(1))/1.04))
Y(6)=12.3+15.* (T-17.199)
IF(Y(6) .GE. 97.8)Y(6)=97.8
C TORQ COMPUTES MIRRLESS DIESEL TORQUE AS A FUNCTION
C OF FUEL SETTING
TORQ=550.*Y(6)
Y(7)=TORQ
DELAY=1.-EXP(-(T-17.199)/.15)
Y(7)=Y(7)-6765.
Y(7)=Y(7)*DELAY
Y(7)=Y(7)+6765.
C QD IS DIESEL TORQUE MODIFIED BY REDUCTION GEAR
QD=-3.72*TORQ*ETA
C Y(8) IS DIESEL RPM
Y(8)=223.*(-Y(1))
C Y(9) IS BEARING LOAD TORQUE LIMIT
Y(9)=20400.+88.6*Y(8)
DY(1)=(QD-Y(4))*8.64E-6
C THRUST IS REDUCED BY THRUST DEDUCTION FACTOR
Y(5)=.98*Y(5)
DY(2)=(Y(5)-RT)*3.33E-6
DY(3)=Y(2)
C Y(10) IS SHIP'S SPEED IN KNOTS
Y(10)=.591*Y(2)
IF(T .GT. 20.)DT=1.
IF(Y(2) .LE. 0.)FTIME=T
RETURN
END

```



## APPENDIX I

B & W 7K98FF Drive Train

Figure (I-1) is a sketch of the 7K98FF drive train. The  $WR^2$  of the engine was not available in the literature surveyed. An official of the Burmeister and Wain Corporation provided the following weights:

Piston ..... 4.18 tons

Crosshead... 3.35 tons

Crank ..... 4.97 tons

From the "Shock and Vibration Handbook", Vol. 3, p. 38-2, the following expression was found for finding the  $WR^2$  of a diesel:

$$J = \left( \frac{W_p}{2} + W_c \left( 1 - \frac{h}{2} \right) \right) R^2$$

$W_p$  = weight of piston, piston pin, and cooling fluid (lb)

$W_c$  = weight of connecting rod (lb)

$h$  = fraction of rod length from the lower center of gravity

$R$  = crank radius (in)

From the above expression, the polar moment of inertia was estimated at  $4.25 \times 10^3$  lb-ft-sec $^2$ .





$$I_{\text{DRIVE TRAIN}} = 12365 + 1050/R \quad \text{lb-ft-sec}^2$$

$R = \text{PITCH RATIO}$

TK98FF DRIVE TRAIN ARRANGEMENT  
FIG (I-1)



```

SUBROUTINE EQSIM
REAL J
COMMON T, DT, Y(20), EY(20), STIME, ETIME, NEWDT
C
C      REVERSING WITH 8W7K9EFF AND CRPP
C      Y(1) IS SHAFT SPEED IN RPS
C      Y(2) IS SHIP'S SPEED IN FPS
C      Y(3) IS DISTANCE TRAVELED IN FT
C      Y(4) IS PITCH DIAMETER RATIO FOR CRPP
C
C      VA=.96*Y(2)
C      DENOM=VA*VA+Y(1)*Y(1)*225.
C
C      J=VA/SQRT(DENOM)
C      Y(5) IS HYDRAULIC FLUID FLOW TO CRPP IN GAL/SEC
C      Y(5)=1.+.435*Y(1)
C      EY(6)=-.0526-.0109*Y(4)*Y(4)*Y(5)
C      IF(Y(6)<=.LE.-1.)Y(6)=-1.
C      PD=Y(4)
C      CALL CRPP (J,CO,CT,AP1,AP8,BP1,BP8,AM3,AM1,BM1,AM4,BM2,AM2,BM2
C,Z,AM0,BM0,AP4,BP4,PD)
C      Y(6) IS PROPELLOR TORQUE
C      Y(6)=5720.*DENOM*CO
C      Y(7) IS PROPELLOR THRUST
C      Y(7)=442.*DENOM*CT
C      THRUST IS REDUCED BY THRUST DEDUCTION FACTOR
C      Y(7)=.98*Y(7)
C      RT IS SHIP RESISTANCE IN LBS
C      RT=1C4, 8*Y(2)*Y(2)
C      SHAFT COMPUTES SHAFT FRICTION AS A FUNCTION OF SHAFT SPEED
C      SN=Y(1)
C      CALL SHAFT (SN,QF)
C      THE 7K9EFF IS DIRECTLY COUPLED TO THE PROPELLOR, THUS ENGINE AND
C      SHAFT RPM ARE IDENTICAL
C      PPM=60.*Y(1)
C      Y(11)=RPM
C      Y(3) IS FUEL SETTING
C      Y(8)=.924+.46545.*((1.-EXP((-T+21.)*.5))*
C      QF=Y(8)

```



```

CALL BURNE (WF,TDRQ)
Y(9)=TDRQ
DELAY=1.*EXP(-(T-21.)/.15)
Y(9)=Y(9)-31100.
Y(2)=Y(9)*DELAY
Y(9)=Y(9)+31100.

C THE SHAFT MOMENT OF INERTIA, Y(10), IS AFFECTED BY PROPELLOR
C PITCH RATIO DUE TO ENTRAINED WATER
Y(10)=6.28*(12365.+1150.*ABS(Y(4)))
CY(1)=(TDRQ-QF-Y(6))/Y(10)
DY(2)=(Y(7)-FT)*3.33E-6
DY(3)=Y(2)
IF(T .GT. 30.)DT=1.
IF(Y(2) .LE. 0.)FTIME=T
RETURN
END

```



29 OCT 76

DEC 77

24119

Thesis  
F78795

135292

Freeman

Digital simulation of  
ship propulsion trains  
utilizing gas turbine  
and diesel prime mo-

DISPLAY

19 SEP 76 vers.

29 OCT 76

24119

DEC 77

Thesis  
F78795

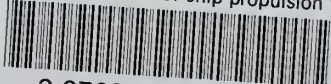
135292

Freeman

Digital simulation of  
ship propulsion trains  
utilizing gas turbine  
and diesel prime mo-  
vers.

thesF78795

Digital simulation of ship propulsion tr



3 2768 001 96009 9  
DUDLEY KNOX LIBRARY